

2014

## APPLICATION OF POLYMER SYSTEMS TO THE DETECTION AND RETENTION OF EXPLOSIVES

Jonathan N. Canino  
University of Rhode Island, Jon.Canino@gmail.com

Follow this and additional works at: [https://digitalcommons.uri.edu/oa\\_diss](https://digitalcommons.uri.edu/oa_diss)

Terms of Use

All rights reserved under copyright.

---

### Recommended Citation

Canino, Jonathan N., "APPLICATION OF POLYMER SYSTEMS TO THE DETECTION AND RETENTION OF EXPLOSIVES" (2014). *Open Access Dissertations*. Paper 262.  
[https://digitalcommons.uri.edu/oa\\_diss/262](https://digitalcommons.uri.edu/oa_diss/262)

This Dissertation is brought to you by the University of Rhode Island. It has been accepted for inclusion in Open Access Dissertations by an authorized administrator of DigitalCommons@URI. For more information, please contact [digitalcommons-group@uri.edu](mailto:digitalcommons-group@uri.edu). For permission to reuse copyrighted content, contact the author directly.

APPLICATION OF POLYMER SYSTEMS TO THE  
DETECTION AND RETENTION OF EXPLOSIVES

BY

JONATHAN N CANINO

A DISSERTATION SUBMITTED IN PARTIAL FULFILLMENT OF THE  
REQUIREMENTS FOR THE DEGREE OF  
DOCTOR OF PHILOSOPHY  
IN  
ANALYTICAL CHEMISTRY

UNIVERSITY OF RHODE ISLAND

2014

DOCTOR OF PHILOSOPHY DISSERTATION  
OF  
JONATHAN N CANINO

APPROVED:

Thesis Committee:

Major Professor      Jimmie Oxley

Co- Major Professor   James Smith

Sze Yang

Otto Gregory

Nasser H. Zawia  
DEAN OF THE GRADUATE SCHOOL

UNIVERSITY OF RHODE ISLAND  
2014

## **ABSTRACT**

Obtaining, handling, and storing of explosives, especially primaries such as triacetone triperoxide (TATP), presents significant obstacles to instrument manufacturers and K-9 trainers. Microencapsulation techniques were used to trap TATP in a plastic matrix rendering it safe to handle, store at room temperature, and release by heating. Detection of most explosive vapor is a challenge for current instrumentation. This work provides a study of polymer systems for the pre-concentration of explosive vapor for use with portable explosive detection technologies, specifically molecularly imprinted polymers (MIPs).

## **ACKNOWLEDGMENTS**

I would like to thank everyone who made this work possible. My advisors Dr. Jimmie Oxley and Dr. James Smith, who guided me along this journey. My family Alison, Elizabeth, and Frank Canino, without your love and support I wouldn't be half the person I am today. My co-workers and fellow graduate students, I have not accomplished anything in this work without your help. My committee members, for their help and guidance. Lastly, my love Stephanie Guertin, not only would this work be the worse without your influence and care, but so would I.

## **PREFACE**

This thesis is prepared in the manuscript format. Chapter 1 has been submitted to the Journal of Energetic Materials. Chapter 2 is in preparation to be submitted to the Journal of Energetic Materials. Both have been prepared following the guidelines of that journal.

## TABLE OF CONTENTS

<b>ABSTRACT</b> .....	<b>ii</b>
<b>ACKNOWLEDGMENTS</b> .....	<b>iii</b>
<b>PREFACE</b> .....	<b>iv</b>
<b>TABLE OF CONTENTS</b> .....	<b>v</b>
<b>LIST OF TABLES</b> .....	<b>vi</b>
<b>LIST OF FIGURES</b> .....	<b>vii</b>
<b>CHAPTER 1</b> .....	<b>1</b>
Insensitive TATP Training Aid by Microencapsulation .....	1
<b>CHAPTER 2</b> .....	<b>57</b>
Investigation of Molecularly Imprinted Polymers with Trinitrotoluene .....	57
<b>SUPPORTING INFORMATION</b> .....	<b>82</b>

## LIST OF TABLES

TABLE	PAGE
<b>Chapter 1</b>	
Table 1. Baking and Purification Temperatures.....	26
Table 2. Overall Results .....	27
Table 3. Encapsulation Repeatability Tests.....	28
Table 4. Storage Stability .....	29
Table 5. Sensitivity Tests.....	30
<b>Chapter 2</b>	
Table 1. Imprinting Results Summary.....	78

## LIST OF FIGURES

FIGURE	PAGE
<b>Chapter 1</b>	
Figure 1. Microcapsules and microspheres .....	31
Figure 2. TGA of PS-TATP microspheres trace (solid); TGA derivative (dotted line); at 2°/min (left) & 20°/min (right).....	32
Figure 3. IR spectra corresponding to peak release in Fig. 2 .....	33
Figure 4. Comparison of PS unknown (middle) IR to pure TATP (bottom) & TATP decomposition (top).....	34
Figure 5. TGA of PC-TATP microspheres trace (solid); TGA derivative (dotted line); at 2°/min (left) & 20°/min (right).....	35
Figure 6. IR spectra of TATP from PC microspheres .....	36
Figure 7. TGA of PSf-TATP microspheres trace (solid); TGA derivative (dotted line); at 2°/min (left) & 20°/min (right).....	37
Figure 8. DSC of PSf: TATP microspheres (solid line), Tg (dotted line).....	38
Figure 9. Comparison of PSf-TATP (middle) IR to pure TATP (bottom) & TATP decomposition (top).....	39
Figure 10. TGA of PEI-TATP microspheres trace (solid); TGA derivative (dotted line); at 2°/min (left) & 20°/min (right) .....	40
Figure 11. DSC of PEI: TATP microspheres (solid line), Tg (dotted line).....	41
Figure 12. Comparison of PEI-TATP (middle) IR to pure TATP (bottom) & TATP decomposition (top).....	42

FIGURE	PAGE
Figure 13. TGA of PLGA-TATP microspheres trace (solid); TGA derivative (dotted line); at 2°/min (left) .....	43
Figure 14. IR spectra of TATP from PLGA microspheres.....	44
Figure 15. TGA of PVBVAVA-TATP microspheres trace (solid); TGA derivative (dotted line); at 2°/min (left) & 20°/min (right) .....	45
Figure 16. IR spectra of TATP from PVBVAVA microspheres.....	46
Figure 17. TGA of P4MS-TATP microspheres trace (solid); TGA derivative (dotted line); at 2°/min .....	47
Figure 18. IR spectra of TATP from P4MS microspheres .....	48
Figure 19. TGA of PEM-TATP microspheres trace (solid); TGA derivative (dotted line); 895cm <sup>-1</sup> IR signal (dash line); at 2°/min.....	49
Figure 20. IR spectra of TATP from PEM microspheres (right); Mix of PEM decomposition and TATP (left) .....	50
Figure 21. TGA of PMMA-TATP microspheres trace (solid); TGA derivative (dotted line); 889cm <sup>-1</sup> IR signal (dash line); at 2°/min.....	51
Figure 22. IR spectra of TATP from PMMA microspheres (right); Mix of PMMA decomposition and TATP (left) .....	52
Figure 23. Blank vs. early polystyrene microspheres vs. PS microspheres after changing PVA and baking for 20 minutes at 150°C.....	53
Figure 24. Polycarbonate microspheres after baking .....	54
Figure 25. Release profile of TATP from polycarbonate .....	55

FIGURE	PAGE
Figure 26. Prototype microsphere heater (right); TATP crystals deposited on aluminum wool (left) .....	56

## Chapter 2

Figure 1. Generalized synthesis of a MIP .....	79
Figure 2. Structural and functional monomers tested .....	80
Figure 3. From left to right: TNT aromatic protons with no aniline, 1 molar equivalent aniline, and 10 molar equivalents aniline .....	81

## CHAPTER 1

Insensitive TATP Training Aid by Microencapsulation

Authors:

Oxley, J. C. University of Rhode Island\*, Smith, J. L. University of Rhode Island,

Canino, J. N. University of Rhode Island

Corresponding Author\*:

Professor Jimmie Oxley

Pastore Hall, URI

51 Lower College Rd.

Kingston, RI 02881

Email: [joxley@chm.uri.edu](mailto:joxley@chm.uri.edu)

Phone: 401-874-2103

Fax: 401-874-5072

Manuscript submitted to the Journal of Energetic Materials

## **Abstract**

There is a need in the explosives detection community for an insensitive, storage-stable source of triacetone triperoxide (TATP). To achieve this, the solvent evaporation microencapsulation technique was used to disperse TATP in a plastic matrix. This lowered the shock sensitivity greatly and prevented loss of TATP at room temperature, allowing for easy long term storage. It was then demonstrated that pure TATP vapor was released on demand from the matrix by heating.

## **Introduction**

Triacetone triperoxide (TATP) is a primary explosive with a high room temperature vapor pressure (0.052mm Hg) [1]. The high sensitivity and vapor pressure make it impractical for military or industrial use. It is quite easy to synthesize, making it a favored explosive of terrorist organizations and thrill-seeking amateur chemists around the world. The detection of TATP is thus of great interest to military and security agencies. Unfortunately, as a primary explosive, it is highly hazardous to handle. Despite this, two communities require this explosive or at least the explosive scent: bomb sniffing dogs and companies manufacturing trace explosive detection instruments. For the manufacturers, obtaining, handling, and storing any explosive is a significant obstacle; thus, it is our intention that the protocols developed in this study can be transitioned to other energetics materials.

The approach discussed herein is encapsulation of the explosive with sufficient polymer that it is subject to combustion rather than to detonation. Microencapsulation procedures distinguish between two types of microparticles:

microcapsules and microspheres. *Microcapsules* have a discrete polymer shell which surrounds either pure core material or a microsphere-like matrix of polymer and core material. Microcapsules are capable of higher loadings of core material. A *microsphere* is a polymer matrix with the desired core material dispersed throughout the polymer (Fig. 1). They can have maximum theoretical loadings of up to 50% core material [2].

<Figure 1>

There are numerous physical methods used for microencapsulation [3–6]. Pan coating is a well-established encapsulation process that is still widely used in the pharmaceutical industry [3, 6]. Particles of core material are sprayed with solubilized polymer while they are tumbled in a “pan.” The pan is usually heated to facilitate evaporation of organic solvents. The polymer coats the particles as they rotate in the pan and the solvent evaporates, leaving a polymer shell. Particle size is controlled by size of core particles, pan rotation speed, and addition rate of solubilized polymer. Disadvantages of the pan coating approach include potential for aggregation of particles and adherence of particles and aggregates to walls of the pan as the polymer coating hardens. Because TATP is sensitive to explosive initiation from shock, friction, and heat, tumbling inside a heated container is not prudent.

Fluidized bed coating, also called Wurster coating [3], is similar to pan coating except air jets replace the tumbling pan. Air currents move the core material past a nozzle that sprays them with the solubilized or molten polymer. The spraying nozzle can either be tangential to, above, or below the substrate. The position of the nozzle changes the performance of the coating [3]. As with pan coating, this method applies

to solid core material. Particle size is controlled by the original size of the core particles and polymer coating rates by spray conditions. It is prone to the same disadvantages as pan coating.

In spray drying, solid core material is mixed with solubilized polymer in a reservoir and sprayed out a nozzle into a collection chamber [3–5]. The chamber is large enough to allow the solvent to evaporate before the particles reach the bottom. When the solvent evaporates, the core material is left with a solid polymer shell. Spray cooling is a similar technique [3–5] where a molten, rather than a solubilized, polymer is used. The polymer cools and hardens as the droplet surrounding the core material falls into the collection chamber. In both methods the particle size is controlled by the type of nozzle used. For purposes herein, this method would be limited by the number of polymers that melt at temperatures safe for handling TATP.

The solvent evaporation technique uses emulsions and volatile organic solvents to make microspheres rather than microcapsules [2, 7, 8]. The polymer and the core material are dissolved in a volatile organic solvent which becomes the dispersed phase. All three, the polymer, the core material, and the solvent, must be immiscible with a second liquid phase, which will be used as the continuous phase. Using a surfactant and rapid stirring, an emulsion is used to create droplets which harden into solid microspheres as the dispersed phase solvent evaporates. The surfactants, stirring speed, rate of dispersed phase evaporation, and amount of solvent used in the dispersed and continuous phase all affect particle size [7, 8]. Particle size often varies between one to two orders of magnitude inside a batch.

Co-acervation uses emulsions and solubility to make microcapsules. It is most commonly performed using a water/oil mix with the oil being the core material [9]. The polymer is dissolved in water and oil is emulsified into the aqueous solution. A change in conditions (temperature, pH, addition of a salt, addition of an anti-solvent) lowers the solubility of polymer in water causing the polymer to reform [3, 10, 11]. The reforming polymer collects at the surface of the oil droplets, forming a shell. Particle size is controlled by stirring time, size of emulsion droplet, and the changing solubility of the polymer in the solvent [3].

Supercritical carbon dioxide is showing considerable promise as a means of promoting microencapsulation. Carbon dioxide acts as an organic solvent and solvent removal is accomplished by simply venting the pressurized chamber. The rapid expansion of supercritical solution (RESS) and the gas anti-solvent (GAS) methods as applied to microencapsulation have been recently reviewed [3]. RESS is similar to spray drying; polymer dissolved in supercritical carbon dioxide is sprayed at atmospheric pressure with the core material forming particles as the carbon dioxide flashes off. Nozzle dimensions determine particle size. The GAS method uses supercritical fluid to co-precipitate the core and shell material from solution. The particles formed in GAS would be similar to microspheres in core/shell material distribution although it is unclear whether actual spheres would form rather than random shapes.

Co-extrusion is a continuous process that encapsulates liquid samples [4]. A syringe pump with two feeds is used, one with coating material and the other with core material. The coating line surrounds the core material line, and the pump is adjusted

to form droplets of core material in the center with the coating material surrounding the outside. As with spray cooling, the drops fall from a sufficient height to allow the polymer shell to harden before impact. It may be possible to use molten, rather than solubilized, polymer in this system. Particle size is controlled by the flow rate of the pump and the nozzle dimensions. This method allows for highly repeatable particle sizes.

Lastly, a chemical method called interfacial polymerization is a batch process where the microspheres are created at the interface of an emulsified solution [3, 4, 12]. A monomer is dissolved in the continuous phase of the emulsion, and a second monomer is dissolved in the dispersed phase along with the core material. The emulsion is stirred to make droplets, and a cross-linker is added to start polymerization. The copolymer forms at the interface of the continuous and dispersed phases, making a shell around the dispersed phase droplet. This method requires that both the shell (i.e. polymer) and the core material (i.e. TATP) be solvated in the dispersed phase. Residual odors associated with unreacted monomers and short chain polymers are of concern. The desired product of this study should be free of odors other than the explosive (i.e. TATP).

After review of the literature, the solvent evaporation technique was selected. This technique required no special equipment and involved limited heating, a major concern with encapsulation of energetic materials. This technique resulted in microspheres, rather than microcapsules. The resulting lower loading of the core material in microspheres was considered advantageous for reducing the sensitivity of TATP, making the microspheres safer to handle.

## Experimental Section

A pre-made polymer (0.5 to 1 g) was dissolved in 7 to 10 mL of solvent, usually dichloromethane (DCM). The active ingredient was added to this solution with stirring and this organic mixture was added, with vigorous stirring (IKA RW20 mechanical stirrer, 900 rpm), to a 200 mL solution of 2% polyvinyl alcohol (PVA) in water. No specific particle size was desired; a concentration of PVA was selected to yield microspheres that could be easily analyzed at 200x zoom on an optical microscope (100 $\mu$ m-300 $\mu$ m). While 2-4% PVA produced particles in this range, using less PVA increased filtration rate; thus, 2% aqueous PVA solution was chosen. The mixture was stirred at 900 rpm to remove the solvent and yield the hardened polymer spheres. Time required to remove the organic solvent depended on the solvent: dichloromethane, 1 hour; chloroform, 3 hours; toluene, overnight. After evaporation of the organic solvent, ~600 mL of water was added with stirring to the foamy white mixture to aid filtration. After 5 to 10 minutes, the microspheres were recovered by vacuum filtration, rinsed with ~200 mL water, and dried under vacuum until the microspheres no longer clumped together. The microspheres were weighed and stored for further analysis. By this route, the active ingredients TATP, DADP (diacetone diperoxide), TNT (2,4,6-trinitrotoluene), HMTD (hexamethylene triperoxide diamine), and naphthalene were encapsulated.

Polystyrene (PS) was purchased from Acros Organics (average molecular weight 250,000). Other polymers tested include polysulfone (PSf) (Acros Organics, Mw 75,000); polyethylmethacrylate (PEM) (Acros Organics, Mw 340,000);

poly(lactic-co-glycolic acid) (PLGA) (Sigma Aldrich, Mw 50,00-75,000); polycarbonate (PC) (Acros Organics, Mw 45,000); polyetherimide (PEI) (Sigma Aldrich, Mw not listed, categorized by melt index); poly (vinyl butyral-co-vinyl alcohol-co-vinyl acetate) (PVBVAVA) (Sigma Aldrich, Mw 50,000-80,000); Poly(methyl methacrylate) (PMMA) (Sigma Aldrich, Mw 30,000); Poly(4-methylstyrene) (P4MS) (Sigma Aldrich, Mw ~72,000). Poly(vinyl alcohol) (PVA) was purchased from Acros Organics (88% hydrolyzed, Mw 20,000-30,000) or Sigma Aldrich (98-99% hydrolyzed, Mw 31,000-50,000) and used as a surfactant. Initially, PVA, 88% hydrolyzed, was found to contaminate the microspheres with tetramethylbutane dinitrile; therefore, the source of PVA was altered. All solvents were HPLC-grade, purchased from Fisher: n-hexane; dichloromethane; chloroform; toluene.

Microspheres were baked at various temperatures for several reasons (Table 1). Polymers with promise as shell materials were baked to remove the residual DCM and surface TATP from the spheres. In addition to providing a cleaner odor, this baking allowed for more accurate determination of the loading of TATP. Most spheres were baked for 24 hours; later it was found that a 48 hour bake was required for complete removal of DCM from polycarbonate. To achieve a pure headspace for polystyrene, a purification bake was required to remove residual monomer and other contaminants from polystyrene. This purification was done by baking blank polystyrene microspheres at 150°C for 20 minutes. These microspheres were re-dissolved in DCM and then used to make a new batch of microspheres free of headspace contaminants.

<Table 1>

Percent loadings of explosive and release profiles of the microspheres were determined using a Thermal Analysis Q5000 thermal-gravimetric analyzer (TGA) with the off-gas routed through a heated transfer line to a Nicolet 6700 infrared spectrometer (FT-IR) using a 20 cm path length vapor cell. The cell and the transfer line were kept at 170°C in order to avoid decomposition of TATP vapor. The furnace and scale of the TGA were purged continuously with nitrogen. The purge gas was vented through a heated transfer line to the gas cell of the FT-IR. It should be noted that the first derivative of mass loss in the TGA was usually identical to the total intensity plot from the IR. Pure TATP exhibited four major IR bands at 1194, 1378, 3005, and 2953  $\text{cm}^{-1}$ ; however, these overlapped with TATP decomposition products. A unique band at 895-899 $\text{cm}^{-1}$  was used to track TATP in the presence of decomposition products. TGA oven programs were varied by polymer and solvent used. Once the solvent was removed by isothermal heating, a heat ramp program was used to determine loading. Samples were heated at 2°C/min or 20°C/min from 40°C to a temperature determined by the thermal stability of the polymer being tested. TATP decomposition vapor signal was obtained by running TATP vapor from the TGA through the IR transfer line while the line was held at 250°C.

The glass transition point ( $T_g$ ) of the polymers were determined by differential scanning calorimetry (DSC) (TA Instruments Q100, calibrated against indium and sapphire). Samples were sealed in hermetic aluminum pans and run in duplicate. The starting temperature was 40°C and ramped at 20°C/min to end temperatures ranging from 200-400°C, depending on the polymer. Two sets of samples were each run twice

to obtain the Tg of a polymer. Microspheres of the polymers were analyzed using the same methods as the Tg experiments, with the exception that thermal cycling was impossible as heating released the core material.

The purity of the released TATP vapor was determined by gas chromatography using a mass spectrometer detector (GC/MS). An Agilent 6890N GC with a 5973 mass selective detector and a Varian VF-200ms column was used for normal headspace analysis; a Thermo Fisher Trace GC Ultra with an ISQ mass spectrometer and a Varian PoraPLOT Amines column was employed for analysis of low molecular weight gases released from the microspheres. To generate these headspace signatures, 100 mg of microspheres were added to a ~11 mL headspace vial, which was sealed and placed in an oven. The oven was rapidly heated to 150°C, and the vial was allowed to equilibrate at temperature for 1 minute. The vial was removed and 1 mL of vapor manually injected into the GC. Before the syringe was reused, it was cleaned with three rinses of volatile solvent, initially acetone and later pentane. The syringe barrel was then baked at ~90°C for ~10 minutes, while the plunger dried in air.

The method for the most headspace runs on the Agilent system was as follows. The inlet was set to 110°C splitless injection with a 20 mL/min purge at 0.5 minutes. The pressure was 1.5 psi for 3 minutes, ramped 10 mL/min to 2.5 psi and held for 4 minutes, ramped 10 mL/min to 1.5 psi and held for 3 minutes, then maintained at 1.5 psi for a 3 minute post-run. The initial oven temperature was 40°C which was held for 2 minutes, ramped 20°C/min to 60°C, slowed to 2.5°C/min to 70°C, 30°C/min to 100°C, 10°C/min to 150°C, 30°C/min to 200°C, and then maintained at 310°C post run for 3 minutes. The mass spectrometer transfer line was kept at 150°C. The

method for the low molecular weight region of the headspace, run on the Thermo system, was as follows. The inlet was set to 100°C splitless injection with a 30 mL/min purge at 2 minutes. The carrier gas flow through the column was set to a constant pressure of 10 psi for the entire method. The initial oven temperature was 35°C which was ramped 30°C/min to 220°C and held for 20 minutes. The mass spectrometer transfer line was kept at 200°C.

Small-scale explosivity device (SSED) tests were done to compare the energetic character of pure TATP to that of encapsulated TATP. A Winchester 0.303 shell was filled with 1g of the test material, sealed inside a heavy-walled steel chamber, and initiated with a RP-3 detonator. The more of the cartridge adhering to the base, the less the explosive power was judged to be. [13, 14].

Detonation tests were performed on a large scale using 3" long and 3/4" diameter stainless steel pipes. The microsphere synthesis was scaled up to 5g of polycarbonate (PC) and 2.5g of triacetone triperoxide (TATP) to make sufficient microspheres for this test. The yield for this scale up was ~5.2g of microspheres with average loading of 13.8% TATP by mass. The pipes were lined with anti-static bags which were cut about 1 1/2" above the top of the pipe and formed to the interior of the pipe using cardboard tubes to tamp the bags down. The threads of the pipe were covered with masking tape and then the exposed anti-static bag was cut and folded down over the threads to prevent loose material from falling into the threads. A 0.31 inch hole was drilled through the bottom end cap of the pipe. The TATP and microspheres were then put into separate pre-weighed plastic pop-top containers and weighed again. This allowed easy filling of the pipes at the range and the mass used

could be determined later. At the range the pipes had a detonator inserted through the bottom of the pipe, going through the plastic bag to ensure good contact with the contents of the pipe once filled. The pipes were filled using a paper funnel and zip-tied to a wooden stake that was placed inside a cardboard concrete form inside a 55 gallon steel drum. The drum was filled with sand on the bottom and around the concrete form. A wooden dowel was placed on top of the opening in the concrete form and sand bags were placed on top of that. Following the range safety guidelines, the detonator was initiated from a safe distance, and once the all clear was given the remains of the pipe were recovered using magnets to sweep the sand. Three shots were done: TATP (5.26 g), PC+TATP (8.64 g), and sand. The remains of the pipe were recovered using magnets to sweep the sand.

## **Results and Discussion**

Thermo-gravimetric (TGA) experiments with polystyrene (PS) encapsulated TATP showed that the release of residual dichloromethane (DCM) could be separated from the release of the encapsulated TATP. This permitted accurate quantification of the mass loading of TATP. The ability to selectively release DCM and TATP was important for purification of the microspheres. The presence of DCM would interfere with the olfactory response of canines to the target material.

The first derivative traces of the polystyrene (PS) solvent-dried microspheres with TATP [PS-TATP] (baked 24 hours at 80°C) indicate three weight loss steps. IR monitoring of the off-gas (Fig. 2) clearly indicated that the first two weight loss steps were loss of TATP (Fig. 3). A third weight loss was observed towards the end of the

TGA run (~70 minutes on Fig. 2, ~280°C) was not identified, its IR did not match TATP, TATP decomposition gases, nor PS decomposition as generated by PS alone. It was concluded that this third loss was related to the presence of TATP in the PS microspheres and TGA analysis of TATP in PS microspheres was modified to use 250°C as the maximum temperature.

<Figure 2>

<Figure 3>

<Figure 4>

Thermal analysis of the polycarbonate (PC) TATP microspheres [PC-TATP] proceeded as with polystyrene. Figure 5 shows release of TATP began at approximately 88°C and continued for 100 degrees at the given scan rate. The IR spectrum of the off-gas indicated pure TATP (Fig. 6); only near the end of the 20°C/min TGA run (above 181°C) were IR bands suggesting other species observed.

<Figure 5>

<Figure 6>

The polysulfone (PSf) encapsulated TATP [PSf-TATP] TGA trace behaved similarly to PS encapsulated TATP [PS-TATP], but weight losses shifted to higher temperatures. Since these microspheres were not baked, the TGA showed the loss of DCM at about 100°C and IR confirmed this. TATP release began around 139°C and reached a maximum at about 167°C (Fig. 7). Unfortunately, the TATP release temperature was close to the decomposition temperature of TATP as observed by DSC (Fig. 8). This, along with the occurrence of extra peaks in the off-gas IR (Fig. 9), suggested that some TATP decomposition was occurring with TATP release. This

same problem was observed with a similar high temperature resistant thermoplastic, polyetherimide (PEI). Polysulfone was discarded as a suitable shell material for TATP due to the overlap of TATP decomposition with release of TATP vapor.

<Figure 7>

<Figure 8>

<Figure 9>

The polyetherimide (PEI) TATP microspheres [PEI-TATP] behaved in a similar manner to polysulfone with TATP: release began at 140°C (Table 2, Fig. 10). The main peak of the TATP exotherm in DSC matches the maximum loss of TATP at 195°C (Table 2, Fig. 11). The IR off-gas from the PEI-TATP microspheres was strong but not pure TATP. As with the PSf-TATP microspheres, the IR spectra appeared to be a mix of TATP and TATP decomposition products. The improved signal strength shows even better correlation between the unknown spectra and that seen in TATP decomposition (Fig. 12). The correlation of IR signal and DSC with the decomposition of TATP for both PSf and PEI suggested that the release of TATP in these polymers was driven by TATP decomposition.

<Figure 10>

<Figure 11>

<Figure 12>

TGA of the poly(D,L-lactide-co-glycolide) (PLGA) TATP microspheres [PLGA-TATP] included a baking period for one hour at 60°C to remove the DCM. The IR of the off-gas showed that along with the DCM, TATP was released as well. Furthermore, as soon as the temperature was ramped (1°C/min) after the baking

period, TATP loss resumed (Fig. 13). To determine if this low-temperature release of TATP began even lower than the “bake out” temperature of 60°C, the PLGA-TATP microspheres were heated from 40°C to 250°C at a constant rate of 5°C/min. TATP release was first observed at ~46°C. This release could be a result of TATP on the surface of the microsphere prior to release of TATP inside the microspheres. Nevertheless, PLGA was discarded as a potential shell material because the polymer was not stable at room temperature, requiring refrigerated storage.

<Figure 13>

<Figure 14>

The poly(vinyl butyral-co-vinyl alcohol-co-vinyl acetate) (PVBVAVA) TATP microspheres [PVBVAVA-TATP] made with this polymer exhibited three weight losses in the TGA trace (2°C/min). IR monitoring of the off-gas showed TATP in all three mass loss regions. The first mass loss was likely surface TATP with some DCM. The second mass loss (started at ~53°C) and third (started at ~76°C) were pure TATP. The TGA suggested that TATP was constantly being released, with release accelerating after 76°C. This polymer was discarded as a potential shell material because of its strong odor.

<Figure 15>

<Figure 16>

The poly-4-methylstyrene (P4MS) TATP microspheres [P4MS-TATP] behaved like polystyrene. There were two TATP releases and a weight loss that could not be attributed to a pure species. The TGA derivative curve (Fig. 17) showed 3 peaks: TATP loss (peak 1 and 2) and a third weight loss unattributed to TATP. TATP

release temperature appeared lower ( $\sim 75^{\circ}\text{C}$ ) than that of PS-TATP ( $88^{\circ}\text{C}$ ), which was surprising considering the small modification to the polymer structure.

<Figure 17>

<Figure 18>

When polyethylmethacrylate (PEM) TATP microspheres [PEM-TATP] were heated in the TGA, decomposition of PEM was observed by IR that overlapped with TATP release. TATP release was observed by following an IR peak ( $894\text{ cm}^{-1}$ ) unique to TATP (Fig. 19); this allowed rough determination of TATP release temperature. TATP release was pure at the start but quickly overwhelmed by decomposition of PEM. As seen in the IR traces (Fig. 20) TATP release did not directly correspond to any of the peaks seen in the total IR intensity trace. PEM was discarded because its decomposition overlapped with TATP release.

<Figure 19>

<Figure 20>

Polymethylmethacrylate (PMMA) TATP microspheres [PMMA-TATP] exhibited the same decomposition problems seen with PEM-TATP: polymer decomposition overlapped with TATP release. A peak unique to TATP in the IR was used to roughly determine the release temperature (Fig. 21), but PMMA was discarded as a shell material due to its decomposition overlapping with TATP release.

<Figure 21>

<Figure 22>

As shown in Table 2, the temperature of initial TATP release was determined by ramping samples slowly ( $2^{\circ}\text{C}/\text{min}$ ) to  $300\text{-}320^{\circ}\text{C}$ . The release “max” temperature

was determined as the peak of the first derivative of TGA trace. Some polymer microspheres had IR signatures for off-gas indicating pure TATP, while others suggested TATP plus TATP decomposition products. In polystyrene the release of TATP started at 77°C. The release in polystyrene was near to the glass transition temperature (T<sub>g</sub>) of polystyrene (109°C) and the melting point of TATP (95°C) [15]. The release of TATP vapor was assumed to be related to one or both of these temperatures. Supporting glass transition temperature was release observed with PVBVAVA-TATP microspheres. The TATP vapor appeared substantially below its melting point. However, with polycarbonate, TATP release began at 88°C, which was far below the glass transition temperature. Furthermore, with polysulfone and polyetherimide, both with high glass transition temperatures, (190°C and 220°C, respectively) TATP release was not observed until 139-140°C, well above the melting point of TATP but below the T<sub>g</sub> of either polymer. The IR of the TGA off-gas and independent DSC runs of PSf-TATP and PEI-TATP shed light on the release mechanism. In both cases the off-gas was clearly a mixture of TATP and TATP decomposition products. The DSC of the microspheres showed the “max” release of TATP was at approximately the same temperature as the temperature of the DSC exothermic maximum.

To examine the factors governing TATP release, in addition to changing the polymer matrix, the core material was also changed. Diacetone diperoxide (DADP) was encapsulated in PC and PSf. The six-membered ring with diperoxide functionalities is chemically very similar to the nine-membered TATP ring with triperoxide functionalities. It is a possible side product of TATP synthesis with a

melting point of 133°C [15]. DADP was encapsulated using polycarbonate and polysulfone and the release temperature determined by TGA. The results are shown in Table 2.

<Table 2>

In selecting the preferred polymer for encapsulation of the explosive, ideal candidates were subjected to three criteria as follows: 1) the polymer/explosive combination must meet solubility constraints amenable to our preparation method; 2) the desired polymer must have long-term shelf-life; 3) the release of the core material (explosive) must be pure (type A release), not contaminated by release of polymer or polymer decomposition products (type B) or by explosive decomposition products (type C) (Table 2). The solvent evaporation method requires that both the polymer and the core material (the explosive) be soluble in readily removable solvent, i.e. dichloromethane or chloroform, and be insoluble in a second solvent which is immiscible with the first, i.e. water. For example, using toluene or ethyl acetate produced no useful spheres with polystyrene due to difficulty removing the solvent at room temperature. While heating can be used to aid in solvent removal, it has been shown to decrease encapsulation efficiency [7, 8]. For polyvinylchloride, Nylon 6/6, and polyurethane, no suitable solvent system could be found. However, this does not rule out the possibility that suitable microspheres could be made by one of the other methods reviewed. Polymer instability at room temperature ruled out PLGA. The presence of polymer decomposition products in the microsphere off-gases ruled out the use of PMMA as shell materials, while the evidence of TATP decomposition in the microspheres of PSf and PEI discouraged use of those polymers. After the above

exclusions, the acceptable polymers were polystyrene, poly-4-methylstyrene, and polycarbonate.

The purity of the evolved vapor released by the microspheres was confirmed by headspace analysis using GC/MS. Headspace was examined first and led to several changes to the microsphere production process. The headspace of PS microspheres was compared to that of a headspace vial that was crimped shut with nothing inside but air. This air sample control revealed background from the syringe and vial associated with the heating cycle used for the microspheres. Contaminants (Fig. 23) consisted of ethylbenzene, styrene, and tetramethylbutanedinitrile. As discussed in the experimental section, the source of the tetramethylbutanedinitrile was the PVA. A new source of PVA lacking the contaminant was found. The styrene and ethylbenzene were thought to be residual in the polystyrene. To remove these contaminants, “baking” of empty polystyrene microspheres was required (see experimental section). This approach successfully removed the remaining contaminant peaks from PS microspheres, but the process more than doubled the effort required to make the spheres.

<Figure 23>

In contrast to polystyrene, polycarbonate was devoid of contaminants in the normal headspace. Polycarbonate was considered a more desirable polymer than polystyrene because with little effort pure TATP vapor was achieved. Note that all microspheres were subject to gentle heating to remove DCM or any surface TATP. The TATP release temperature near 90°C was sufficiently high to allow bake off of contaminating solvents from the microspheres while not triggering the release of

TATP. Nearly all TATP was released from the PC-TATP by 170°C (Fig. 25) which was just below where TATP decomposition began between 170°C and 180°C.

<Figure 24>

<Figure 25>

As shown in Figure 25, once TATP released from the microspheres reached a maximum at a given temperature, the weight loss gradually declined. The trace (Fig. 25) of PC-TATP microspheres suggests that this release behavior can be manipulated. Heating to 90°C releases a certain amount of TATP, but the release slows considerably over an hour. A new rapid release can be obtained if the temperature is raised to 100°C. For the application desired, TATP generation, Figure 25 shows that the microspheres could be used serially. Sufficient TATP for training could be released at a given temperature and at a later time more TATP could be released by heating to a higher temperature.

Repeatability of the microcapsule loading was tested by comparing ten replicate batches of PS and PC microspheres. The results showed little difference in loading between PC and PS with slightly less loss in mass from the blank of polycarbonate. These microspheres were baked at 80°C for 24 hours; later GC/MS studies indicated 48 hours was required for complete removal of DCM.

<Table 3>

Using TGA-IR to check loadings of the microspheres shelf-stability was investigated. Samples were stored at room temperature after initial experiments revealed that TATP was retained in the microspheres until released by heating. Samples of polystyrene, polysulfone, and polycarbonate spheres were left at room

temperature for one to two years. The loss of TATP from the microspheres over time at room temperature was negligible as the data in Table 4 shows.

<Table 4>

The SSED and pipe tests showed similar results, with PC-TATP microspheres performing similarly to a blank. In the SSED test 1g of 12.9% by weight PC-TATP microspheres failed to damage the shell casing aside from opening a hole in the side. This damage was similar to that seen in an empty shell with only the detonator inside. The TATP test destroyed the shell walls and left only the primer base. This damage was characteristic of initiation of an energetic material. In the pipe tests the damage of the PC-TATP microspheres (14% by weight TATP) was similar to that of an identical pipe filled with sand. Pure TATP fragmented the pipe into several large pieces. Flame tests on both 12.9% and 14% TATP microspheres showed that they did not flash ignite or propagate a flame as pure TATP would. Microspheres with higher loadings, 19-20% TATP by weight, did propagate a small blue flame across the top of a line of microspheres that was ignited at one end by a propane torch. All microspheres loaded with TATP (14%-20%) would “pop” when held under the flame of a propane torch for 10-20 seconds. Under the flame the microspheres would melt and begin to char before the melted mass would burst open, making a loud popping noise. Microspheres with no TATP encapsulated did not exhibit the same behavior. It was supposed that this “pop” was TATP vapor building up in the molten plastic, then combusting to create the loud popping sound.

<Table 5>

The intended use of these microspheres was to provide the TATP scent to bomb sniffing canines without the hazard of working with bulk TATP. A prototype device was made for the release of the TATP from the microspheres for this purpose. The prototype used a resistive heater to heat the microspheres to about 150°C for a few seconds. This heating profile released most of the encapsulated TATP without decomposing it. The microspheres were placed in a 1 mL glass vial which was open at the top and which fit snugly into a larger glass vial that contained the heater. A small piece of aluminum wool was placed just inside the 1 mL vial which was joined at the top to another larger glass vial by means of a rubber septum. The released TATP was collected on a piece of aluminum wool which acted as a condenser for the TATP vapor. The heater was controlled by a variable autotransformer. The power was switched on for 3 minutes which brought the microspheres to about 150°C, then switched off; the whole setup was allowed to sit for further 3 minutes. The TATP could be seen deposited on the surface of the aluminum wool. The scent provided was easily detected by dogs from the local bomb squad that were imprinted the same morning on pure TATP vapor.

<Figure 26>

## **Conclusions**

TATP can be encapsulated inside a polymer matrix to increase handling and storage safety. Volatile solvents, i.e. DCM, can be removed without releasing significant amounts of TATP. This allowed for purification of the vapor signature of the microspheres, which is important for use in canine training. Polycarbonate was the

preferred polymer for encapsulation of TATP because it released TATP in the temperature range desired and was sufficiently pure for use from the manufacturer. SSED and pipe tests indicated that the microspheres were insensitive to shock at the scales tested. Flame tests of the microspheres showed significantly reduced sensitivity to flame over pure TATP; however, they were not completely insensitive to flame. Microspheres of TATP can be stored for long periods of time at room temperature, and the trapped TATP can be released with heating on demand. Encapsulating TATP significantly reduced the risks of handling and storing of TATP. Microspheres of TATP provide a way to supply TATP that is easy to handle and store to canine trainers and instrument manufacturers.

## **References**

- [1]- Oxley J, Smith J, Shinde K, Moran J. 2005. Determination of the Vapor Density of Triacetone Triperoxide (TATP) Using a Gas Chromatography Headspace Technique. *Propellants, Explos Pyrotech* 30:127–130.
- [2]- Li M, Rouaud O, Poncelet D. 2008. Microencapsulation by solvent evaporation: state of the art for process engineering approaches. *Int J Pharm* 363:26–39.
- [3]- Jyothi NVN, Prasanna PM, Sakarkar SN, et al. 2010. Microencapsulation techniques, factors influencing encapsulation efficiency. *J Microencapsul* 27:187–97.
- [4]- Madene A, Jacquot M, Scher J, Desobry S. 2006. Flavour encapsulation and controlled release - a review. *Int J Food Sci Technol* 41:1–21.

- [5]- Risch S. 1995. Encapsulation: overview of uses and techniques. ACS Symp Ser 2-7.
- [6]- Madan P. L. 1978. Methods of preparing microcapsules: mechanical methods. Pharm Technol 2:24-61.
- [7]- Freitas S, Merkle H, Gander B. 2005. Microencapsulation by solvent extraction/evaporation: reviewing the state of the art of microsphere preparation process technology. J Control release 102:313-332.
- [8]- O'Donnell P, McGinity J. 1997. Preparation of microspheres by the solvent evaporation technique. Adv Drug Deliv Rev 28:25-42.
- [9]- Poncelet D. 2002. Powder Research to Promote Competitive Manufacture of Added-Value Food Ingredients. 1-48.
- [10]- Saihi D, Vroman I, Giraud S, Bourbigot S. 2005. Microencapsulation of ammonium phosphate with a polyurethane shell part I: Coacervation technique. React Funct Polym 64:127-138.
- [11]- Lazko J, Popineau Y, Legrand J. 2004. Soy glycinin microcapsules by simple coacervation method. Colloids Surf B Biointerfaces 37:1-8.
- [12]- Saihi D, Vroman I, Giraud S, Bourbigot S. 2006. Microencapsulation of ammonium phosphate with a polyurethane shell. Part II. Interfacial polymerization technique. React Funct Polym 66:1118-1125.

[13]- Oxley J, Smith J, Rogers E, et al. 1999. Small-scale explosivity testing. *J Energ Mater* 17:331–343.

[14]- Oxley JC, Smith JL, Resende E. 2001. Determining explosivity part II: comparison of small-scale cartridge tests to actual pipe bombs. *J Forensic Sci* 46:1070–1075.

[15]- Oxley JC, Smith JL, Bowden PR, Rettinger RC. 2013. Factors Influencing Triacetone Triperoxide (TATP) and Diacetone Diperoxide (DADP) Formation: Part I. *Propellants, Explos Pyrotech* 38:244–254.

Table 1 – Baking and Purification Temperatures

Polymer	Bake (°C)	Purification (°C)
Poly(4-methylstyrene) (P4MS)	60	-
Polymethylmethacrylate (PMMA)	60	-
Polystyrene (PS)	80	150
Polycarbonate (PC)	80	-
Polysulfone (PSf)	120	-
Polyetherimide (PEI)	120	-

Table 2 – Overall Results

Polymer	Tg 20°C/min (°C)	TATP Start Loss 2°C/min (°C)	TATP Max Loss 2°C/min (°C)	TATP Max Loss 20°C/min (°C)	DSC Max Endotherm 20°C/min (°C) TATP	DSC Max Exotherm 20°C/min (°C) TATP	DSC Max Endotherm 20°C/min (°C) DADP	DSC Max Exotherm 20°C/min (°C) DADP	DADP Start Loss 2°C/min (°C)	DADP Max Loss 2°C/min (°C)	Polymer Decomp (°C)	Release Type
Triacetoneperoxide (TATP)	-	-	-	-	98	238	-	-	-	-	-	-
Diacetoneperoxide (DADP)	-	-	-	-	-	-	133	253	-	-	-	-
Poly(DL-lactide-co-glycolide) (PLGA)	45-50*	~46, 60	-	-	-	-	-	-	-	-	-	A**
Polyethylmethacrylate (PEM)	63*	65	142	-	-	-	-	-	-	-	-	B
Poly (vinyl butyral-co-vinyl alcohol-co-vinyl acetate) (PVBVAVA)	64	77	93	102	89	-	-	-	-	-	-	A
Poly(4-methyl styrene) (P4MS)	104*	75	~124, 190	-	-	-	-	-	-	-	-	A
Polyethylmethacrylate (PMMA)	105*	77	154	-	-	-	-	-	-	-	-	B
Polystyrene (PS)	109	77	152	163	63	231	-	-	-	-	443*	A
Polycarbonate (PC)	148	88	135	168	87	-	132	-	103, 134	160	480-485*	A
Poly sulfone (PSf)	190	139	167	183	93	184	-	-	149	197	530-535*	C
Polyetherimide (PEI)	220	140	195	197	93	199	-	-	-	-	-	C

\* Literature Value

\*\* Polymer Decomposes at Room Temperature

Table 3 – Encapsulation Repeatability

All samples baked at 80°C for 24 hours		
Sample	% TATP	Std Dev
Polystyrene	19.1	1.0
Polycarbonate	19.2	2.0
Blanks	% Mass Lost	Std Dev
Blank PS	0.25	0.04
Blank PC	0.17	0.008

Table 4 – Storage Stability

Polymer	% TATP Initial	238 Days	322 Days	432 Days	446 Days	771 Days	873 Days
Polystyrene	16.0	-	-	15.8	-	-	15.9
Polysulfone	19.7	-	19.6	-	-	19.6	-
Polycarbonate	25.7		-	-	25.5	-	-

Table 5 – Sensitivity Tests

	TATP	PC-TATP (13-14%)
Flame	Flash burn	If flame held on it, will "pop"
SSED	Violence similar to TNT	Did not initiate
Pipe Tests	Fragmented the pipe	Damage similar to sand

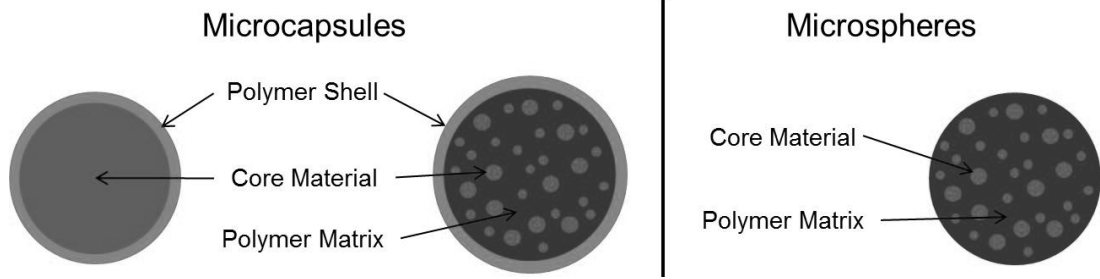


Fig. 1 - Microcapsules and microspheres

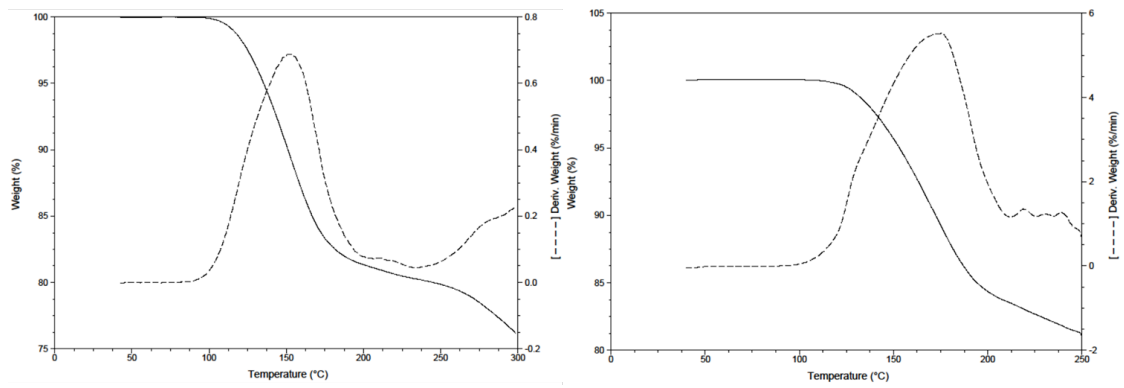


Fig. 2 - TGA of PS-TATP microspheres trace (solid); TGA derivative (dotted line); at 2<sup>o</sup>/min (left) & 20<sup>o</sup>/min (right)

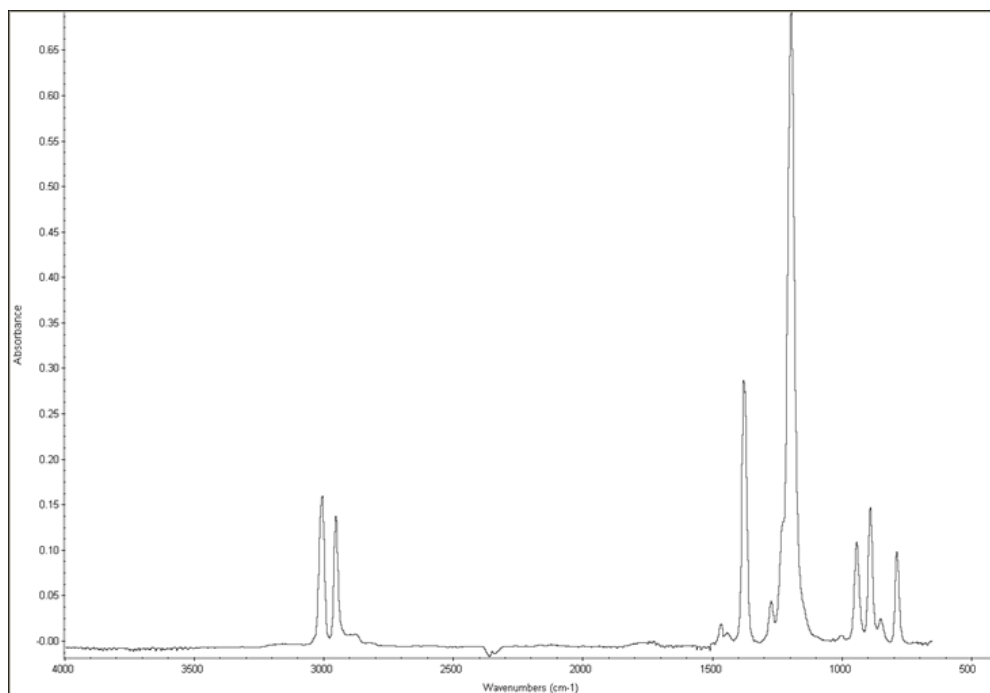


Fig. 3 – IR spectra corresponding to peak release in Fig. 2

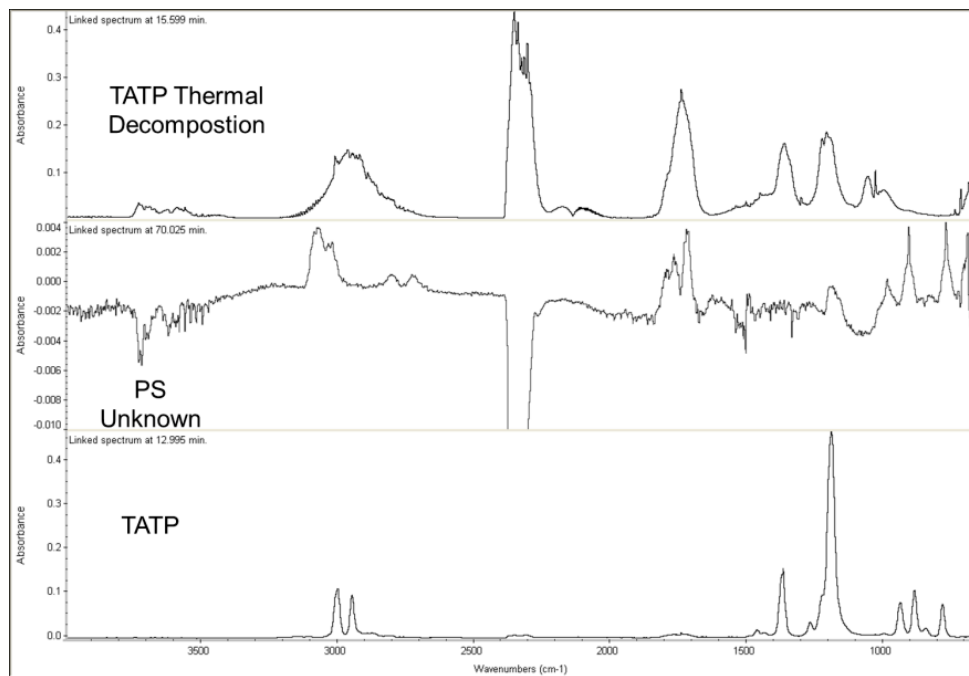


Fig. 4 – Comparison of PS unknown (middle) IR to pure TATP (bottom) & TATP decomposition (top)

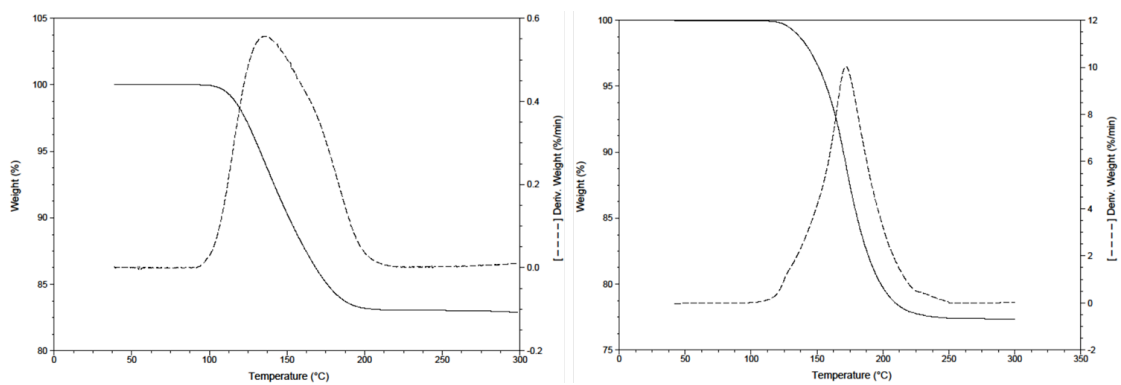


Fig. 5 - TGA of PC-TATP microspheres trace (solid); TGA derivative (dotted line); at 2°/min (left) & 20°/min (right)

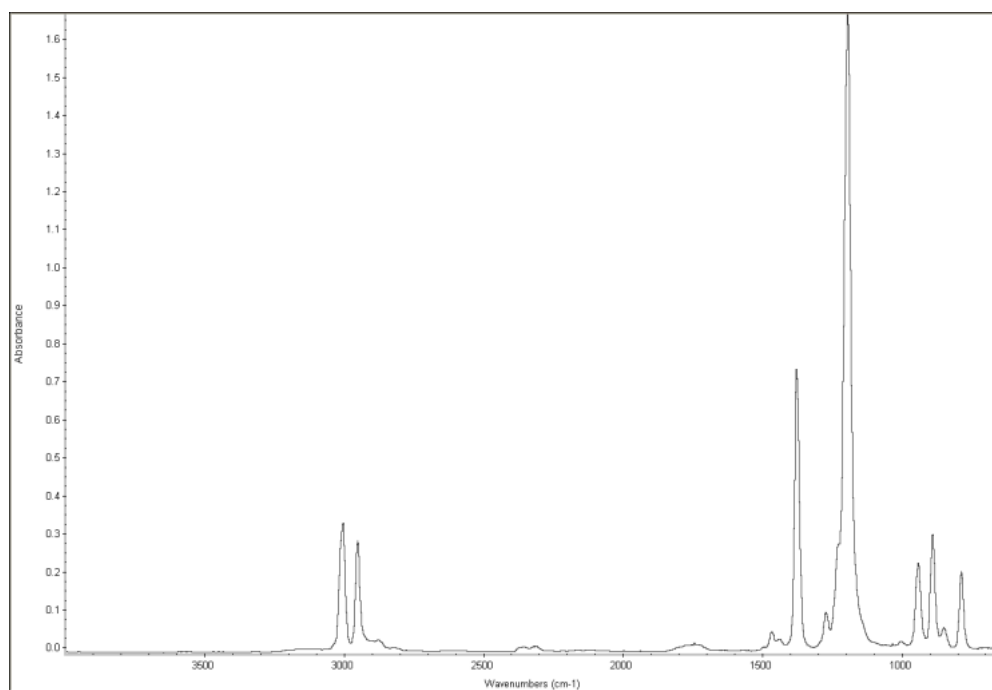


Fig. 6 - IR spectra of TATP from PC microspheres

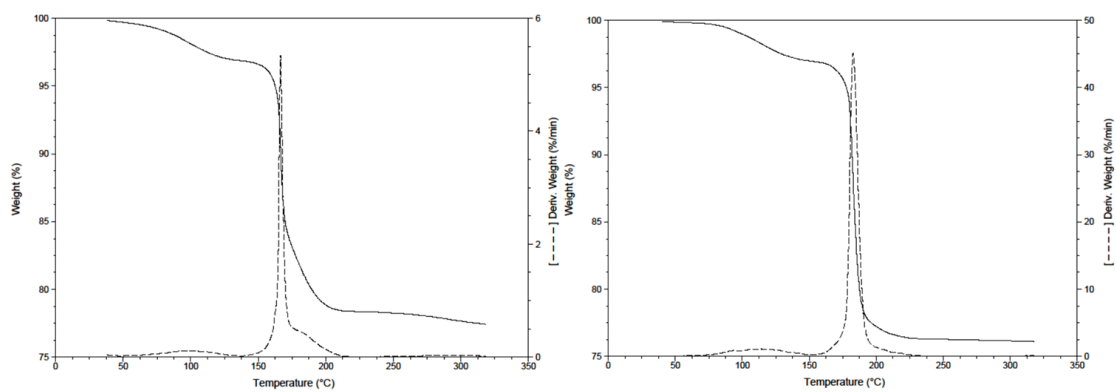


Fig. 7 – TGA of PSf-TATP microspheres trace (solid); TGA derivative (dotted line); at 2<sup>o</sup>/min (left) & 20<sup>o</sup>/min (right)

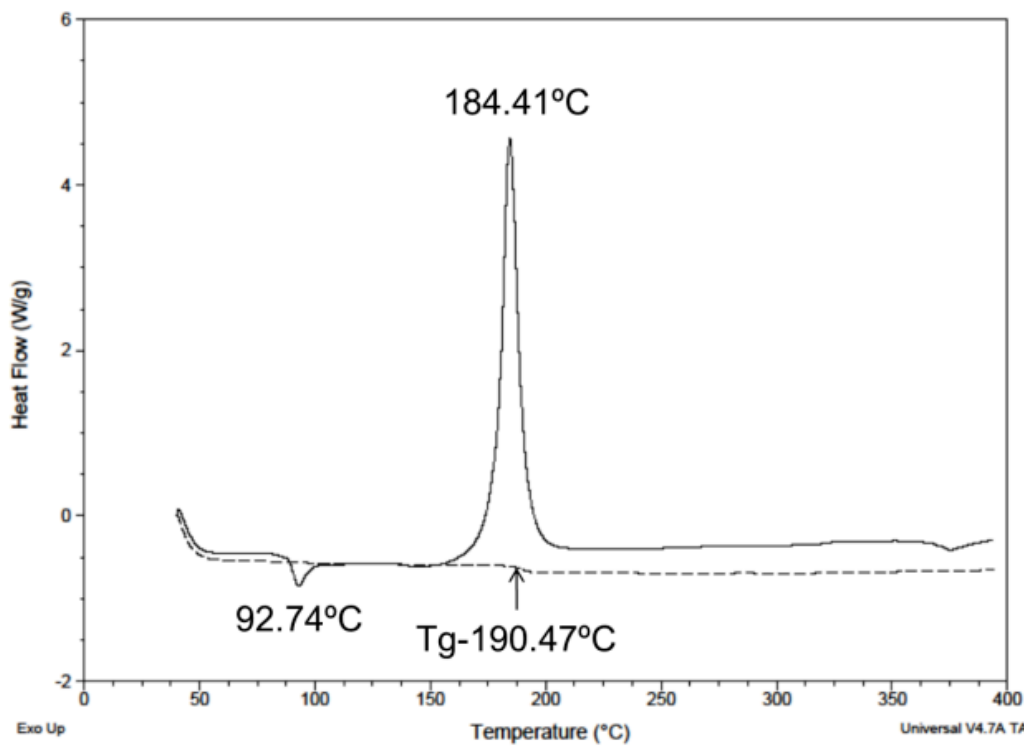


Fig. 8 - DSC of PSf: TATP microspheres (solid line), Tg (dotted line)

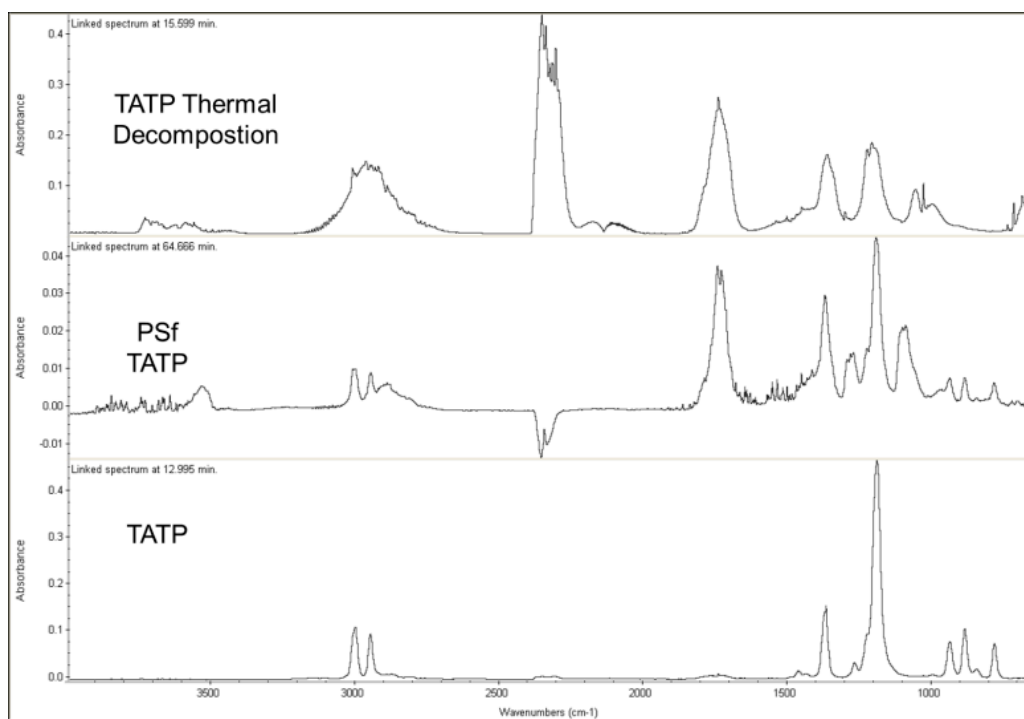


Fig. 9 - Comparison of PSf-TATP (middle) IR to pure TATP (bottom) & TATP decomposition (top)

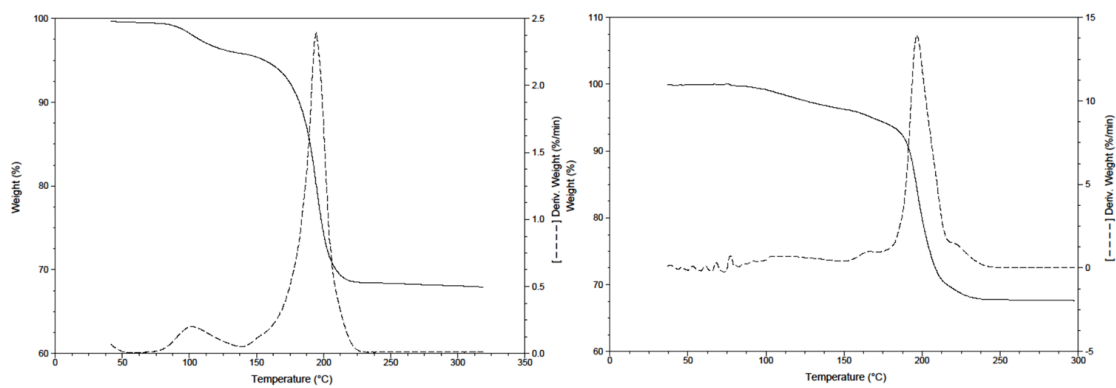


Fig. 10 - TGA of PEI-TATP microspheres trace (solid); TGA derivative (dotted line); at 2<sup>o</sup>/min (left) & 20<sup>o</sup>/min (right)

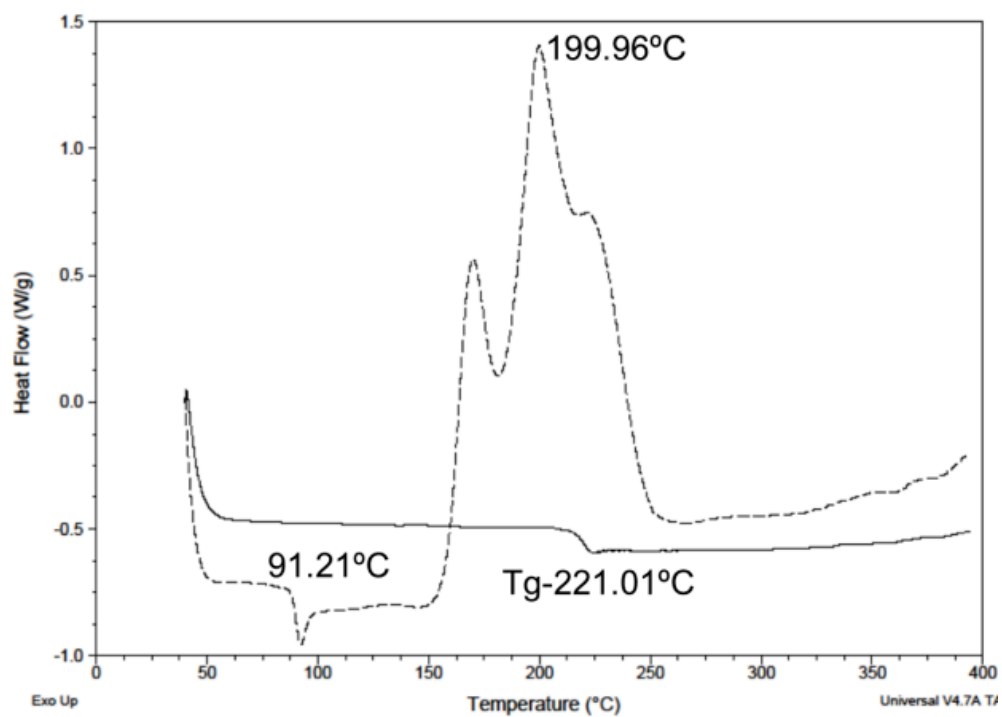


Fig. 11 - DSC of PEI: TATP microspheres (solid line), Tg (dotted line)

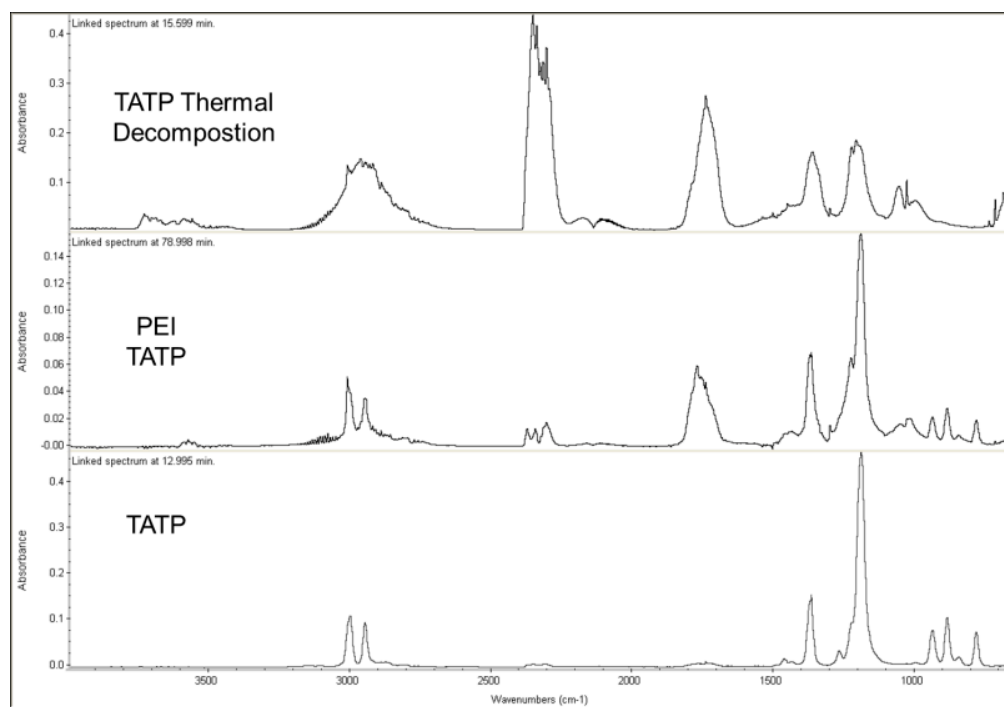


Fig. 12- Comparison of PEI-TATP (middle) IR to pure TATP (bottom) & TATP decomposition (top)

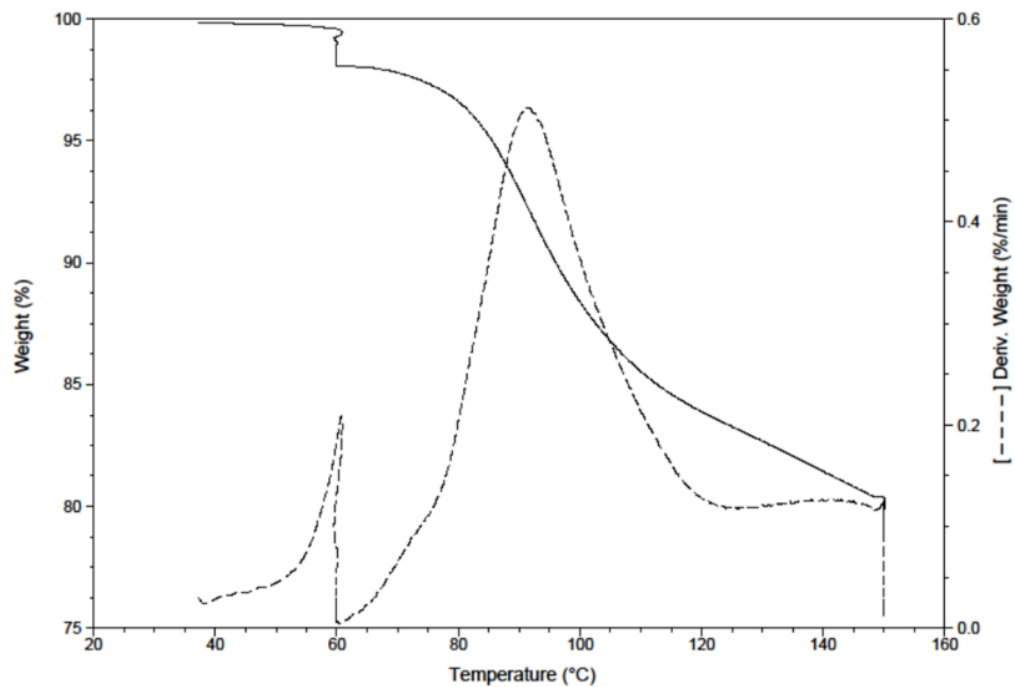


Fig. 13 - TGA of PLGA-TATP microspheres trace (solid); TGA derivative (dotted line); at 2°/min (left)

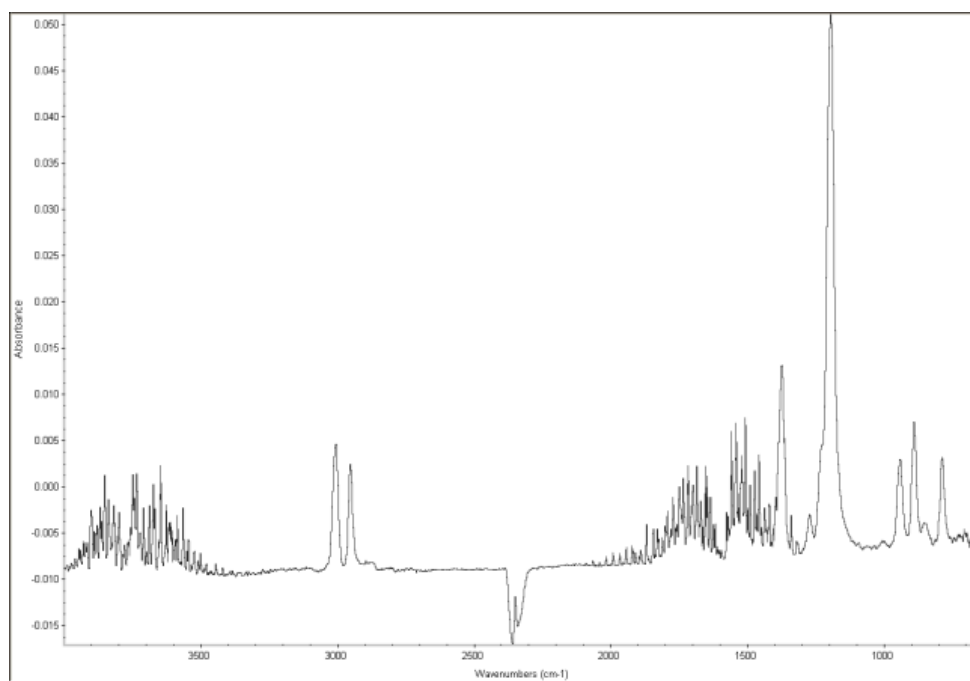


Fig. 14 - IR spectra of TATP from PLGA microspheres

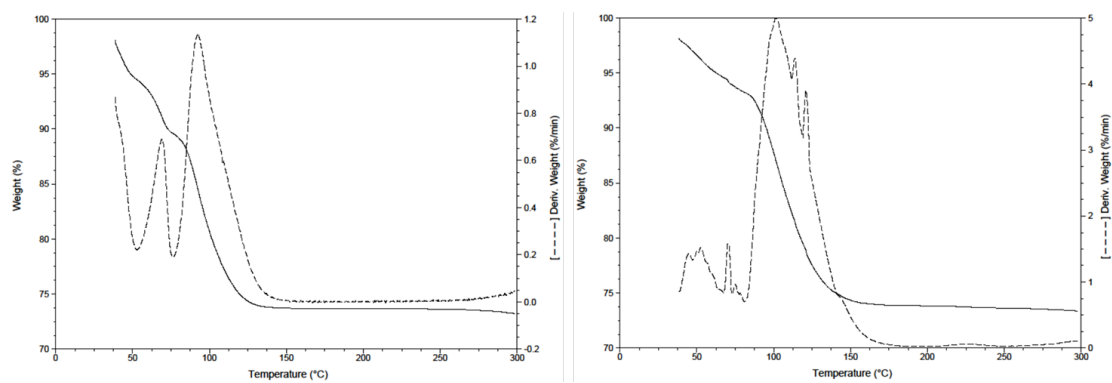


Fig. 15 - TGA of PVBVAVA-TATP microspheres trace (solid); TGA derivative (dotted line); at 2°/min (left) & 20°/min (right)

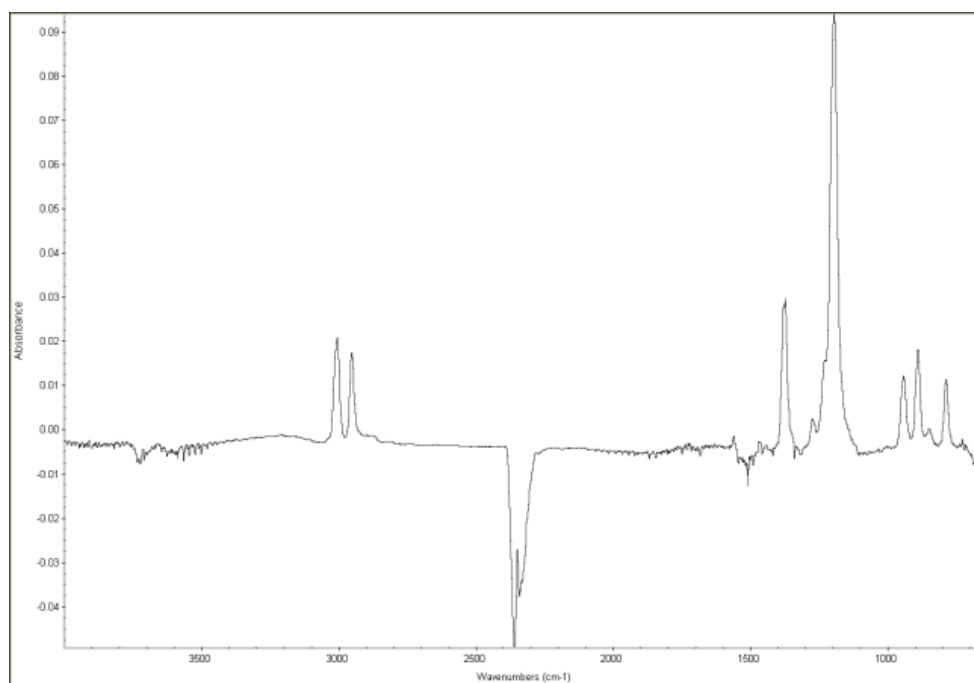


Fig. 16 - IR spectra of TATP from PVBVVA microspheres

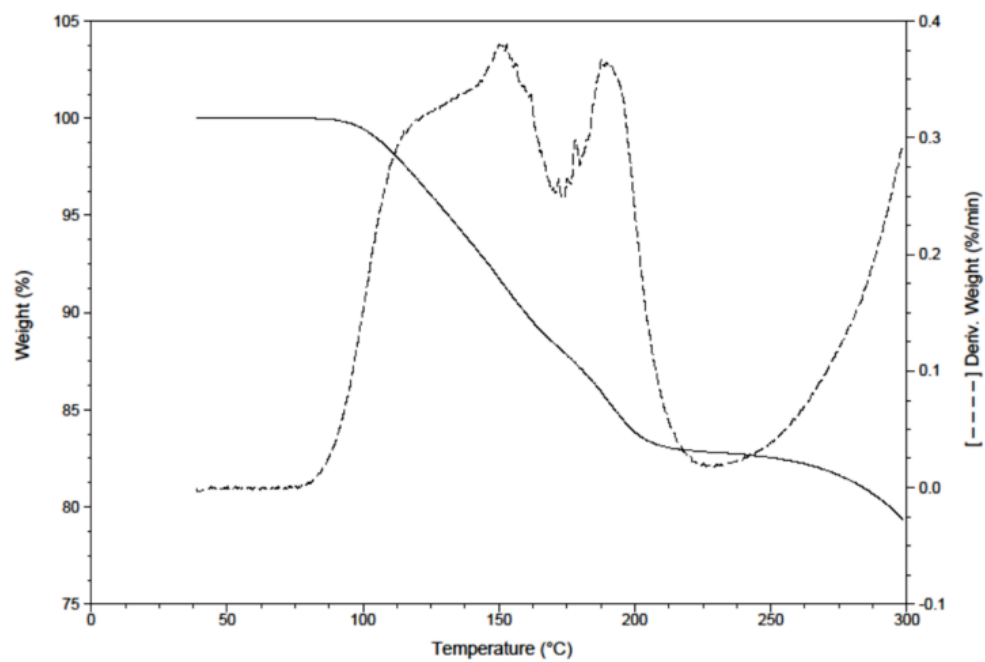


Fig. 17 - TGA of P4MS-TATP microspheres trace (solid); TGA derivative (dotted line); at 2°/min

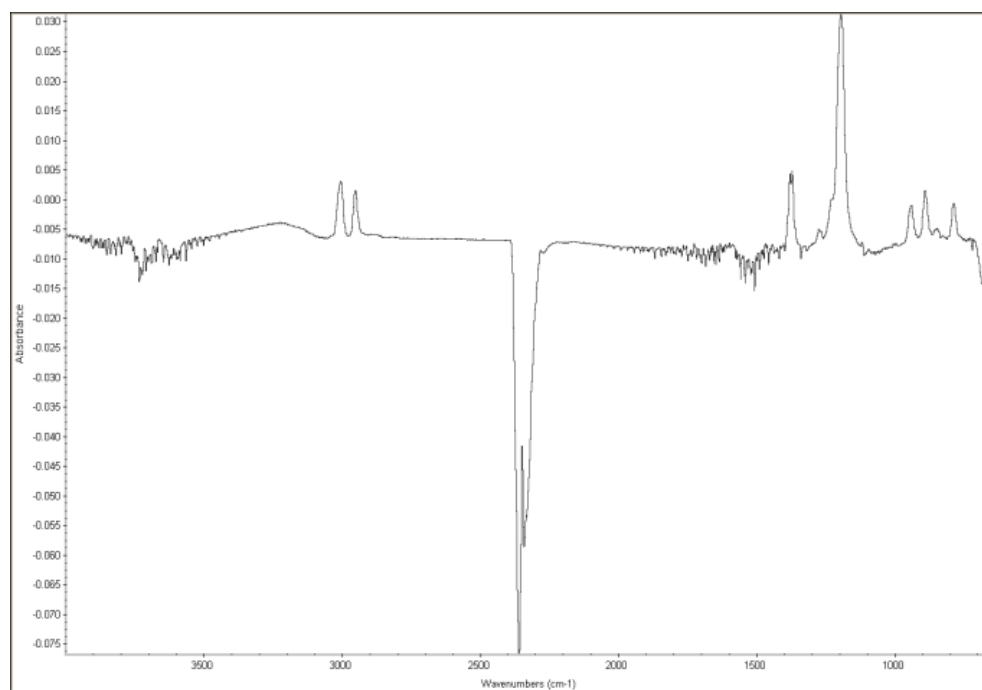


Fig. 18 - IR spectra of TATP from P4MS microspheres

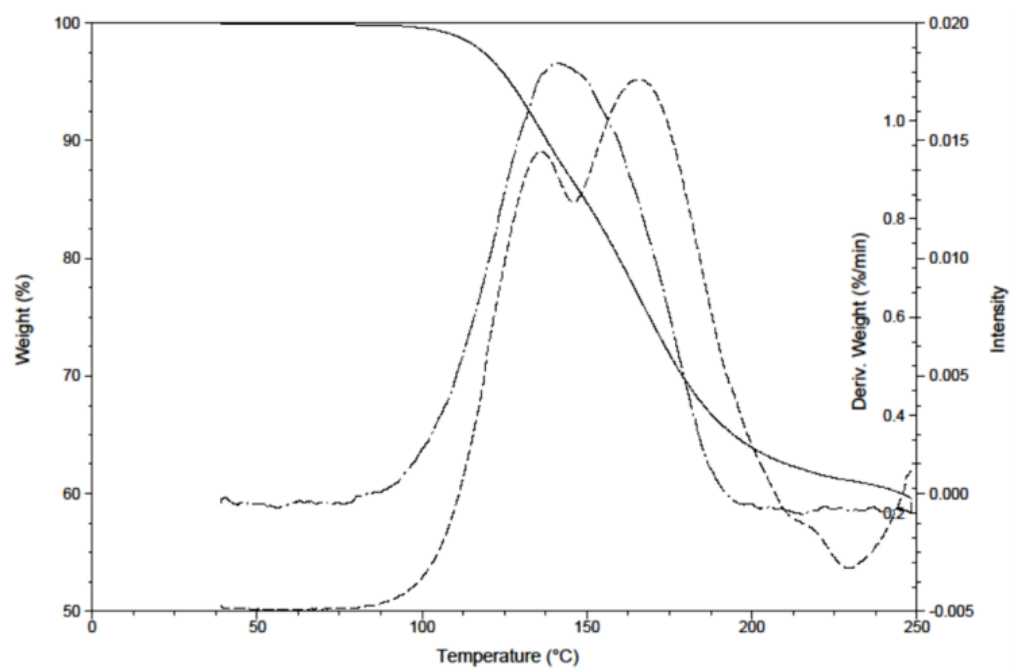


Fig. 19 - TGA of PEM-TATP microspheres trace (solid); TGA derivative (dash line); 895cm<sup>-1</sup> IR signal (dot-dash line); at 2°/min

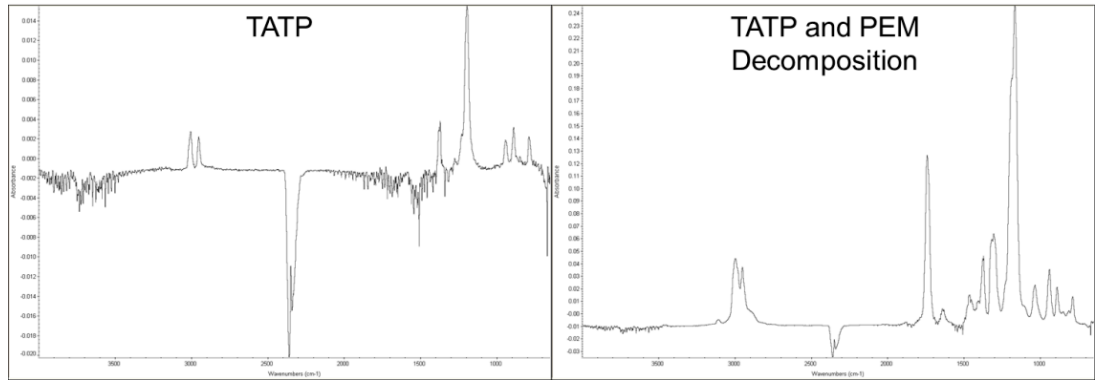


Fig. 20 - IR spectra of TATP from PEM microspheres (right); Mix of PEM decomposition and TATP (left)

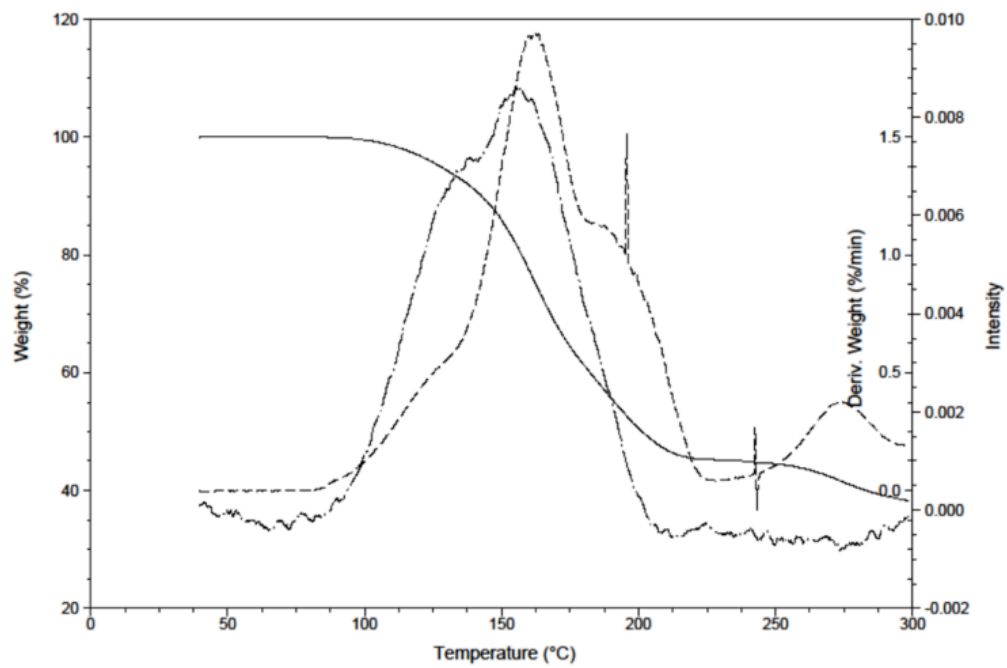


Fig. 21 - TGA of PMMA-TATP microspheres trace (solid); TGA derivative (dash line); 889cm<sup>-1</sup> IR signal (dot-dash line); at 2°/min

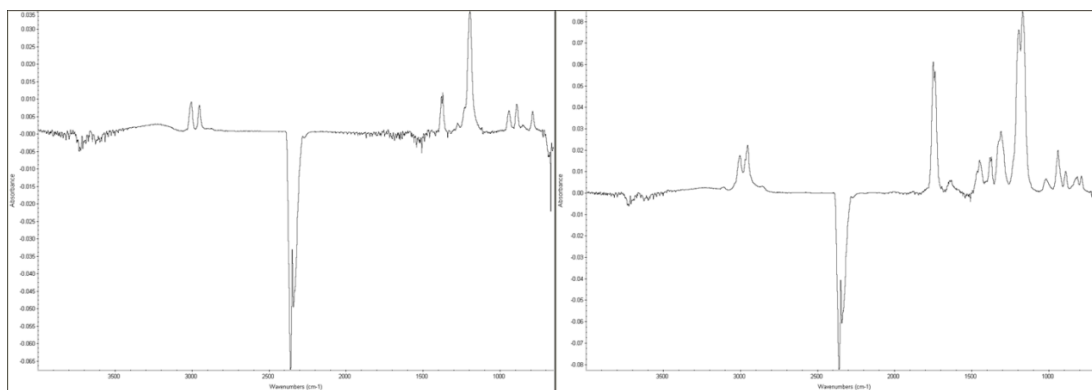


Fig. 22 - IR spectra of TATP from PMMA microspheres (right); Mix of PMMA decomposition and TATP (left)

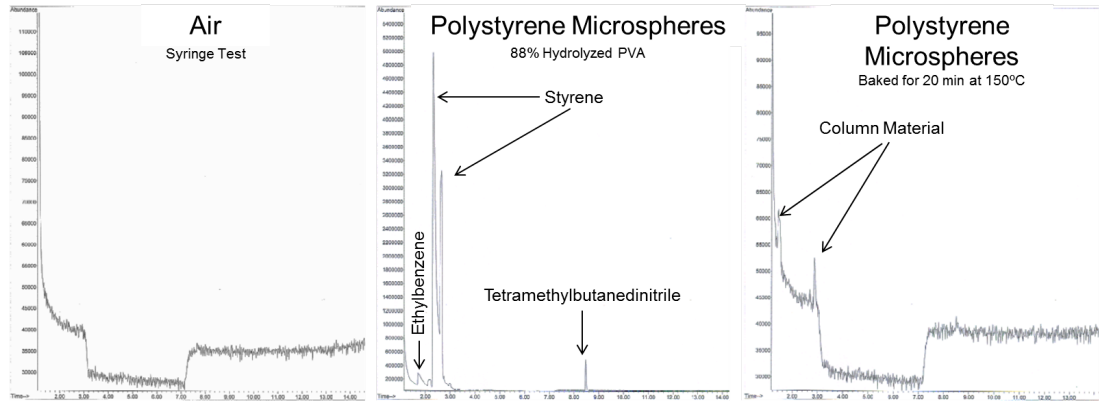


Fig. 23 – Blank vs. early polystyrene microspheres vs. PS microspheres after changing PVA and baking for 20 minutes at 150°C

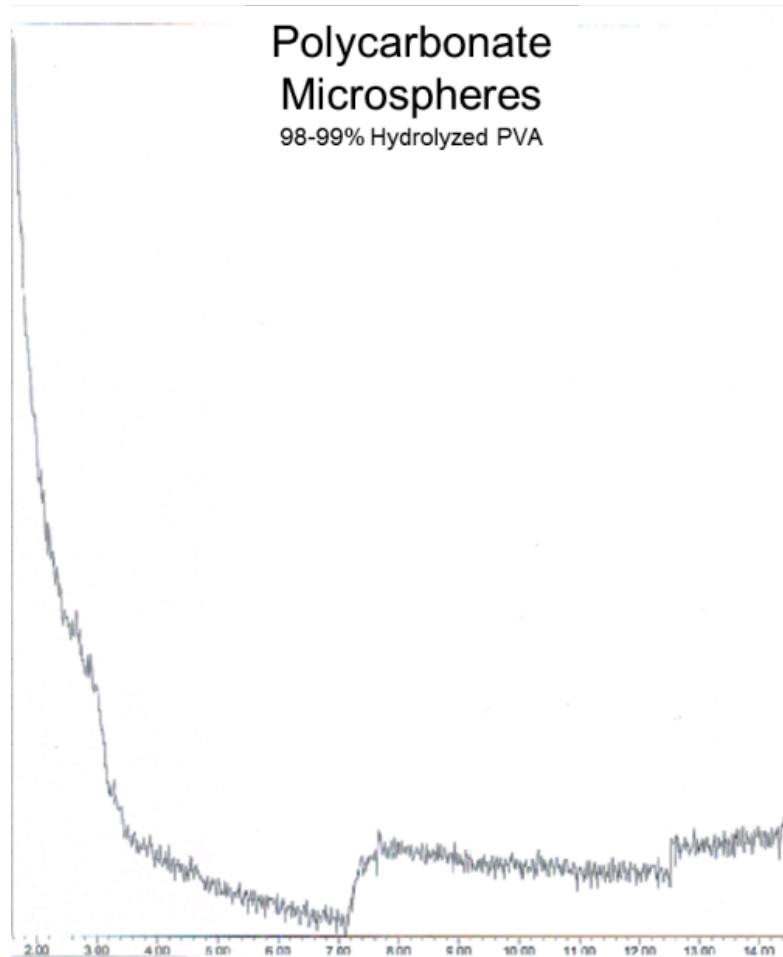


Fig. 24 – Polycarbonate microspheres after baking

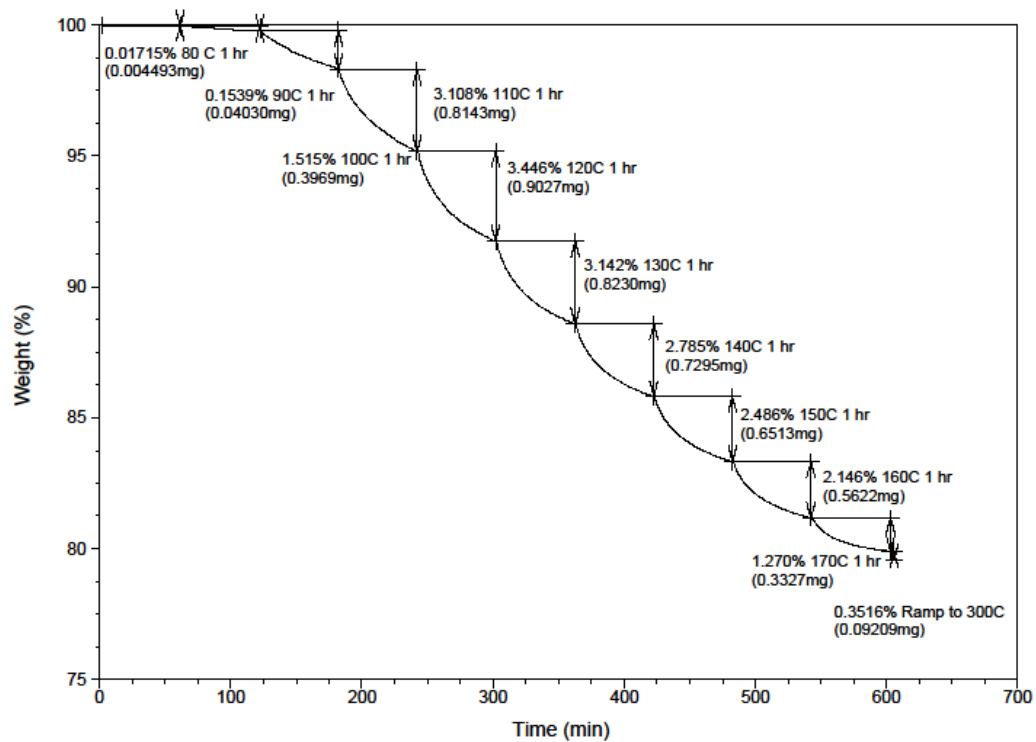


Fig. 25 – Release profile of TATP from polycarbonate

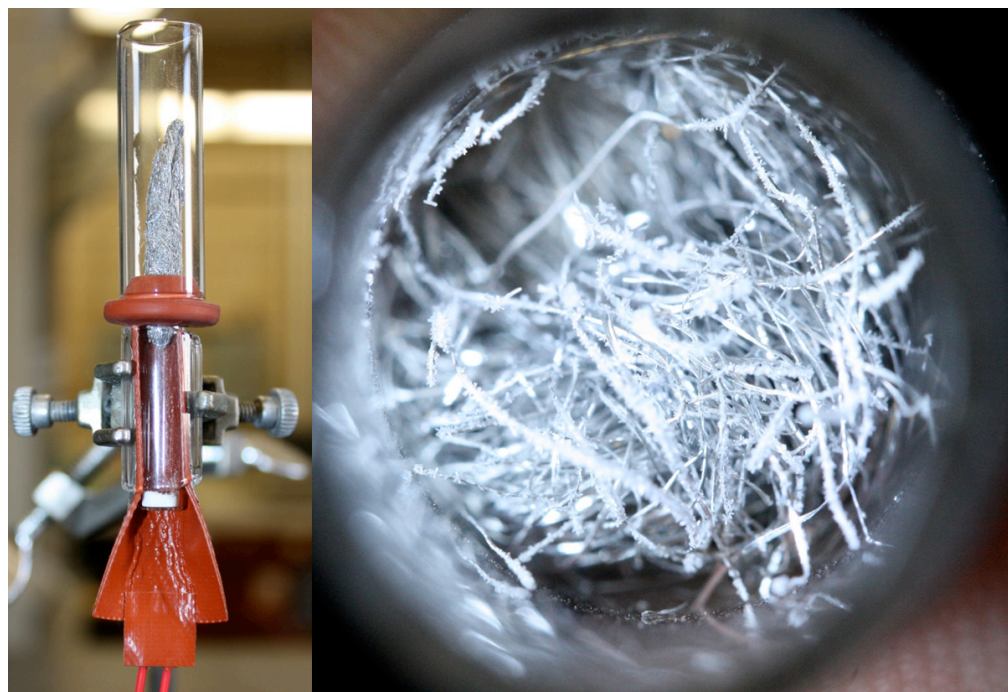


Fig. 26 - Prototype microspherule heater (right); TATP crystals deposited on aluminum wool (left)

## CHAPTER 2

Investigation of Molecularly Imprinted Polymers with Trinitrotoluene

Authors:

Oxley, J. C. University of Rhode Island\*, Smith, J. L. University of Rhode Island,

Canino, J. N. University of Rhode Island

Corresponding Author\*:

Professor Jimmie Oxley

Pastore Hall, URI

51 Lower College Rd.

Kingston, RI 02881

Email: [joxley@chm.uri.edu](mailto:joxley@chm.uri.edu)

Phone: 401-874-2103

Fax: 401-874-5072

Manuscript in process

## **Abstract**

Molecularly imprinted polymers (MIPs) have potential applications to the field of trace explosives detection. Imprinting conditions from the literature were replicated with variable success. Review of literature addressing explosives imprinting was sparse leaving pertinent mechanistic questions unanswered. Some novel imprinting experiments alongside NMR studies were performed to provide insight into the mechanism of explosive imprinting.

## **Introduction**

Molecularly imprinted polymers (MIPs) are copolymer systems designed to bind specific analytes, akin to a man-made antibody. Specific binding sites are created by coordinating the target analyte (termed “template”) to a functional group on a monomer (termed “functional monomer”). Once the functional monomer and the template are bound or coordinated in solution, the monomer is polymerized using a second monomer (“structural monomer”) to bridge between functional monomers. The template is extracted, leaving a binding site tailored to the template.

<Figure 1>

Molecular imprinting was pioneered in the early 1970’s by Gunther Wulfe [1]. That work and a majority of the research in the field since then centered on imprinting biological molecules. Early work used covalent bonding between the template and functional monomer to create binding sites. Later work by Klaus Mosbach used non-covalent attractions to create binding sites [2]. Non-covalent imprinting appears to be the more popular approach; one source estimates that 90% of MIP publications use

non-covalent approach [3]. The authors credit this prevalence to the simpler synthetic routes, a closer mimicry of the natural processes of selective molecule formation, and a broader range of monomers and template molecules. The broad range of monomers and templates can be attributed to the ubiquity of non-covalent interactions. Most functional groups are susceptible to non-covalent interactions and this type of imprinting merely exploits these interactions.

There are two major obstacles to creating MIPs: finding the correct ratio template: functional monomer: structural monomer and template removal after imprinting is complete. If the ratio of component monomers is not correct, imprinting will fail. Even after successful imprinting, if the polymer lacks rigidity, removal of the template can cause binding site collapse or distortion and prevent function. Conversely, if the polymer has high rigidity, diffusion will be poor and template removal difficult, rendering the binding site unusable. Even in successful MIPs removal can be partially complete [3]. This latter situation is important for analytical applications as MIPs designed to pick up and release targeted analytes into a detector can act as a source of background contamination by continuous release of low levels of template.

Success or failure of imprinting is traditionally measured by binding or uptake experiments. A MIP with template removed is allowed to equilibrate in solution containing known concentration of template. After various time intervals, the concentration of template remaining in the solution is measured. The amount of template lost from solution is a measure of binding strength between MIP and template. A successful MIP should bind more template than a control polymer made

under identical conditions without template. Furthermore, the MIP should be sufficiently selective as to not bind molecules of similar functionality. For example, an MIP designed to bind 2,4,6-trinitrotoluene (TNT) should not also bind 2,4-dinitrotoluene (2,4-DNT).

A comprehensive review of the literature for MIPs, both in general and with respect to explosives, is summarized in Supporting Information 1. Resulting from this review we conclude as follows:

1. Only a few functional monomers were used for explosives applications: methacrylic acid (MAA), acrylamide (AA), methacrylamide (MAM), phenyltrimethoxysilane (PTMS), aminopropyl-trimethoxysilane (APTES), bisaniline, and 2-(trimethoxysilylethyl)pyridine (TMSE-Pyr).
2. Of functional polymers mentioned in 1, only three were used by more than one author: MAA (six authors [8, 14, 15, 16, 17, 18]), AA (5 authors [8, 19, 20, 21, 22]), and APTES (two authors [5, 6]).
3. Only 2 out of 15 authors [20, 23] imprinted a template other than TNT or DNT.
4. Most work done in the field was with the MAA and TNT system with the goal of developing a novel sensor through surface plasmon resonance [21, 23], cyclic voltammetry [15, 24], or fluorescence quenching [18]. Each author, therefore, used different analytical techniques to measure success. This made comparison of imprinting effectiveness across authors ambiguous. In addition, some authors [7] demonstrated interest in desorption efficiency rather than the sorption efficiency of the polymers.

MIPs are particularly relevant to the field of explosives detection. Many instruments cannot detect explosive vapor due to the low vapor pressures involved [4]. A way to selectively pre-concentrate explosive vapors from a shipping container or a room may dramatically improve the ability of current instruments to detect trace amounts of explosive vapors. In addition, possibilities for novel explosive detection techniques utilizing MIPs are wide-ranging.

## **Experimental Section**

*MIP Syntheses:* Preliminary imprinting work was done following the work of Ellen Holthoff [5]. The functional monomer was aminopropyltriethoxysilane (APTES) and the structural monomer was methyltriethoxysilane (C1 TriEOS). These along with 1M hydrochloric acid were mixed and stirred. A solution of TNT was added and the whole mixture vortexed for 30 seconds. The resulting red solution was then spin-coated onto surfaceenhanced Raman spectroscopy substrates. Later, a similar formulation, as outlined in the work of Xie, was tested [6]. The only major differences were the ratio of reactants, the use of sodium acetate as the catalyst rather than hydrochloric acid, and the use of various substrates instead of spin-coating. In early formulations, the MIP was coated on various substrates: glass wool, sand, silica gel, and steel wool. While the coating was eventually successful on glass and steel wool, the synthesis was changed to bulk, also called block, polymerization to allow easier template extraction and analysis.

<Figure 2>

Synthesis of the APTES MIPs varied with the different monomer and solvent ratios, but the basic synthetic procedure was similar (see Supplement 2). The APTES, TNT or 2,4-DNT, and C1-TriEOS were vortexed in a vial for 5 to 10 minutes, with an excess of ethanol if the polymer was to be used as a coating but with minimal ethanol for block polymers. Catalyst, usually hydrochloric acid, was added and mixed by vortexing. The resulting solution was either dripped onto the substrate to be coated or left in the vial to form a block polymer. Samples were allowed to cure for 3 days at room temperature or left in an oven at 40°C overnight, due to time concerns. Block polymers were ground into a powder using a pill crusher before extraction.

Synthesis conditions for phenyltrimethoxysilane (PTMS), trimethoxytrifluoropropyl-silane (TMOTFS), and triethoxythienylsilane (TEOTES) were similar. Tetraethoxysilane (TEOS) was used as a structural monomer for all three. PTMS was selected based on the work of Lordel et al. [7]. TMOTFS was selected because of its use as a stationary phase in chromatography of explosives and TEOTES was also a good medium for explosives.

Solid TNT or hexahydro-1,3,5-trinitro-1,3,5-triazine (RDX) was weighed into a test tube; the monomers were added by syringe in the appropriate ratios along with a stir bar. Initially minimal solvent (1 mL of acetonitrile and isopropanol or methanol) was added to dissolve the explosive. The reaction was then mixed by vortexing. The ammonium hydroxide catalyst was then added by syringe and mixed again by vortexing. The homogeneous mixture was put in a water bath at 60°C with magnetic stirring. It was later discovered that the Meisenheimer complex of TNT which formed on the addition of the ammonium hydroxide was miscible in the monomers after

sufficient reaction time, so vortex mixing was not required or helpful. Thereafter, the test tube with only the monomers, catalyst, and TNT was placed in a 60°C water bath with magnetic stirring. In either case the sol gel was allowed to cure until hardened. This was usually overnight but could take up to a week under some reaction conditions. Initial reactions were allowed to react at room temperature, but reaction times were unacceptably long. Once samples were determined to be solid by visual inspection and probing with a spatula, they were removed from the bath and placed in an oven overnight at 120°C. Controls and MIPs were baked separately, and the oven was purged for an hour at 350°C to ensure that controls were not exposed to TNT vapor. The block polymers were then ground into a powder with a pill crusher before extraction.

Some PTMS based MIPs were instead coated onto steel wool. To do this the above procedure was changed to allow for dip coating of steel wool. To each reaction test tube 3 mL of methanol and acetonitrile were added before the ammonium hydroxide catalyst. After addition of the catalyst, the reaction was mixed using vortexing. A pre-weighed sample of steel wool, sometimes pre-treated with a UV ozone generator, was then submerged in the now homogenous reaction solution for 30 minutes. The wool was then removed and placed into a metal tin in a dark room to cure for several weeks. The coating appeared to cure completely; however, pooling of the coating towards the bottom of the wool and on the surface of the tin indicated faster curing was necessary for uniform coating on the surface of the wool.

The most successful imprinting followed the work of Bunte [8]. A magnetic stir bar and 120 mL of polyvinyl alcohol (PVA, 31,000-50,000 molecular weight)

were added to a 3-necked round bottom flask which was heated in a water bath to 60°C with magnetic stirring. The atmosphere in the flask was then purged with nitrogen for 1.5 hours, while a chloroform solution (25 mL) of 9.91 g of ethylene glycol dimethacrylate (EGDMA), 0.69 g of methacrylic acid (MAA), 200 mg of azobisisobutyronitrile (AIBN), and 454 mg of TNT was added by syringe to the stirring PVA solution. The reaction was allowed to proceed for 24 hours before the reaction solution was added to ~500 mL of water to aid with filtration. The copolymer was then collected using vacuum filtration.

A number of approaches were used to remove template molecules. Initially, for PTMS, TMOTFS, and TEOTES polymers, Soxhlet extraction was used with acetone, acetonitrile, or methanol for times ranging from a few hours to overnight. Later, it was discovered that solvent rinsing using vacuum filtration and alternating solvents was faster and more effective. Progress of extraction could be judged visually by coloration of the polymer and extraction solvent. With template removal the dark red-brown color of the polymer faded to a whitish-grey. The extraction was judged complete when the solvent remained clear to the eye after rinsing. Solvents used for the rinsing step of each reaction can be found in Supporting Information 2; in general acetone, methanol, and acetonitrile were judged best. The successful extraction was then confirmed with an Agilent 8453 UV-Visible spectrometer (UV-Vis); this was especially important when the template was RDX which imparted no color to the polymer. If the rinse solution of 90% water:10% methanol passed through the polymer and appeared clean by UV-Vis, then template was considered fully extracted. For APTES MIPs various extraction procedures were attempted: 1) that

used by Holthoff [5] which soaked the MIP in a solution of ethanol, acetonitrile, and acetic acid (8:2:1) from 1 hour to 13 days; 2) refluxing in the same solution; 3) Soxhlet extraction with methanol, acetone, or acetonitrile; or 4) solvent rinsing using vacuum filtration with the Holthoff extraction solution, cyclohexane, hexane, dichloromethane, acetone, acetonitrile, and methanol. MAA MIPs and control were Soxhlet extracted overnight with chloroform.

***Evaluation of MIP Performance:*** We attempted to assess analyte pickup by placing MIPs in a solution containing a known amount of the analyte (TNT or 2,4-DNT). See experiments 1 to 34 in Supporting Information 2. The MIP solutions were shaken for 1 to 24 hours and examined using an Agilent 7890 gas chromatograph with a micro-electron capture detector (GC- $\mu$ ECD) for loss of the analyte. Analyte loss (uptake) was not observed for any MIP solutions. Sometimes an increase in TNT or 2,4-DNT was observed instead of a decrease. This increase in template concentration was attributed to the template's greater affinity for the solvents used than the MIP binding sites.

The success of imprinting was judged by sorption experiments using UV-Vis. A solvent system of 90% water:10% methanol was adopted for the UV-Vis experiments to prevent the problems with competing solvent and MIP affinity from the GC experiments. This system couldn't be used on the GC- $\mu$ ECD as it would damage the detector. For the UV-Vis experiments, 15(+/-0.2)mg of extracted sample was weighed out and added to a disposable 5mL plastic syringe with a 0.2 $\mu$ m syringe filter attached. About 3mL of acetonitrile was added to the syringe, pushed through

the sample, and collected in a quartz cuvette. The acetonitrile was checked by UV-Vis (water blank) to see if residual solvent or TNT was present. If the signal was above baseline, then the process was repeated until the signal matched that of clean acetonitrile. Next ~3mL of 90:10 water:methanol was pushed through the syringe to rinse out the acetonitrile. This was also checked by UV-Vis and repeated until no baseline variation was observed. Then 3mL of a TNT solution of known concentration (15  $\mu\text{g}/\text{mL}$  TNT in 90:10 water:methanol) was pushed through the syringe. This solution was collected and analyzed by UV-Vis to determine decrease in TNT concentration by comparison with the standard TNT solution. Quantification was completed by comparison with calibration curves. The procedure was repeated starting with the acetonitrile rinses as above to remove the bound TNT. Four additional replicates were obtained using the same 15 mg sample. Alongside these tests were tests of uptake from separate MIP samples. In these experiments the procedure was the same except the samples were not cleaned and retested. Each sample was made using a new 15 mg aliquot of polymer. Similar experiments were done with RDX for RDX imprinted MIPs.

***Nuclear Magnetic Resonance (NMR) Experiments:*** TNT was dissolved into deuterated solvent [chloroform ( $\text{CDCl}_3$ ) for MAA, PTMS, TMOTFS, TEOTES; aniline and acetonitrile ( $\text{d}^3\text{-ACN}$ ) for APTES (due to an interaction of the monomer with chloroform)]. As molar equivalents of functional monomer (1 to 4  $\mu\text{L}$  depending on the monomer) were added via syringe,  $^1\text{H-NMR}$  chemical shifts of aromatic and aliphatic protons of TNT were noted. See Supporting Information 4. It was expected

that differences in positions of chemical shifts of the complexed and the uncomplexed TNT would be observed. However, since only a single chemical shift was observed for the aromatic and the aliphatic protons, the exchange between free and bound TNT must be fast on the NMR timescale, and the observed chemical shifts must be intermediate between those of the bound and unbound TNT. At higher monomer-to-TNT ratios, more TNT should be bound, and there would be a corresponding change in the chemical shift ( $\Delta\delta$ ).

## **Results and Discussion**

A summary of MIP performance in terms of percent TNT uptake by the MIP relative to the untemplated polymer (the control) are shown in Table 1. A comprehensive list of imprinting conditions and results can be found in Supporting Information 2 and 3, respectively. Table 1 clearly shows that the MIP using MAA was most effective, while some success was had with PTMS and TEOTES.

<Table 1>

MIPs made using APTES were unsuccessful with TNT. As TNT was added to the polymerization reaction, a red color appeared which suggested that APTES and TNT form a Meisenheimer complex. This red color was observed with other functional monomers, but in APTES the color remained despite extensive attempts to extract the TNT template. Additionally, unique to APTES was that the red Meisenheimer was observed after the addition of APTES with no additional base required. GC- $\mu$ ECD and UV-Vis experiments were done on the extracts and no TNT was observed. The inability to extract the template meant that if imprinting was

successful, no binding sites could be freed to allow uptake of TNT. Interestingly, when 2,4-DNT was used as the template with APTES, no red color was observed.

Extracting the TNT template from PTMS MIPs with alternating acetone, acetonitrile, and methanol rinses proved to be the most efficient way to remove most of the red coloration. With this functional monomer, most work focused on adjusting the ratios of template: functional monomer: structural monomer. The varied results from different ratios of PTMS MIP formulations showed that the correct ratio of components has a large effect on imprinting efficiency (Table 1). The 90:10 water:methanol solution used in the UV-Vis uptake experiments was selected to be close to the percolation solution used by Lordel [7]. The most successful ratio was 1:8:40, with a 227% improvement compared to the control. While these results show some increase in affinity for TNT, the increase in binding was not as high as desired. This MIP was designed by Lordel et al. as a solid phase extraction media, but their testing was primarily done as if it were a stationary phase, which made comparison of results difficult. The work of Lordel et al. [7] showed that PTMS polymers had great potential as stationary phases and as extraction media but did not directly measure initial binding capacity. Indeed, although both MIPs and controls in that work showed excellent binding of TNT during the percolation step, the difference was retention through the washing step. The excellent uptake by both MIP and control would have made the MIP a failure by our metrics, in which the MIP was required to uptake dramatically more analyte than the control.

Tests of PTMS and RDX MIPs showed no significant increase in pickup over the controls. The reason for this was unclear, but there are a few possible

explanations. Since no Meisenheimer complex (i.e. red color) formed when RDX was added to the polymerization reaction, it was difficult to judge extraction efficiency. Judging extraction efficiency by UV-Vis was also difficult due to weak UV absorbance by RDX. It was possible that the RDX template was not removed efficiently or that the template: structural monomer: functional monomer ratio was not optimal or that PTMS was not a good functional monomer for RDX. Indeed, control polymers using PTMS showed lower retention of RDX than of TNT, e.g. 0.48  $\mu\text{g}$  of RDX per mg of polymer versus 0.94  $\mu\text{g}$  of TNT per mg of polymer.

Two novel functional monomers were tested, TEOTES and TMOTFS, chosen because it was noted that they had good affinity for explosives. Only TEOTES showed promise for molecular imprinting, with 159% pickup compared to the control (Table 1). TMOTFS pickup was less than the control, but the difference was within the standard deviation. While the performance of either monomer might have been improved by changing the ratios used, neither pickup was sufficiently impressive to pursue at this time.

The most successful MIP used MAA, following the work of Bunte [8]. The reason for its success is unclear. Porogens have been shown to be important to successful imprinting; volatile solvent play the role of porogens increasing surface area of the MIPs [9]. Chloroform, a porogen, was the dispersed phase solvent for the MAA/EGDMA system and may contribute to a successful imprinting. Water can also function as a porogen. A few PTMS reactions [7, and experiments 58, 59, and 78-85, Supporting Information 2] used excess water; however, our experiments did not show any improved TNT binding ability by the PTMS MIPs made using excess water.

Ethanol has also previously been used as a porogen. In this work, it was added to the TEOTES reactions to slow suspected self-polymerization and encourage copolymerizing with TEOS.

Simple NMR titration experiments were performed to attempt to identify the best functional monomer and to probe its interaction with the analyte [10, 11]. The technique monitors chemical shift when aliquots of one component (the titrant) are added to a solution of the second component. Initially we attempted to add a solution of TNT to a solution of one of the functional monomers (MAA); however, the low solubility of TNT made the volume of titrant so large that dilution effects became significant. Instead, the monomer of interest was added to a solution of TNT. The change in chemical shift ( $\Delta\delta$ ) of the TNT protons, 2.7 ppm for the methyl protons and 8.9 ppm for the aliphatic protons, was monitored. We anticipated that maximum  $\Delta\delta$  would indicate optimal ratio of functional monomer to template.

<Figure 3>

MAA and TMOTFS titrations showed very little change over a 1 to 10 functional monomer to TNT ratio. The changes observed were not high enough to distinguish from noise or volume change effects. The results of the MAA and TMOTFS titrations were very similar. This was surprising considering MAA was the best and TMOTS almost the worst functional monomer (Table 1). Furthermore, the pickup of TNT by MAA was so successful (795%) that an observable  $\Delta\delta$  was expected. The successful MAA MIP used the 1:4:25 ratio so the largest  $\Delta\delta$  was expected around the 1:4 TNT:MAA point; instead it was around the 1:8 ratio. It was not expected that the titration of MAA and TMOTFS would lead to similar results.

Evidently the titration experiment was not probing the interactions of TNT as expected.

PTMS, aniline, and TEOTES had similar results in the titration experiments; all three had a linear change in chemical shift with increasing amounts of functional monomer. Experiments with PTMS showed that this linear increase continued up to a 200:1 ratio. It was supposed that this was a  $\pi$ -stacking interaction and that it would continue as concentration of the monomer increased effectively to infinity. This conflicted with the original theory that  $\pi$  electron acceptor-donor interactions between the  $\text{NO}_2$  and the monomer were the cause of imprinting. While this still could be true for non-aromatic explosives, no imprinting was ever witnessed using RDX. Controls for this consistently performed similar to or better than MIPs; it was not expected that coordination would be observed with RDX.

In an effort to eliminate some of the complexities of the NMR titration study, the titration of nitromethane with PTMS was performed. This appeared to be a good starting point because of the simple nature of the nitromethane molecule and the prevalence of the  $-\text{NO}_2$  functionality in explosives. The resulting plot of the  $\Delta\delta$  of the methyl protons on nitromethane appears very similar to that seen for the TNT protons.

## **Conclusions**

The earliest literature involving molecularly imprinted polymers appeared in the 1970s. References to explosives appear after 2000. The primary approach for discovery of a new MIP is combinatorial, which is labor-intensive, time consuming, and costly. This explains the prevalence of MAA in explosive MIPs, since it has been

shown to work. To grow as a field and technique, further research into the basic mechanisms of formation and template release is required and predictive experiments and models need to be developed.

The two most successful MIPs were 1:4:25 MAA and 1:8:40 PTMS with 795% and 227% uptake compared to controls. Efforts to identify reasons for success/failure of the various formulations included NMR titration experiments. The results did not distinguish MAA as a good candidate for a MIP monomer, despite experimental results showing imprinting success. It is clear that the success of imprinting cannot be predicted using the simple model used in these experiments.

Further review of NMR titration literature showed that the interactions are complex [12, 13], much more involved than the simple equilibria assumed in the experiments performed. At a minimum, the interaction of the monomer with itself must be accounted for with self-titration. The complex nature of the equilibria must also be taken into consideration and volume effects compensated for or eliminated. In addition, modeling work is needed to examine possible interactions between the monomers and templates that overcome dimerization and sensitivity in the NMR. Further development of general screening methods to evaluate potential functional monomers is needed; ideally it would give insight as to best ratios of template to monomer and easing design novel MIPs for both explosives and other compounds.

## References

- [1]- Wulff G, Sarhan A, Zabrocki K. 1973. Enzyme-analogue built polymers and their use for the resolution of racemates. *Tetrahedron Lett* 14:4329–4332.

- [2]- Arshady R, Mosbach K. 1981. Synthesis of substrate-selective polymers by host-guest polymerization. *Die Makromol Chemie* 182:687–692.
- [3]- Mingdi, Y, Ramstrom, O. 2005. *Molecularly imprinted materials : science and technology*. Marcel Dekker, New York
- [4]- Marshall M, Oxley JC. 2011. *Aspects of Explosives Detection*. Elsevier
- [5]- Holthoff E, Stratis-Cullum D. 2010. A Nanosensor for Explosives Detection Based on Molecularly Imprinted Polymers ( MIPs ) and Surfaced- enhanced Raman Scattering ( SERS ).
- [6]- Xie C, Liu B, Wang Z, et al. 2008. Molecular Imprinting at Walls of Silica Nanotubes for TNT Recognition of highly uniform silica nanotubes for the recognition of of silica through the strong acid - base pairing interaction. 80:437–443.
- [7]- Lordel S, Chapuis-Hugon F, Eudes V, Pichon V. 2010. Development of imprinted materials for the selective extraction of nitroaromatic explosives. *J Chromatogr A* 1217:6674–80.
- [8]- Bunte G, Hürttlen J, Pontius H, et al. 2007. Gas phase detection of explosives such as 2,4,6-trinitrotoluene by molecularly imprinted polymers. *Anal Chim Acta* 591:49–56.

- [9]- Bunte G, Heil M, Röseling D, et al. 2009. Trace Detection of Explosives Vapours by Molecularly Imprinted Polymers for Security Measures. *Propellants, Explos Pyrotech* 34:245–251.
- [10]- Sellergren B, Lepisto M, Mosbach K. 1988. Highly Enantioselective and Substrate-Selective Polymers Obtained by Molecular Imprinting Utilizing Noncovalent Interactions . NMR and Chromatographic Studies on the Nature of Recognition. *J Am Chem Soc* 435:5853–5860.
- [11]- Idziak I, Benrebouh A, Deschamps F. 2001. Simple NMR experiments as a means to predict the performance of an anti-17 -ethynylestradiol molecularly imprinted polymer. *Anal Chim Acta* 435:137–140.
- [12]- Macomber RS. 1992. An introduction to NMR titration for studying rapid reversible complexation. *J Chem Educ* 69:375.
- [13]- Ansell RJ, Kuah KL. 2005. Imprinted polymers for chiral resolution of (+/-)-ephedrine: understanding the pre-polymerisation equilibrium and the action of different mobile phase modifiers. *Analyst* 130:179–87.
- [14]- Pérez-Moral N, Mayes A. 2004. Comparative study of imprinted polymer particles prepared by different polymerisation methods. *Anal Chim Acta* 504:15–21.

- [15]- Alizadeh T, Zare M, Ganjali MR, et al. 2010. A new molecularly imprinted polymer (MIP)-based electrochemical sensor for monitoring 2,4,6-trinitrotoluene (TNT) in natural waters and soil samples. *Biosens Bioelectron* 25:1166–72.
- [16]- Roeseling D, Tuercke T, Krause H, Loebbecke S. 2009. Microreactor-Based Synthesis of Molecularly Imprinted Polymer Beads Used for Explosive Detection  
Abstract : 1007–1013.
- [17]- Stringer RC, Gangopadhyay S, Grant SA. 2010. Detection of nitroaromatic explosives using a fluorescent-labeled imprinted polymer. *Anal Chem* 82:4015–9.
- [18]- Stringer RC, Gangopadhyay S, Grant SA. 2010. Use of Quantum Dot-Labeled Imprinted Polymer Microparticles for Detection of Nitroaromatic Compounds. *Proc SPIE* 7673:767304–767306.
- [19]- Xie C, Zhang Z, Wang D, et al. 2006. Surface molecular self-assembly strategy for TNT imprinting of polymer nanowire/nanotube arrays. *Anal Chem* 78:8339–46.
- [20]- Liang Y, Gu L, Liu X, et al. 2011. Composites of Polyaniline Nanofibers and Molecularly Imprinted Polymers for Recognition of Nitroaromatic Compounds. *Chem – A Eur J* 17:5989–5997.

- [21]- Bao H, Wei T, Li X, et al. 2012. Detection of TNT by a molecularly imprinted polymer film-based surface plasmon resonance sensor. *Chinese Sci Bull* 57:2102–2105.
- [22]- Guan G, Liu R, Mei Q, Zhang Z. 2012. Molecularly imprinted shells from polymer and xerogel matrices on polystyrene colloidal spheres. *Chemistry* 18:4692–8.
- [23]- Riskin M, Ben-amram Y, Tel-vered R, et al. 2011. Molecularly Imprinted Au Nanoparticles Composites on Au Surfaces. 3082–3088.
- [24]- Riskin M, Tel-Vered R, Bourenko T, et al. 2008. Imprinting of molecular recognition sites through electropolymerization of functionalized Au nanoparticles: development of an electrochemical TNT sensor based on pi-donor-acceptor interactions. *J Am Chem Soc* 130:9726–33.
- [25]- Booker K, Bowyer MC, Holdsworth CI, McCluskey A. 2006. Efficient preparation and improved sensitivity of molecularly imprinted polymers using room temperature ionic liquids. *Chem Commun (Camb)* 1730–2.
- [26]- Walker NR, Linman MJ, Timmers MM, et al. 2007. Selective detection of gas-phase TNT by integrated optical waveguide spectrometry using molecularly imprinted sol-gel sensing films. *Anal Chim Acta* 593:82–91.

- [27]- Turner NW, Holmes N, Brisbane C, et al. 2009. Effect of template on the formation of phase-inversed molecularly imprinted polymer thin films: an assessment. *Soft Matter* 5:3663.
- [28]- Riskin M, Tel-Vered R, Willner I. 2010. Imprinted Au-Nanoparticle Composites for the Ultrasensitive Surface Plasmon Resonance Detection of Hexahydro-1,3,5-trinitro-1,3,5-triazine (RDX). *Adv Mater* 22:1387–1391.
- [29]- Lordel S, Chapuis-Hugon F, Eudes V, Pichon V. 2011. Selective extraction of nitroaromatic explosives by using molecularly imprinted silica sorbents. *Anal Bioanal Chem* 399:449–58.
- [30]- Stringer RC, Gangopadhyay S, Grant SA. 2011. Comparison of molecular imprinted particles prepared using precipitation polymerization in water and chloroform for fluorescent detection of nitroaromatics. *Anal Chim Acta* 703:239–44.

Table 1 – Imprinting Results Summary

Functional monomer	Structural monomer	TNT:FM:SM	MIP ( $\mu\text{g}$ TNT/mg poly)	Std Dev	Control ( $\mu\text{g}$ TNT/mg poly)	Std Dev	TNT uptake over control
PTMS	TEOS	1:8:18	1.54	0.20	1.62	0.13	95%
TMOTFS	TEOS	1:4:20	0.39	0.06	0.41	0.03	97%
PTMS	TEOS	1:23:102	1.31	0.19	1.20	0.39	109%
PTMS	TEOS	1:8:36	1.41	0.23	1.20	0.39	118%
PTMS	TEOS	1:2:9	1.51	0.02	1.20	0.39	126%
PTMS	TEOS	1:10:50	0.98	0.43	0.74	0.20	133%
PTMS	TEOS	1:4:27	0.99	0.06	0.74	0.13	133%
TEOTES	TEOS	1:4:20	1.04	0.15	0.65	0.05	159%
PTMS	TEOS	1:8:40	1.32	0.10	0.41	0.03	227%
MAA	EGDMA	1:4:25	1.2	0.10	0.20	0.03	795%
APTES	C1-TriEOS	1:10:368	0.12	0.21	0.11	0.07	110%
RDX							
PTMS	TEOS	1:4:18	0.36	0.08	0.47	0.14	76%
2,4-DNT							
APTES	C1-TriEOS	1:10:368	0.11	0.03	0.11	0.07	101%

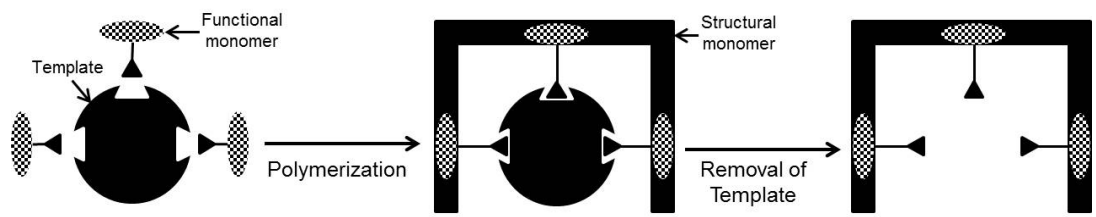


Fig. 1 – Generalized synthesis of a MIP

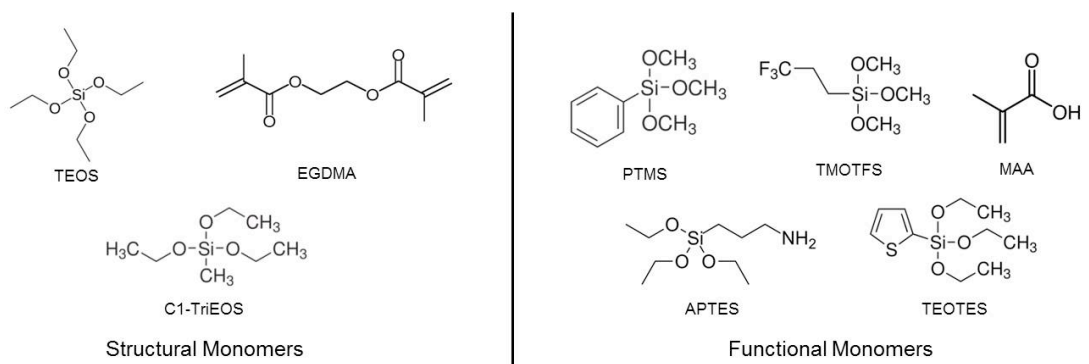


Fig. 2 – Structural and functional monomers tested

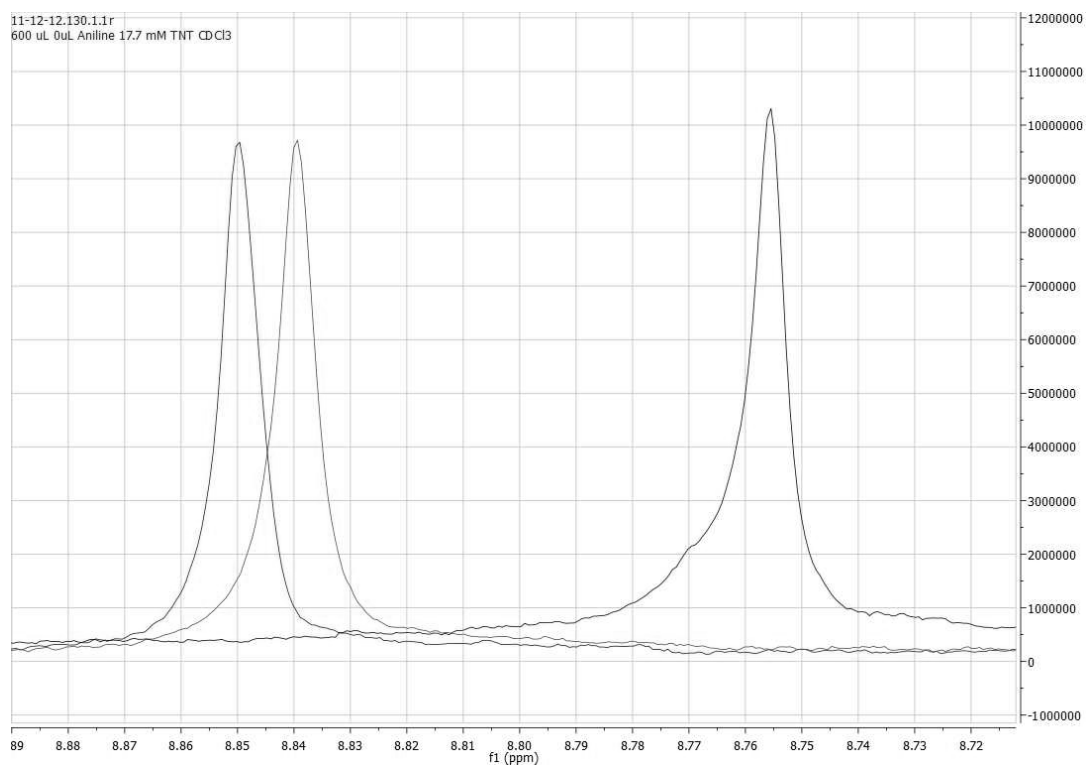


Fig. 3 – From left to right: TNT aromatic protons with no aniline, 1 molar equivalent aniline, and 10 molar equivalents aniline

## SUPPORTING INFORMATION

### Supporting Information 1

Year	Author	Reference	Template	Monomer	Crosslinker	Initiator	MIP formation
2004	Mayes	14	Propanol	MAA	EGDMA	DMPAP	5 ways
2006	Booker	25	Trans-aconitic acid	Ionic liquids & NMR titration			
2006	Xie	19	TNT	Acrylamide (AA)	EGDMA	AIBN	Nanotubes
2007	Bunte	8	TNT, 2,4-DNT	methacrylic acid MAA or acrylamide	ethylene glycol dimethacrylate EGDMA	AIBN	Suspension polymerization
2007	Walker	26	TNT	2-(trimethoxysilylethyl)pyridine (TMSE-Pyr)	Bis(trimethoxysilylethyl)benzene (BTEB)	Tetrabutylammonium fluoride (TBAF)	Zerogel bulk polymerization
2008	Riskin	24	Picric Acid, imprinting for TNT	p-aminothiophenol	Au nanoparticles		electropolymerization
2008	Xie	6	TNT	Aminopropyltriethoxysilane (APTES)	TEOS	Sodium acetate buffer (pH 5.1)	Nanotubes
2009	Bunte	9	TNT				
2009	Turner	27	TNT, DNT	Methacrylamide (MAM)	Acrylonitrile (AN), EDGMA	AIBN	MIP films
2009	Roesling	16	TNT	MAA	EGDMA	UV	Microreactors making microspheres
2010	Alizadeh	15	TNT	MAA	EGDMA	AIBN	Bulk polymerization, ground & added to carbon paste
2010	Stringer	17	TNT, DNT	MAA	EGDMA		
2010	Riskin	28	Kemp's acid, imprinting for RDX	Bisaniline	Au nanoparticles		Electropolymerization
2010	Lordel	7	DNT	Phenyltrimethylsiloxane (PTMS)	Tetraethoxysilane (TEOS)	Ammonia	Bulk Polymerization
2010	Holthoff	5	TNT	APTES	Methyltriethoxysilane (C1-TriEOS)	HCl	Spincoating onto SERS substrate
2010	Stringer	18	TNT, DNT	MAA	EGDMA	365nm UV	Bulk polymerization
2011	Riskin	23	Citric acid imprint for PETN or NG & maleic acid or fumaric acid, imprint for EGDN	Bisaniline	Au nanoparticles		Electropolymerization
2011	Lordel	29	DNT	PTMS	TEOS	Ammonia	Bulk polymerization
2011	Stringer	30	TNT, DNT	MAA	EGDMA, EGDA	AIBN, ACVA	Suspension polymerization
2011	Liang	20	DNB	AA	EGDMA	AIBN	Films onto polyaniline nanofibres
2012	Bao	21	TNT	AA	EGDMA	AIBN	Polymer Films
2012	Guan	22	TNT	AA	EGDMA	AIBN	Films on polystyrene spheres

## Supporting Information 2

	Author	Solvent	Structural Monomer	Functional Monomer	Catalyst	Template	Substrate	Extraction Method	Analysis Methods	#	TNT; polymer:crosslink
1	Triton	40 mL EtOH*	3 mL C1-TriEOS	112 $\mu$ L APTES + 90 $\mu$ L MPTMS	200 $\mu$ L 1M HCl	1.6 mL of 1800 $\mu$ g/mL 2,4-DNT	Glass Wool	Holthoff extraction solution (8:2:1 EtOH:ACN:Acetic Acid), Soxhlet	GC/ $\mu$ ECD uptake	9	
2	Triton	40 mL EtOH*	3 mL C1-TriEOS	112 $\mu$ L APTES + 90 $\mu$ L MPTMS	200 $\mu$ L 1M HCl	None (control)	Glass Wool	Holthoff extraction solution, Soxhlet	GC/ $\mu$ ECD uptake	7	
3	Holthoff	40 mL EtOH*	3 mL C1-TriEOS	112 $\mu$ L APTES + 90 $\mu$ L MPTMS	200 $\mu$ L 1M HCl	3.52 mL 1020 $\mu$ g/mL TNT	Glass Wool	Holthoff extraction solution, Soxhlet	GC/ $\mu$ ECD uptake	2	
4	Triton	40 mL EtOH*	3 mL C1-TriEOS	112 $\mu$ L APTES	200 $\mu$ L 1M HCl	3.0(+/-) 0.2)mg 2,4-DNT	Sand	Holthoff extraction solution	GC/ $\mu$ ECD uptake, UV-Vis extract, TGA	2	
5	Triton	40 mL EtOH*	3 mL C1-TriEOS	112 $\mu$ L APTES	200 $\mu$ L 1M HCl	None (control)	Sand	Holthoff extraction solution	GC/ $\mu$ ECD uptake, UV-Vis extract, TGA	1	
6	Triton	40 mL EtOH*	3 mL C1-TriEOS	112 $\mu$ L APTES	200 $\mu$ L 1M HCl	None (control)	Silica Gel	Holthoff extraction solution	GC/ $\mu$ ECD uptake, UV-Vis extract, TGA	1	
7	Triton	40 mL EtOH*	3 mL C1-TriEOS	112 $\mu$ L APTES	200 $\mu$ L 1M HCl	3.0(+/-) 0.2)mg 2,4-DNT	Silica Gel	Holthoff extraction solution	GC/ $\mu$ ECD uptake, UV-Vis extract, TGA	2	
8	Triton	40 mL EtOH*	3 mL C1-TriEOS	112 $\mu$ L APTES	200 $\mu$ L 1M HCl	291(+/-) 5)mg DNT	Sand	Holthoff extraction solution	GC/ $\mu$ ECD uptake, UV-Vis extract, TGA	2	10x DNT amt
9	Triton	40 mL EtOH*	3 mL C1-TriEOS	112 $\mu$ L APTES	200 $\mu$ L 1M HCl	291(+/-) 5)mg DNT	Silica Gel	Holthoff extraction solution	GC/ $\mu$ ECD uptake, UV-Vis extract, TGA	2	10x DNT amt
10	Holthoff	40 mL EtOH*	3 mL C1-TriEOS	112 $\mu$ L APTES	200 $\mu$ L 1M HCl	1 mL of 3.6 mg/mL TNT solution	Sand	Holthoff extraction solution	GC/ $\mu$ ECD uptake, UV-Vis extraction	2	

11	Holthoff	40 mL EtOH*	3 mL C1-TriEOS	112 $\mu$ L APTES	200 $\mu$ L 1M HCl	None (control)	Sand	Holthoff extraction solution	GC/ $\mu$ ECD uptake, UV-Vis extraction	1	
12	Holthoff	40 mL EtOH*	3 mL C1-TriEOS	112 $\mu$ L APTES	200 $\mu$ L 1M HCl	1 mL of 3.6 mg/mL TNT solution	Glass Wool	Holthoff extraction solution, Soxhlet	GC/ $\mu$ ECD uptake, UV-Vis extraction	2	
13	Holthoff	40 mL EtOH*	3 mL C1-TriEOS	112 $\mu$ L APTES	200 $\mu$ L 1M HCl	None (control)	Glass Wool	Holthoff extraction solution, Soxhlet	GC/ $\mu$ ECD uptake, UV-Vis extraction	1	
14	Xie	41 mL EtOH*	1.8 mL C1-TriEOS	354 $\mu$ L APTES	1.8 mL pH 5 Sodium Acetate Buffer	53.7 (+/-1) mg TNT	Sand	Holthoff extraction solution	GC/ $\mu$ ECD uptake, UV-Vis extraction	2	
15	Xie	41 mL EtOH*	1.8 mL C1-TriEOS	354 $\mu$ L APTES	1.8 mL pH 5 Sodium Acetate Buffer	53.7 (+/-1) mg TNT	Sand	Holthoff extraction solution	GC/ $\mu$ ECD uptake, UV-Vis extraction	2	
16	Holthoff	20 mL EtOH	2.2 mL C1-TriEOS	70 $\mu$ L APTES	125 $\mu$ L 1M HCl	1 mL of 6.8 mg/mL TNT	Sand	Holthoff extraction solution	GC/ $\mu$ ECD uptake	2	
17	Holthoff	20 mL EtOH	2.2 mL C1-TriEOS	70 $\mu$ L APTES	125 $\mu$ L 1M HCl	1 mL of 6.8 mg/mL TNT	Glass Wool	Holthoff extraction solution	GC/ $\mu$ ECD uptake	2	Drop-coated
18	Holthoff	20 mL EtOH	2.2 mL C1-TriEOS	70 $\mu$ L APTES	125 $\mu$ L 1M HCl	None (control)	Sand	Holthoff extraction solution	GC/ $\mu$ ECD uptake	1	
19	Holthoff	20 mL EtOH	2.2 mL C1-TriEOS	70 $\mu$ L APTES	125 $\mu$ L 1M HCl	None (control)	Glass Wool	Holthoff extraction solution	GC/ $\mu$ ECD uptake	1	Drop-coated Initial Experiment
20	Lordel	2 mL ACN	480 $\mu$ L C1-TriEOS	110 $\mu$ L PTMS	200 $\mu$ L 1M NaOH	91 mg DNT	Block	N/A	N/A	1	Experiment 1:1:5
21	Lordel	1mL MeOH, 1mL ACN	480 $\mu$ L C1-TriEOS	110 $\mu$ L PTMS	200 $\mu$ L 1M HCl	91mg DNT	Block	Solvent Rinse (MeOH, ACN, Acetone), soxhlet	GC/ $\mu$ ECD uptake	1	60C oven to cure 1:1:5
22	Lordel	1mL EtOH, 1mL ACN	480 $\mu$ L C1-TriEOS	110 $\mu$ L PTMS	200 $\mu$ L 1M HCl	91mg DNT	Block	Solvent Rinse (MeOH, ACN, Acetone), soxhlet	GC/ $\mu$ ECD uptake	1	60C oven to cure 1:1:5
23	Lordel	1mL MeOH, 1mL ACN	480 $\mu$ L C1-TriEOS	110 $\mu$ L PTMS	200 $\mu$ L 1M NaOH	91mg DNT	Block	Solvent Rinse (MeOH, ACN, Acetone), soxhlet	GC/ $\mu$ ECD uptake	1	60C oven to cure 1:1:5
24	Lordel	1mL EtOH,	480 $\mu$ L C1-TriEOS	110 $\mu$ L PTMS	200 $\mu$ L 1M NaOH	91mg DNT	Block	Solvent Rinse (MeOH, ACN,	GC/ $\mu$ ECD uptake	1	60C oven to cure

25	Lordel	5mL EtOH, 5mL ACN	480 uL C1- TriEOS	110 uL PTMS	200uL 1M HCL	113.5mg TNT	Glass Wool	Acetone), soxhlet	GC/uECD uptake	1	Dip Coat 1:1:5	1:1:5
26	Lordel	5mL MeOH, 5mL ACN	480 uL C1- TriEOS	110 uL PTMS	200uL 1M NaOH	113.5mg TNT	Glass Wool	Soxhlet	GC/uECD uptake	1	Dip Coat 1:1:5	
27	Holthoff	1mL EtOH, 1mL ACN	2.2mL C1- TriEOS	70 uL APTES	125 uL 1M HCl	1 mL of 6.8 mg/mL TNT	Block	Holthoff extraction solution, refluxed in extraction solution, soxhlet, solvent rinse (MeOH, ACN, acetone)	GC/uECD uptake, UV-Vis uptake	2	1:10:368, 60C oven to cure	
28	Holthoff	1mL EtOH, 1mL ACN	2.2mL C1- TriEOS	70 uL APTES	125 uL 1M HCl	None (control)	Block	Holthoff extraction solution, refluxed in extraction solution, soxhlet, solvent rinse (MeOH, ACN, acetone)	GC/uECD uptake, UV-Vis uptake	0	60C oven to cure	
29	Holthoff	20 mL EtOH	2.2 mL C1- TriEOS	70 uL APTES	125 uL 1M HCl	1 mL of 6.8 mg/mL TNT	Glass Wool	Holthoff extraction solution, Soxhlet	GC/uECD uptake	1	Dip Coat, sent to Triton	
30	Holthoff	20 mL EtOH	2.2 mL C1- TriEOS	70 uL APTES	125 uL 1M HCl	None (control)	Glass Wool	Holthoff extraction solution, Soxhlet	GC/uECD uptake	1	Dip Coat, sent to Triton	
31	Lordel	1mL EtOH, 1mL ACN	2 mL C1- TriEOS	440 uL PTMS	800uL of 30% NH4 Hydroxide	113.5mg TNT	Block	Soxhlet, solvent rinse (MeOH, acetone)	GC/uECD uptake	5	40C in oven to cure 1:4:20	
32	Lordel	1mL MeOH, 1mL ACN	2 mL C1- TriEOS	440 uL PTMS	800uL of 30% NH4 Hydroxide	113.5mg TNT	Block	Soxhlet, solvent rinse (MeOH, acetone)	GC/uECD uptake	4	40C in oven to cure 1:4:20	
33	Lordel	1mL EtOH, 1mL ACN	2 mL C1- TriEOS	440 uL PTMS	800uL of 30% NH4 Hydroxide	None (control)	Block	Soxhlet, solvent rinse (MeOH, acetone)	GC/uECD uptake	3	40C in oven to cure	
34	Lordel	1mL MeOH, 1mL ACN	2 mL C1- TriEOS	440 uL PTMS	800uL of 30% NH4 Hydroxide	None (control)	Block	Soxhlet, solvent rinse (MeOH, acetone)	GC/uECD uptake	3	40C in oven to cure	
35	Lordel	N/A	2 mL C1- TriEOS	440 uL PTMS	800uL of 30% NH4 Hydroxide	113.5mg TNT	Block	Soxhlet, solvent rinse (MeOH, acetone)	GC/uECD uptake, UV-Vis uptake, TGA/IR	6	40C in oven to cure 1:4:20	

36	Lordel	N/A	2 mL C1-TriEOS	440 uL PTMS	800uL of 30% NH4 Hydroxide	None (control)	Block	Soxhlet, solvent rinse (MeOH, acetone)	GC/μECD uptake, UV-Vis uptake, TGA/IR	7	40C regulated bath
37	Lordel	3mL MeOH, 3mL ACN	2 mL C1-TriEOS	440 uL PTMS	800uL of 30% NH4 Hydroxide	113.5mg TNT	Steel Wool	N/A	UV-Vis uptake	1	Sent to Triton 1:4:20
38	Lordel	3mL MeOH, 3mL ACN	2 mL C1-TriEOS	440 uL PTMS	800uL of 30% NH4 Hydroxide	None (control)	Steel Wool	N/A	UV-Vis uptake	1	Sent to Triton
39	Lordel	N/A	2 mL C1-TriEOS	440 uL PTMS	500uL 50% NaOH	None (control)	Block	Solvent Rinse (MeOH, Acetone)	UV-Vis uptake templated polymer	1	
40	Lordel	N/A	2 mL C1-TriEOS	440 uL PTMS	500uL 37% HCl	None (control)	Block	Solvent Rinse (MeOH, Acetone)	UV-Vis uptake templated polymer	1	
41	Lordel	N/A	2 mL C1-TriEOS	440 uL PTMS	500uL 37% HCl	113.5mg TNT	Block	Solvent Rinse (MeOH, Acetone)	UV-Vis uptake templated polymer	1	1:4:20
42	Lordel	1mL Isopropanol, 1mL ACN	2 mL C1-TriEOS	440 uL PTMS	500uL 37% HCl	113.5mg TNT	Block	Solvent Rinse (MeOH, Acetone)	UV-Vis uptake templated polymer	1	1:4:20
43	Lordel	N/A	2 mL C1-TriEOS	440 uL PTMS	800uL 1M NaOH	None (control)	Block	Solvent Rinse (MeOH, Acetone)	UV-Vis uptake templated polymer	1	
44	Lordel	N/A	2 mL C1-TriEOS	440 uL PTMS	800uL 10% NaOH	None (control)	Block	Solvent Rinse (MeOH, Acetone)	UV-Vis uptake templated polymer	1	
45	Lordel	N/A	2 mL C1-TriEOS	440 uL PTMS	800uL 20% NaOH	None (control)	Block	Solvent Rinse (MeOH, Acetone)	UV-Vis uptake templated polymer	1	
46	Lordel	N/A	2 mL C1-TriEOS	440 uL PTMS	800uL 20% NaOH	113.5mg TNT	Block	Solvent Rinse (MeOH, ACN, Acetone)	UV-Vis uptake templated polymer	1	1:4:20
47	Lordel	N/A	1 mL C1-TriEOS	220 uL PTMS	400uL of 30% Ammonium Hydroxide	57.2mg TNT	Block	Solvent Rinse (MeOH, ACN, Acetone)	UV-Vis uptake templated polymer	1	1:4:20
48	Lordel	N/A	1 mL C1-TriEOS	220 uL PTMS	400uL of 30% Ammonium Hydroxide	None (control)	Block	Solvent Rinse (MeOH, ACN, Acetone)	UV-Vis uptake templated polymer	1	

49	Lordel	3mL ACN	2 mL C1-TriEOS	440 uL PTMS	800uL of 30% Ammonium Hydroxide	11.1mg RDX	Block	Solvent Rinse (MeOH, Acetone)	UV-Vis uptake templated polymer	3	RDX 1:4:20
50	Lordel	1.5mL ACN	1 mL C1-TriEOS	220 uL PTMS	400uL of 30% Ammonium Hydroxide	55.5mg RDX	Block	Solvent Rinse (MeOH, Acetone)	UV-Vis uptake templated polymer	3	RDX 1:4:20
51	Lordel	3mL ACN	2 mL C1-TriEOS	440 uL PTMS	800uL of 30% Ammonium Hydroxide	None (control)	Block	Solvent Rinse (MeOH, Acetone)	UV-Vis uptake templated polymer	3	RDX
52	Lordel	N/A	1 mL TEOS	220 uL PTMS	400uL of 30% Ammonium Hydroxide	56.7mg TNT	Block	Solvent Rinse (MeOH, Acetone)	UV-Vis uptake templated polymer	4	1:4:18
53	Lordel	N/A	1 mL TEOS	220 uL PTMS	400uL of 30% Ammonium Hydroxide	None (control)	Block	Solvent Rinse (MeOH, Acetone)	UV-Vis uptake templated polymer	3	
54	Lordel	1.5mL ACN	1 mL TEOS	220 uL PTMS	440uL of 30% Ammonium Hydroxide	55.5mg RDX	Block	Solvent Rinse (MeOH, Acetone, ACN)	UV-Vis uptake templated polymer	5	RDX 1:4:18
55	Lordel	1.5mL ACN	1 mL TEOS	220 uL PTMS	440uL of 30% Ammonium Hydroxide	None (control)	Block	Solvent Rinse (MeOH, Acetone, ACN)	UV-Vis uptake templated polymer	2	RDX 1:4:18
56	Lordel	N/A	1 mL TEOS	220 uL PTMS	440uL of 30% Ammonium Hydroxide	56.7mg TNT	Block	Solvent Rinse (MeOH, Acetone)	UV-Vis uptake templated polymer	3	1:4:18
57	Lordel	N/A	1 mL TEOS	220 uL PTMS	440uL of 30% Ammonium Hydroxide	None (control)	Block	Solvent Rinse (MeOH, Acetone)	UV-Vis uptake templated polymer	1	
58	Lordel	2mL Water	1 mL TEOS	220 uL PTMS	440uL of 30% Ammonium Hydroxide	56.7mg TNT	Block	Solvent Rinse (MeOH, Acetone, ACN)	UV-Vis uptake templated polymer	5	1:4:18
59	Lordel	2mL Water	1 mL TEOS	220 uL PTMS	440uL of 30% Ammonium Hydroxide	None (control)	Block	Solvent Rinse (MeOH, Acetone, ACN)	UV-Vis uptake templated polymer	3	

60	Lordel	N/A	1 mL TEOS	220 uL PTMS	400uL of 30% Ammonium Hydroxide	28.4mg TNT	Block	Solvent Rinse (MeOH, Acetone, ACN)	UV-Vis uptake templated polymer	3	1:8:36
61	Lordel	N/A	0.5 mL TEOS	110 uL PTMS	400uL of 30% Ammonium Hydroxide	56.7mg TNT	Block	Solvent Rinse (MeOH, Acetone, ACN)	UV-Vis uptake templated polymer	1	1:2:9
62	Lordel	N/A	1 mL TEOS	440 uL PTMS	400uL of 30% Ammonium Hydroxide	56.7mg TNT	Block	Solvent Rinse (MeOH, Acetone, ACN)	UV-Vis uptake templated polymer	1	1:8:18
63	Lordel	N/A	1 mL TEOS	440 uL PTMS	400uL of 30% Ammonium Hydroxide	None (control)	Block	Solvent Rinse (MeOH, Acetone, ACN)	UV-Vis uptake templated polymer	1	
64	Lordel	N/A	1.5 mL TEOS	220 uL PTMS	400uL of 30% Ammonium Hydroxide	56.7mg TNT	Block	Solvent Rinse (MeOH, Acetone, ACN)	UV-Vis uptake templated polymer	1	1:4:27
65	Lordel	N/A	1.5 mL TEOS	220 uL PTMS	400uL of 30% Ammonium Hydroxide	None (control)	Block	Solvent Rinse (MeOH, Acetone, ACN)	UV-Vis uptake templated polymer	1	
66	Lordel	1.5mL ACN	1 mL TEOS	220 uL PTMS	880uL of 30% Ammonium Hydroxide	55.5mg RDX	Block	Solvent Rinse (MeOH, Acetone, ACN)	UV-Vis uptake templated polymer	1	RDX, 1:4:18
67	Lordel	1.5mL ACN	1 mL TEOS	220 uL PTMS	880uL of 30% Ammonium Hydroxide	None (control)	Block	Solvent Rinse (MeOH, Acetone, ACN)	UV-Vis uptake templated polymer	1	RDX
68	Lordel	N/A	0.97 mL TEOS	200 uL PTMS	400uL of 30% Ammonium Hydroxide	20mg TNT	Block	Solvent Rinse (MeOH, Acetone, ACN)	UV-Vis uptake templated polymer	3	1:10:50
69	Lordel	N/A	0.97 mL TEOS	200 uL PTMS	400uL of 30% Ammonium Hydroxide	None (control)	Block	Solvent Rinse (MeOH, Acetone, ACN)	UV-Vis uptake templated polymer	3	1:10:50
70	Lordel	N/A	1.16 mL TEOS	220 uL PTMS	400uL of 30% Ammonium Hydroxide	30mg TNT	Block	Solvent Rinse (MeOH, Acetone, ACN)	UV-Vis uptake templated polymer	1	1:8:40

71	Lordel	N/A	1.16 mL TEOS	220 uL PTMS	400uL of 30% Ammonium Hydroxide	None (control)	Block	Solvent Rinse (MeOH, Acetone, ACN)	UV-Vis uptake templated polymer	1	1:8:40
72	Lordel	N/A	1 mL TEOS	220 uL PTMS	400uL of 30% Ammonium Hydroxide	10mg TNT	Block	Solvent Rinse (MeOH, Acetone, ACN)	UV-Vis uptake templated polymer	1	1:23:102
73	New	N/A	0.51 mL TEOS	90 uL TMOTFS	400uL of 30% Ammonium Hydroxide	26mg TNT	Block	Solvent Rinse (MeOH, Acetone, ACN)	UV-Vis uptake templated polymer	2	TMOTFS= trimethoxytrifluoropropyl silane 1:4:20
74	New	N/A	0.51 mL TEOS	90 uL TMOTFS	400uL of 30% Ammonium Hydroxide	None (control)	Block	Solvent Rinse (MeOH, Acetone, ACN)	UV-Vis uptake templated polymer	1	TMOTFS= trimethoxytrifluoropropyl silane
75	New	1mL EtOH	0.51 mL TEOS	100 uL TEOTES	400uL of 30% Ammonium Hydroxide	26mg TNT	Block	Solvent Rinse (MeOH, Acetone, ACN)	UV-Vis uptake templated polymer	2	TEOTES= Triethoxy-2-thenylsilane 1:4:20
76	New	1mL EtOH	0.51 mL TEOS	100 uL TEOTES	400uL of 30% Ammonium Hydroxide	None (control)	Block	Solvent Rinse (MeOH, Acetone, ACN)	UV-Vis uptake templated polymer	2	TEOTES= Triethoxy-2-thenylsilane
77	New	N/A	0.51 mL TEOS	100 uL TEOTES	400uL of 1M Sodium Hydroxide	None (control)	Block	Solvent Rinse (MeOH, Acetone, ACN)	UV-Vis uptake templated polymer	2	TEOTES= Triethoxy-2-thenylsilane
78	Lordel	2mL Water	1 mL TEOS	220 uL PTMS	400uL of 30% Ammonium Hydroxide	28.4mg TNT	Block	Solvent Rinse (MeOH, Acetone, ACN)	UV-Vis uptake templated polymer	3	1:8:36
79	Lordel	2mL Water	0.5 mL TEOS	110 uL PTMS	400uL of 30% Ammonium Hydroxide	56.7mg TNT	Block	Solvent Rinse (MeOH, Acetone, ACN)	UV-Vis uptake templated polymer	1	1:2:9
80	Lordel	2mL Water	1 mL TEOS	440 uL PTMS	400uL of 30% Ammonium Hydroxide	56.7mg TNT	Block	Solvent Rinse (MeOH, Acetone, ACN)	UV-Vis uptake templated polymer	1	1:8:18
81	Lordel	2mL Water	1 mL TEOS	440 uL PTMS	400uL of 30% Ammonium Hydroxide	None (control)	Block	Solvent Rinse (MeOH, Acetone, ACN)	UV-Vis uptake templated polymer	1	

82	Lordel	2mL Water	1.1 mL TEOS	220 uL PTMS	400uL of 30% Ammonium Hydroxide	56.7mg TNT	Block	Solvent Rinse (MeOH, Acetone, ACN)	UV-Vis uptake templated polymer	1	1:8:18
83	Lordel	2mL Water	1.1 mL TEOS	220 uL PTMS	400uL of 30% Ammonium Hydroxide	None (control)	Block	Solvent Rinse (MeOH, Acetone, ACN)	UV-Vis uptake templated polymer	1	
84	Lordel	2mL Water	1.5 mL TEOS	220 uL PTMS	400uL of 30% Ammonium Hydroxide	56.7mg TNT	Block	Solvent Rinse (MeOH, Acetone, ACN)	UV-Vis uptake templated polymer	1	1:4:27
85	Lordel	2mL Water	1.5 mL TEOS	220 uL PTMS	400uL of 30% Ammonium Hydroxide	None (control)	Block	Solvent Rinse (MeOH, Acetone, ACN)	UV-Vis uptake templated polymer	1	
86	Lordel	Excess Water	1 mL TEOS	220 uL PTMS	400uL of 30% Ammonium Hydroxide	56.7mg TNT	Block	Solvent Rinse (MeOH, Acetone)	UV-Vis uptake templated polymer	4	Emulsion MIP, 1:4:18
87	Lordel	Excess Water	1 mL TEOS	220 uL PTMS	400uL of 30% Ammonium Hydroxide	None (control)	Block	Solvent Rinse (MeOH, Acetone)	UV-Vis uptake templated polymer	3	Emulsion Control
88	Holthoff	1mL EtOH, 1mL ACN	0.8mL TEOS	150 uL APTES	125 uL 1M HCl	34mg TNT	Block	Holthoff extraction solution, refluxed in extraction solution, soxhlet, solvent rinse (MeOH, ACN, acetone)	UV-Vis uptake	2	60C oven to cure
89	Holthoff	1mL EtOH, 1mL ACN	2.2mL C1-TriEOS	70 uL APTES	125 uL 1M HCl	1 mL of 5.4 mg/mL 2,4-DNT	Block	Holthoff extraction solution, refluxed in extraction solution, soxhlet, solvent rinse (MeOH, ACN, acetone)	UV-Vis uptake	1	1:10:368, 60C oven to cure

\* Sample volumes were large for the first 14 experiments because a batch was made & split into 15 mL individual samples.

Supporting Information 3

TNT uptake: rinsing and reusing the same sample

Sample name	Sample #	UV-Vis Abs 232 nm	TNT left in soln out of 15 ug/mL	TNT uptake out of 15 ug/mL	Condition Table # Supp Info 2	Ratio	
<b>MIP 1 5-15</b>	1	0.980	10.4	4.60	<b>52</b>	1:4:18	
	2	0.899	9.47	5.53			
	3	0.879	9.23	5.77			
	4	0.938	9.92	5.08			
	*run another day	5	1.26	13.7			1.30
	*run another day	6	1.02	10.9			4.13
	<b>Average</b>			<b>10.6</b>			<b>4.40</b>
<b>MIP 2 5-15</b>	1	0.922	9.73	5.27	<b>52</b>	1:4:18	
	2	0.858	8.99	6.01			
	3	0.854	8.94	6.06			
	4	0.839	8.77	6.23			
	*run another day	5	1.015	10.9			4.11
	<b>Average</b>			<b>9.46</b>			<b>5.54</b>
<b>MIP 1 6-25</b>	1	0.594	6.15	8.85	<b>60</b>	1:8:36	
	2	0.617	6.43	8.57			
	3	0.491	4.95	10.1			
	4	0.461	4.58	10.4			
	5	0.477	4.78	10.2			
	<b>Average</b>			<b>5.38</b>			<b>9.62</b>
<b>MIP 2 6-25</b>	1	0.713	7.56	7.44	<b>61</b>	1:2:9	
	2	0.724	7.69	7.31			
	3	0.814	8.76	6.24			
	4	0.771	8.25	6.75			
	5	0.750	7.99	7.01			
	<b>Average</b>			<b>8.05</b>			<b>6.95</b>
<b>MIP 2 5-30</b>	1	0.676	7.35	7.65	<b>56</b>	1:4:18	
	2	0.724	7.89	7.11			
	3	0.435	4.59	10.4			
	4	0.596	6.43	8.57			
	*run another day	5	0.696	7.57			7.43
	<b>Average</b>			<b>6.77</b>			<b>8.23</b>
<b>MIP 3 6-5</b>	1	0.957	10.6	4.44	<b>56</b>	1:4:18	
	2	0.958	10.6	4.42			
	3	0.977	10.8	4.21			
	4	0.879	9.66	5.34			
	*run another day	5	1.08	12.0			2.99
	<b>Average</b>			<b>10.7</b>			<b>4.28</b>
<b>MIP 4 6-5</b>	1	1.01	11.1	3.89	<b>56</b>	1:4:18	
	2	0.868	9.54	5.46			
	3	0.773	8.45	6.55			
	4	0.771	8.43	6.57			
	*run another day	5	0.960	10.6			4.40
	<b>Average</b>			<b>9.62</b>			<b>5.38</b>
<b>Control 1 5-15</b>	<b>1</b>	<b>0.851</b>	<b>8.99</b>	<b>6.01</b>	<b>53</b>		

*run another day *run another day <b>Average</b>	2	0.728	7.57	7.43		
	3	0.762	7.96	7.04		
	4	0.602	6.11	8.89		
	5	1.20	13.0	1.97		
	6	1.07	11.6	3.42		
			<b>9.21</b>	<b>5.79</b>		
<b>Control 2 5-15</b>  *run another day <b>Average</b>	1	1.02	10.9	4.09	<b>53</b>	
	2	0.911	9.69	5.31		
	3	0.889	9.44	5.56		
	4	0.856	9.06	5.94		
	5	1.02	11.0	4.00		
			<b>10.0</b>	<b>4.98</b>		
<b>Control 1 5-30</b>  *run another day <b>Average</b>	1	1.02	10.9	4.11	<b>57</b>	
	2	1.05	11.2	3.76		
	3	1.04	11.0	3.96		
	4	1.10	11.8	3.24		
	5	1.11	11.9	3.13		
			<b>11.4</b>	<b>3.64</b>		
<b>MIP 1 5-30</b>  *run another day <b>Average</b>	1	1.02	10.9	4.12	<b>58</b>	1:4:18
	2	1.07	11.4	3.58		
	3	1.07	11.4	3.59		
	4	1.09	11.7	3.33		
	5	0.938	9.92	5.08		
			<b>11.1</b>	<b>3.94</b>		
<b>MIP 1 6-5</b>  *run another day <b>Average</b>	1	0.895	9.85	5.15	<b>58</b>	1:4:18
	2	0.843	9.26	5.74		
	3	1.00	11.1	3.90		
	4	0.943	10.4	4.60		
	5	0.858	9.43	5.57		
			<b>10.0</b>	<b>4.99</b>		
<b>MIP 2 6-5</b>  *run another day <b>Average</b>	1	0.903	9.94	5.06	<b>58</b>	1:4:18
	2	0.903	9.94	5.06		
	3	1.03	11.4	3.59		
	4	1.01	11.2	3.78		
	5	0.946	10.4	4.56		
			<b>10.6</b>	<b>4.41</b>		
<b>MIP 1 6-18</b>  *run another day <b>Average</b>	1	0.962	10.3	4.67	<b>78</b>	1:8:36
	2	0.832	8.85	6.15		
	3	0.876	9.35	5.65		
	4	0.953	10.2	4.77		
	5	0.896	9.48	5.52		
			<b>9.65</b>	<b>5.35</b>		
<b>Control 2 5-30</b>  *run another day <b>Average</b>	1	1.13	12.2	2.82	<b>59</b>	
	2	1.12	12.0	3.02		
	3	1.02	10.9	4.08		
	4	1.09	11.6	3.37		
	5	1.108	12.0	3.00		
			<b>11.7</b>	<b>3.26</b>		
<b>Emulsion MIP 6-12</b>	1	1.20	12.8	2.24	<b>86</b>	
	2	1.24	13.2	1.82		
	3	1.24	13.3	1.72		

<b>Average</b>	4	1.08	11.4	3.60			
			<b>12.7</b>	<b>2.34</b>			
<b>Emulsion Cont 6-12</b>	1	1.07	11.3	3.69	<b>87</b>		
	2	0.970	10.1	4.86			
	3	0.920	9.57	5.43			
	4	0.961	10.0	4.96			
	<b>Average</b>			<b>10.3</b>			<b>4.73</b>
<b>MIP 2 6-18</b>	1	0.982	10.6	4.44	<b>79</b>	1:2:9	
	2	0.962	10.3	4.66			
	3	0.942	10.1	4.89			
	4	1.02	10.9	4.06			
	*run another day	5	0.901	9.54			5.46
	<b>Average</b>			<b>10.3</b>			<b>4.71</b>
<b>MIP 3 6-18</b>	1	0.832	8.86	6.14	<b>80</b>	1:8:18	
	2	0.809	8.59	6.41			
	3	0.823	8.75	6.25			
	4	0.937	10.0	4.95			
	*run another day	5	0.854	8.97			6.03
	<b>Average</b>			<b>9.04</b>			<b>5.96</b>
<b>Control 1 6-18</b>	1	0.808	8.35	6.65	<b>81</b>		
	2	0.767	7.90	7.10			
	3	0.996	10.5	4.54			
	4	0.894	9.31	5.69			
	*run another day	5	0.944	10.0			4.96
	<b>Average</b>			<b>9.21</b>			<b>5.79</b>
<b>MIP 4 6-18</b>	1	0.991	10.6	4.43	<b>82</b>	1:8:40	
	2	0.987	10.5	4.47			
	3	0.985	10.5	4.50			
	4	0.997	10.6	4.36			
	*run another day	5	0.954	10.2			4.83
	<b>Average</b>			<b>10.5</b>			<b>4.52</b>
<b>Control 2 6-18</b>	1	0.891	9.29	5.71	<b>83</b>		
	2	1.04	11.0	4.04			
	3	1.07	11.3	3.74			
	4	1.14	12.0	2.99			
	*run another day	5	1.09	11.8			3.22
	<b>Average</b>			<b>11.1</b>			<b>3.94</b>
<b>MIP 5 6-18</b>	1	0.927	9.85	5.15	<b>84</b>		
	2	1.04	11.1	3.85			
	3	1.08	11.5	3.46			
	4	1.04	11.1	3.86			
	*run another day	5	0.928	9.85			5.15
	<b>Average</b>			<b>10.7</b>			<b>4.30</b>
<b>Control 3 6-18</b>	1	1.10	11.6	3.38	<b>85</b>		
	2	1.13	12.0	3.01			
	3	1.14	12.1	2.93			
	4	1.14	12.1	2.93			
	*run another day	5	1.17	12.8			2.20
	<b>Average</b>			<b>12.1</b>			<b>2.89</b>
<b>MIP 3 6-25</b>	1	0.628	6.56	8.44	<b>62</b>	1:8:18	

<b>Average</b>	2	0.617	6.43	8.57		
	3	0.582	6.01	8.99		
	4	0.719	7.63	7.37		
	5	0.840	9.06	5.94		
			<b>7.14</b>	<b>7.86</b>		
<b>Control 1 6-25</b>	1	0.632	6.57	8.43	<b>63</b>	
	2	0.592	6.09	8.91		
	3	0.759	8.08	6.92		
	4	0.845	9.11	5.89		
	5	0.820	8.81	6.19		
<b>Average</b>			<b>7.73</b>	<b>7.27</b>		
<b>MIP 4 6-25</b>	1	0.905	9.82	5.18	<b>64</b>	1:4:27
	2	0.812	8.73	6.27		
	3	0.879	9.52	5.48		
	4	0.884	9.58	5.42		
	5	0.931	10.1	4.87		
<b>Average</b>			<b>9.56</b>	<b>5.44</b>		
<b>Control 2 6-25</b>	1	0.985	10.8	4.23	<b>65</b>	
	2	0.886	9.60	5.40		
	3	0.754	8.02	6.98		
	4	0.840	9.04	5.96		
	5	0.850	9.16	5.84		
<b>Average</b>			<b>9.32</b>	<b>5.68</b>		
<b>TEOTES MIP 1 7-23</b>	1	0.915	9.93	5.07	<b>75</b>	1:4:20
	2	0.875	9.62	5.38		
	3	0.797	8.73	6.27		
	4	0.788	8.63	6.37		
	5	0.794	8.70	6.30		
	6	0.776	8.50	6.50		
<b>Average</b>			<b>9.02</b>	<b>5.98</b>		
<b>TEOTES MIP 2 7-23</b>	1	0.943	10.2	4.76	<b>75</b>	1:4:20
	2	0.883	9.72	5.28		
	3	0.965	10.7	4.35		
	4	0.874	9.61	5.39		
	5	0.833	9.15	5.85		
	6	0.837	9.19	5.81		
<b>Average</b>			<b>9.76</b>	<b>5.24</b>		
<b>MIP 1 7-20</b>	1	1.08	11.8	3.21	<b>68</b>	1:10:50
	2	0.876	9.64	5.36		
	3	0.782	8.55	6.45		
	4	0.778	8.51	6.49		
	5	0.946	10.4	4.56		
	6	0.803	8.80	6.20		
<b>Average</b>			<b>9.62</b>	<b>5.38</b>		
<b>MIP 2 7-20</b>	1	1.02	11.1	3.92	<b>68</b>	1:10:50
	2	0.876	9.63	5.37		
	3	0.930	10.3	4.75		
	4	0.911	10.0	4.96		
	5	0.999	11.0	3.96		
	6	0.976	10.8	4.22		
<b>Average</b>			<b>10.5</b>	<b>4.53</b>		

RDX uptake: rinsing and reusing the same sample.

Sample name	Sample #	UV-Vis Abs 236 nm	RDX left in soln out of 15 ug/mL	RDX uptake out of 15 ug/mL	Condition Table # Supp Info 2	Ratio
<b>MIP 1 5-22</b>	1	0.645	12.7	2.30	<b>54</b>	1:4:18
	2	0.653	12.9	2.15		
	3	0.645	12.7	2.31		
	4	0.660	13.0	2.01		
	<b>Average</b>			<b>12.8</b>		
<b>MIP 1 6-13</b>	1	0.699	13.8	1.18	<b>54</b>	1:4:18
	2	0.708	14.0	1.01		
	3	0.690	13.6	1.38		
	4	0.681	13.4	1.56		
	<b>Average</b>			<b>13.7</b>		
<b>MIP 2 6-13</b>	1	0.665	13.1	1.89	<b>54</b>	1:4:18
	2	0.671	13.2	1.76		
	3	0.659	13.0	2.02		
	4	0.657	12.9	2.06		
	<b>Average</b>			<b>13.1</b>		
<b>MIP 3 6-13</b>	1	0.667	13.1	1.85	<b>54</b>	1:4:18
	2	0.670	13.2	1.78		
	3	0.680	13.4	1.58		
	4	0.675	13.3	1.68		
	<b>Average</b>			<b>13.3</b>		
<b>Control 1 5-22</b>	1	0.684	13.5	1.49	<b>55</b>	
	2	0.669	13.2	1.82		
	3	0.666	13.1	1.88		
	4	0.655	12.9	2.10		
	<b>Average</b>			<b>13.2</b>		
<b>Control 1 6-13</b>	1	0.612	12.0	3.00	<b>55</b>	
	2	0.628	12.3	2.67		
	3	0.632	12.4	2.57		
	4	0.600	11.7	3.25		
	<b>Average</b>			<b>12.1</b>		
<b>MIP 2 5-22</b>	1	0.679	13.4	1.60	<b>66</b>	1:4:18
	2	0.674	13.3	1.71		
	3	0.694	13.7	1.28		
	4	0.698	13.8	1.20		
	<b>Average</b>			<b>13.6</b>		
<b>Control 2 5-22</b>	1	0.656	12.9	2.08	<b>67</b>	
	2	0.663	13.1	1.94		
	3	0.658	13.0	2.04		
	4	0.662	13.0	1.95		
	<b>Average</b>			<b>13.0</b>		

TNT and DNT uptake: using new samples each trial

Sample name	Sample #	UV-Vis Abs 232 nm	TNT left in soln out of 15 ug/mL	TNT uptake out of 15 ug/mL	mg polymer	(ug/ml)/mg poly	3mL vol (ug TNT/mg poly)	Condition Table # Supp Info 2	Ratio
<b>DIP MIP 3 3-6</b>	1	1.14	12.7	2.27				<b>37</b>	1:4:20
<b>DIP MIP 1 3-27</b>	1	1.21	13.4	1.57				<b>37</b>	1:4:20
<b>DIP Control 4 3-6</b>	1	1.03	11.6	3.45				<b>38</b>	
<b>DIP Control 1 3-27</b>	1	1.20	13.2	1.76				<b>38</b>	
<b>MIP 1 6-25</b>	1	0.594	6.15	8.85	14.9	0.594	1.78	<b>60</b>	1:8:36
	2	0.727	7.76	7.24	14.8	0.489	1.47		
	3	0.647	6.82	8.18	15.1	0.542	1.63		
	4	0.802	8.64	6.36	15.1	0.421	1.26		
	5	0.695	7.39	7.61	14.9	0.511	1.53		
	6	0.591	6.16	8.84	14.8	0.597	1.79		
	7	0.631	6.63	8.37	15.1	0.554	1.66		
	8	0.691	7.62	7.38	15.1	0.489	1.47		
	9	0.536	5.85	9.15	15.2	0.602	1.81		
	10	0.622	6.83	8.17	15.1	0.541	1.62		
<b>Average</b>			<b>6.99</b>	<b>8.01</b>			<b>1.60</b>		
<b>MIP 1 7-2</b>	1	0.900	9.28	5.72	14.8	0.386	1.16	<b>60</b>	1:8:36
	2	0.874	8.96	6.04	15	0.403	1.21		
	3	0.906	9.35	5.65	15.2	0.372	1.12		
	4	0.862	8.83	6.17	15	0.412	1.23		
	5	0.902	9.31	5.69	14.8	0.385	1.15		
	6	0.904	9.32	5.68	15.1	0.376	1.13		
	7	0.839	8.54	6.46	14.8	0.437	1.31		



<b>MIP 2 6-25</b>	1	0.713	7.56	7.44	14.9	0.499	1.50	<b>61</b>	1:2:9
	2	0.705	7.50	7.50	14.8	0.507	1.52		
<b>Average</b>			<b>7.53</b>	<b>7.47</b>			<b>1.51</b>		
<b>MIP 3 7-12</b>	1	0.717	7.87	7.13	15	0.475	1.43	<b>72</b>	1:23:102
	2	0.876	9.68	5.32	15.2	0.350	1.05		
	3	Instrument Error		14.9	0.000	0.00			
	4	0.785	8.64	6.36	15.1	0.421	1.26		
	5	0.701	7.69	7.31	14.8	0.494	1.48		
<b>Average</b>			<b>8.47</b>	<b>6.53</b>			<b>1.31</b>		
<b>Control 2 5-15</b>	1	0.718	7.91	7.09	15.1	0.469	1.41	<b>53</b>	
	2	0.733	8.08	6.92	15.2	0.455	1.36		
	3	0.743	8.20	6.80	15	0.454	1.36		
	4	0.421	4.62	10.38	14.8	0.701	2.10		
	5	0.892	9.85	5.15	15.2	0.339	1.02		
	6	0.801	8.84	6.16	14.9	0.413	1.24		
	7	0.775	8.55	6.45	15.1	0.427	1.28		
	8	0.843	9.31	5.69	14.8	0.384	1.15		
	9	0.889	9.82	5.18	15	0.345	1.04		
	10	0.719	7.93	7.07	15.2	0.465	1.39		
<b>Average</b>			<b>8.31</b>	<b>6.69</b>			<b>1.34</b>		
<b>Control 1 7-2</b>	1	0.879	9.03	5.97	14.9	0.401	1.20	<b>53</b>	
	2	0.921	9.53	5.47	14.8	0.370	1.11		
	3	0.850	8.67	6.33	15.1	0.419	1.26		
	4	0.907	9.37	5.63	15.1	0.373	1.12		
	5	0.896	9.23	5.77	15.2	0.380	1.14		
	6	0.948	9.85	5.15	14.9	0.346	1.04		

	7	0.929	9.63	5.37	15	0.358	1.07		
	8	1.10	11.7	3.28	15.2	0.216	0.65		
	9	0.893	9.19	5.81	15.1	0.384	1.15		
	10	0.905	9.34	5.66	14.9	0.380	1.14		
<b>Average</b>			<b>9.56</b>	<b>5.44</b>			<b>1.09</b>		
<b>Control 1 5-30</b>	1	0.804	8.87	6.13	14.8	0.414	1.24		<b>57</b>
	2	0.721	7.95	7.05	15.2	0.464	1.39		
	3	Instrument Error							
	4	0.140	1.50	13.50	15.1	0.894	2.68		
	5	0.925	10.2	4.78	14.9	0.321	0.96		
	6	0.973	10.7	4.25	15	0.284	0.85		
	7	0.833	9.19	5.81	14.9	0.390	1.17		
	8	1.07	11.8	3.15	15	0.210	0.63		
	9	0.967	10.7	4.32	15.2	0.284	0.85		
	10	1.00	11.1	3.93	15.2	0.259	0.78		
<b>Average</b>			<b>9.12</b>	<b>5.88</b>			<b>1.17</b>		
<b>MIP 3 6-25</b>	1	0.628	6.56	8.44	15.1	0.559	1.68		1:8:18
	2	0.749	8.02	6.98	15	0.465	1.40		
<b>Average</b>			<b>7.29</b>	<b>7.71</b>			<b>1.54</b>		
<b>Control 1 6-25</b>	1	0.632	6.57	8.43	14.8	0.569	1.71		<b>63</b>
	2	0.693	7.36	7.64	15	0.509	1.53		
<b>Average</b>			<b>6.97</b>	<b>8.03</b>			<b>1.62</b>		
<b>MIP 4 6-25</b>	1	0.905	9.82	5.18	15.1	0.343	1.03		1:4:27
	2	0.944	10.3	4.69	14.9	0.315	0.94		
<b>Average</b>			<b>10.1</b>	<b>4.93</b>			<b>1.0</b>		
<b>Control 2 6-25</b>	1	0.985	10.8	4.23	15.2	0.278	0.84		<b>65</b>

<b>Average</b>	<b>2</b>	<b>1.07</b>	<b>11.8</b>	<b>3.20</b>	<b>14.8</b>	<b>0.216</b>	<b>0.65</b>		
			<b>11.3</b>	<b>3.71</b>			<b>0.7</b>		
<b>MIP 1 7-12</b>	1	0.813	8.96	6.04	15.2	0.397	1.19		1:10:50
	2	0.629	6.87	8.13	15.4	0.528	1.58		
	3	0.596	6.49	8.51	15.2	0.560	1.68		
	4	0.644	7.04	7.96	15.3	0.520	1.56		
	5	0.694	7.61	7.39	15.2	0.486	1.46		
<b>Average</b>			<b>7.40</b>	<b>7.60</b>			<b>1.49</b>		
<b>MIP 1 7-20</b>	1	1.08	11.8	3.21	15.1	0.213	0.64		1:10:50
	2	1.12	12.2	2.80	15.2	0.184	0.55		
	3	1.15	12.5	2.46	15	0.164	0.49		
	4	1.11	12.2	2.84	15.1	0.188	0.56		
	5	1.16	12.6	2.36	15	0.158	0.47		
<b>Average</b>			<b>12.3</b>	<b>2.73</b>			<b>0.5</b>		
<b>MIP 2 7-20</b>	1	1.02	11.1	3.92	14.9	0.263	0.79		1:10:50
	2	0.873	9.46	5.54	15.1	0.367	1.10		
	3	0.993	10.8	4.19	14.8	0.283	0.85		
	4	1.01	11.0	3.96	14.9	0.266	0.80		
	5	0.952	10.4	4.65	15	0.310	0.93		
<b>Average</b>			<b>10.5</b>	<b>4.45</b>			<b>0.9</b>		
<b>Control 1 7-12</b>	1	1.30	14.5	0.55	15	0.037	0.11		69
	2	1.06	11.7	3.29	14.8	0.223	0.67		
	3	1.07	11.9	3.14	15	0.209	0.63		
	4	1.03	11.4	3.59	14.9	0.241	0.72		
	5	0.98	10.9	4.10	15.2	0.270	0.81		
<b>Average</b>			<b>12.1</b>	<b>2.93</b>			<b>0.6</b>		

<b>Control 1 7-20</b>	1	1.08	12.0	2.99	14.9	0.201	0.60	<b>69</b>
	2	1.05	11.7	3.28	14.9	0.220	0.66	
	3	1.05	11.7	3.28	15.2	0.216	0.65	
	4	1.06	11.8	3.19	15	0.212	0.64	
	5	1.00	11.1	3.89	15.2	0.256	0.77	
<b>Average</b>		<b>11.7</b>	<b>3.33</b>				<b>0.7</b>	
<b>Control 2 7-20</b>	1	0.902	9.98	5.02	14.8	0.339	1.02	<b>69</b>
	2	1.07	11.9	3.06	15.2	0.201	0.60	
	3	1.01	11.2	3.79	15	0.253	0.76	
	4	1.01	11.2	3.82	15.2	0.251	0.75	
	5	1.04	11.5	3.47	14.9	0.233	0.70	
<b>Average</b>		<b>11.2</b>	<b>3.83</b>				<b>0.8</b>	
<b>Control 3 7-20</b>	1	0.919	10.2	4.82	15.1	0.319	0.96	<b>69</b>
	2	0.940	10.4	4.58	14.8	0.310	0.93	
	3	0.948	10.5	4.48	15	0.299	0.90	
	4	0.938	10.4	4.60	15.2	0.303	0.91	
	5	0.921	10.2	4.80	15.2	0.315	0.95	
<b>Average</b>		<b>10.3</b>	<b>4.66</b>				<b>0.9</b>	
<b>MIP 2 7-12</b>	1	0.691	7.58	7.42	15.2	0.488	1.47	<b>70</b>
	2	0.736	8.08	6.92	15.4	0.449	1.35	
	3	0.763	8.39	6.61	15.2	0.435	1.30	
	4	0.784	8.63	6.37	15.3	0.416	1.25	
	5	0.799	8.80	6.20	15.2	0.408	1.22	
<b>Average</b>		<b>8.30</b>	<b>6.70</b>				<b>1.32</b>	
<b>Control 2 7-12</b>	1	1.12	12.4	2.58	15	0.172	0.52	<b>71</b>
	2	1.11	12.4	2.65	15.2	0.174	0.52	



<b>Average</b>	5	0.996	10.8	4.16	15.2	0.273	0.82		
<b>TEOTES 7/19 Control</b>	1	1.06	11.9	3.14	15.2	0.207	0.62	<b>76</b>	
	2	1.05	11.8	3.25	15	0.217	0.65		
	3	1.05	11.7	3.31	15.1	0.219	0.66		
	4	1.07	12.0	3.03	14.9	0.203	0.61		
	5	1.02	11.4	3.65	15	0.243	0.73		
<b>Average</b>			<b>11.7</b>	<b>3.28</b>			<b>0.7</b>		
<b>TEOTES 7/19 Control</b> NaOH could be cause of suspect results	1	1.66	18.7	-3.73				<b>77</b>	
	2	1.72	19.5	-4.46					
	3	1.88	21.3	-6.26					
	4	1.52	17.1	-2.13					
	5	1.76	19.8	-4.85					
<b>Average</b>			<b>19.3</b>	<b>-4.29</b>					
<b>MIP 1 8-17</b>	1	1.2445	13.7	1.3	14.8	0.087	0.26	27	1:10:368
<b>APTES</b>	2	1.2531	13.8	1.2	15	0.079	0.24		
	3	1.2623	13.9	1.1	15.2	0.071	0.21		
	4	1.2576	13.9	1.1	14.9	0.076	0.23		
	5	1.2504	13.8	1.2	15.2	0.080	0.24		
			<b>13.8</b>	<b>1.18</b>			<b>0.24</b>		
<b>MIP 2 8-17</b>	1	1.2765	14.1	0.9	14.8	0.062	0.19	27	1:10:368
<b>APTES</b>	2	1.2737	14.0	1.0	15.1	0.063	0.19		
	3	1.2754	14.1	0.9	14.9	0.063	0.19		
	4	1.4791	16.4	-1.4	14.8	-0.092	-0.28		
	5	1.4782	16.4	-1.4	15.0	-0.091	-0.27		
			<b>15.0</b>	<b>0</b>			<b>0.00</b>		

<b>MIP 1 8-22</b> <b>APTES</b>	1	1.4484	16.0	-1.0	14.8	-0.069	-0.21	88
	2	1.4348	15.9	-0.9	14.9	-0.058	-0.17	
	3	1.421	15.7	-0.7	14.8	-0.048	-0.14	
	4	1.4075	15.6	-0.6	15.1	-0.037	-0.11	
	5	1.4377	15.9	-0.9	14.9	-0.060	-0.18	
			<b>15.8</b>	<b>-0.81</b>			<b>-0.16</b>	
<b>8-28-14 MIP</b> <b>2,4 -DNT APTES</b>		UV-Vis Abs 250 nm						88 1:10:368
	1	1.142	14.5	0.50	15.0	0.033	0.10	
	2	1.1217	14.2	0.77	15.2	0.051	0.15	
	3	1.1498	14.6	0.39	14.9	0.026	0.08	
	4	1.1453	14.5	0.45	15.2	0.030	0.09	
	5	1.1296	14.3	0.66	15.2	0.044	0.13	
<b>Control 1</b> <b>APTES</b>			<b>14.4</b>	<b>0.55</b>			<b>0.1</b>	28
	1	1.1224	14.2	0.76	15.0	0.051	0.15	
	2	1.1751	15.0	0.04	15.2	0.003	0.01	
	3	1.1209	14.2	0.78	15.0	0.052	0.16	
	4	1.1215	14.2	0.78	15.1	0.051	0.15	
	5	1.1526	14.6	0.35	15.0	0.023	0.07	
		<b>14.5</b>	<b>0.5</b>			<b>0.1</b>		

## Supporting Information 4

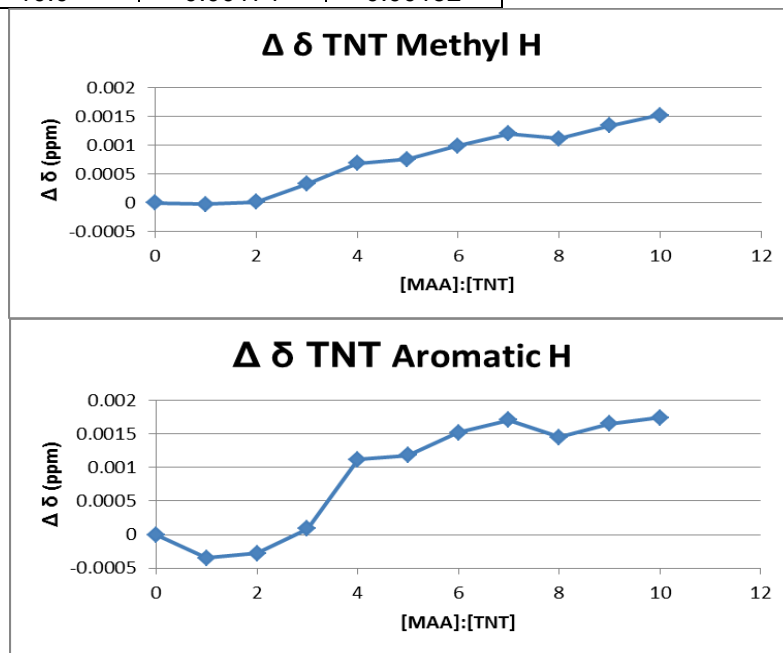
## Comparison of total NMR shift for all monomers

Monomer	Max [Mono]:[TNT]	Aromatic		Methyl	
		Start	End	Start	End
PTMS	20.2:1	0.00198	0.0430	0.00166	0.0352
Aniline	20:1	0.0104	0.0943	0.00659	0.0623
TEOTES	10.4:1	0.00121	0.0106	0.00087	0.00986
Low [MAA]	10:1	-0.0003	0.00174	-0.00002	0.00152
High [MAA] 1	9.7:1	0.00009	0.00070	0.00053	0.00134
High [MAA] 2	9.4:1	0.00055	0.00087	0.00074	0.0015
TMOTFS	9.8:1	0.00001	0.00046	-0.0003	0.00176
Nitromethane	9.8:1	NA	NA	0.0022	0.0234

TNT titrated with MAA lower concentration

Titration of trinitrotoluene (TNT) with methacrylic acid (MAA)					
MAA uL	[MAA] M	[TNT] M	[MAA]:[TNT]	Aromatic TNT ppm	TNT Methyl ppm
0	0	0.0088	0	8.84999	2.71839
2	0.0088	0.0088	1.0	8.85034	2.71841
4	0.0176	0.0088	2.0	8.85027	2.71837
6	0.0264	0.0088	3.0	8.8499	2.71806
8	0.0352	0.0088	4.0	8.84887	2.7177
10	0.044	0.0088	5.0	8.84881	2.71763
12	0.0528	0.0088	6.0	8.84847	2.7174
14	0.0616	0.0088	7.0	8.84828	2.71719
16	0.0704	0.0088	8.0	8.84854	2.71727
18	0.0792	0.0088	9.0	8.84834	2.71705
20	0.088	0.0088	10.0	8.84825	2.71687

Change in chemical shift ( $\Delta\delta$ )			
MAA uL	[MAA]:[TNT]	Aromatic TNT	TNT Methyl
0	0	0	0
2	1.0	-0.00035	-2E-05
4	2.0	-0.00028	2E-05
6	3.0	9E-05	0.00033
8	4.0	0.00112	0.00069
10	5.0	0.00118	0.00076
12	6.0	0.00152	0.00099
14	7.0	0.00171	0.0012
16	8.0	0.00145	0.00112
18	9.0	0.00165	0.00134
20	10.0	0.00174	0.00152

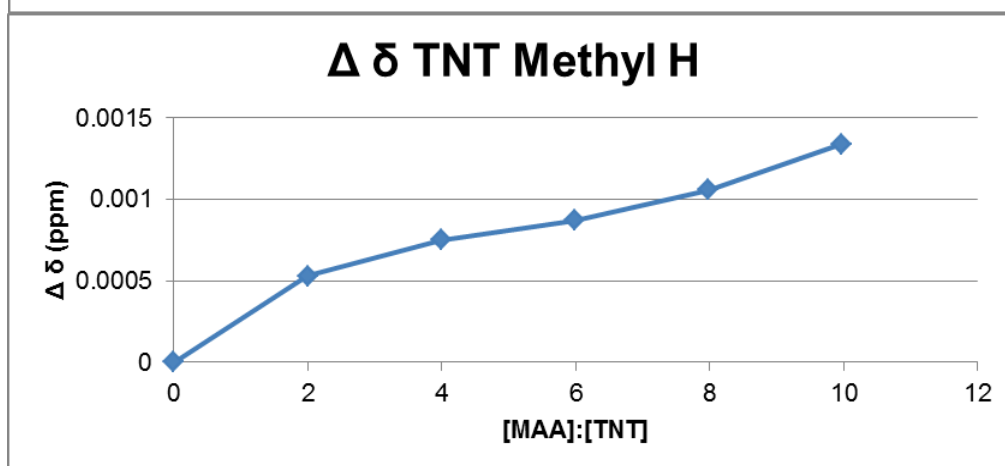
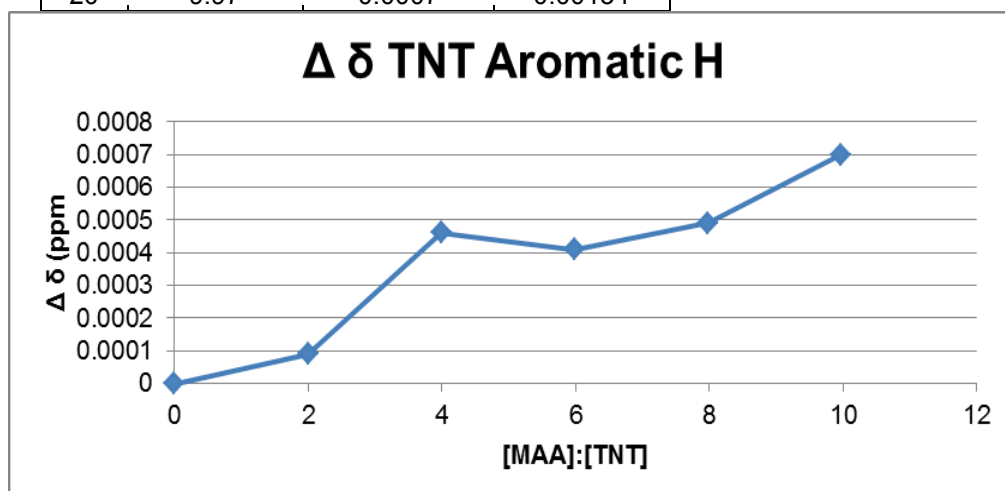


TNT titrated with MAA higher concentration 1

Titration of trinitrotoluene (TNT) with methacrylic acid (MAA)					
MAA uL	[MAA] M	[TNT] M	[MAA]:[TNT]	Aromatic TNT (ppm)	TNT Methyl (ppm)
0	0	0.0177	0	8.8517	2.719
4	0.0353	0.0177	1.99	8.85161	2.71847
8	0.0706	0.0177	3.99	8.85124	2.71825
12	0.1059	0.0177	5.98	8.85129	2.71813
16	0.1412	0.0177	7.98	8.85121	2.71794
20	0.1765	0.0177	9.97	8.851	2.71766

Change in chemical shift ( $\Delta\delta$ )			
MAA uL	[MAA]:[TNT]	Aromatic TNT	TNT Methyl
0	0	0	0
4	1.99	9E-05	0.00053
8	3.99	0.00046	0.00075
12	5.98	0.00041	0.00087
16	7.98	0.00049	0.00106
20	9.97	0.0007	0.00134

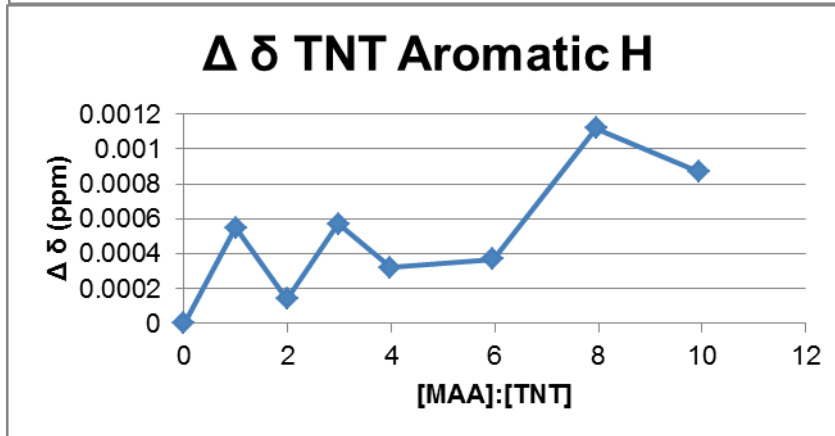
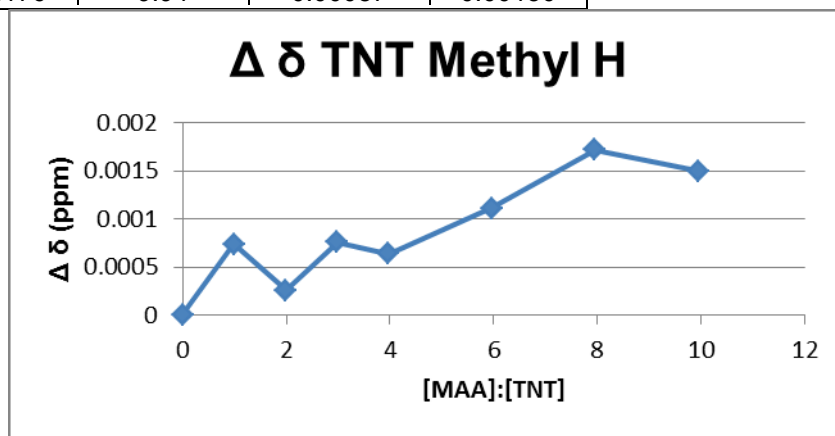


TNT titrated with MAA higher concentration 2

Titration of trinitrotoluene (TNT) with methacrylic acid (MAA)					
MAA $\mu$ L	[MAA] M	[TNT] M	[MAA]:[TNT]	Aromatic TNT (ppm)	TNT Methyl (ppm)
0	0	0.0177	0	8.85160	2.71915
2	0.0176	0.0177	0.99	8.85105	2.71841
4	0.0352	0.0177	1.99	8.85146	2.71889
6	0.0528	0.0177	2.98	8.85103	2.71839
8	0.0704	0.0177	3.98	8.85128	2.71851
12	0.1056	0.0177	5.97	8.85123	2.71804
16	0.1408	0.0177	7.95	8.85048	2.71743
20	0.176	0.0177	9.94	8.85073	2.71765

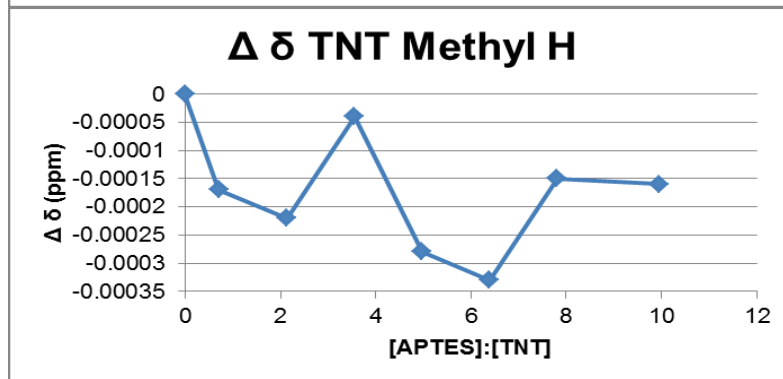
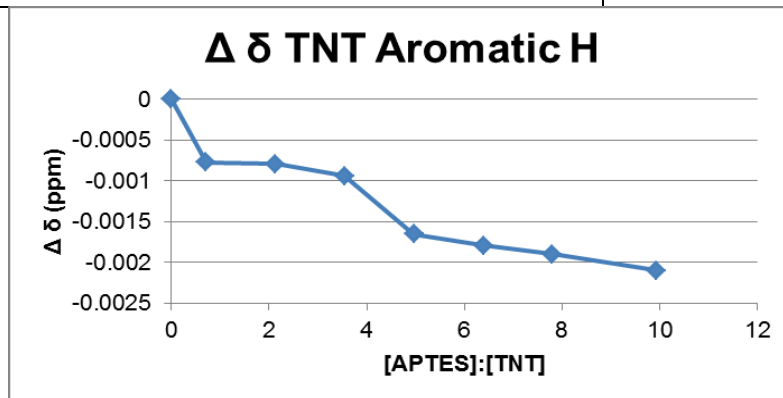
Change in chemical shift ( $\Delta\delta$ )			
[MAA] M	[MAA]:[TNT]	Aromatic TNT	TNT Methyl
0	0	0	0
0.0176	0.99	0.00055	0.00074
0.0352	1.99	0.00014	0.00026
0.0528	2.98	0.00057	0.00076
0.0704	3.98	0.00032	0.00064
0.1056	5.97	0.00037	0.00111
0.1408	7.95	0.00112	0.00172
0.176	9.94	0.00087	0.00150



Titration of trinitrotoluene (TNT) with aminopropyltriethoxy silane (APTES) in deuterated acetonitrile

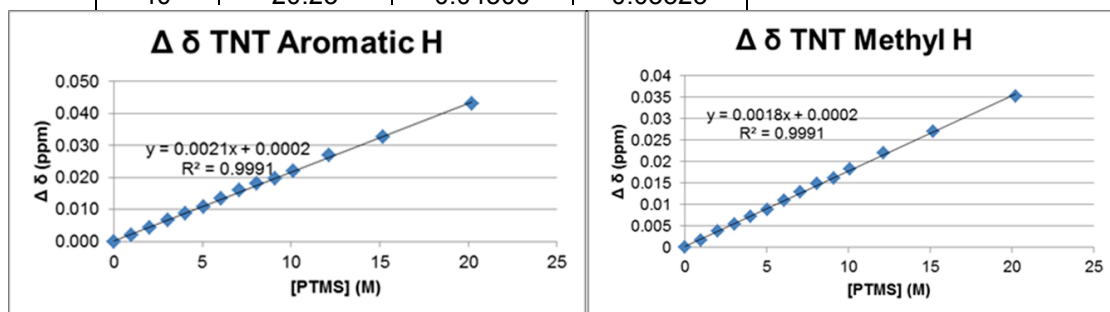
APTES $\mu$ L	[APTES] M	[TNT] M	[APTES]:[TNT]	Aromatic TNT (ppm)	TNT Methyl (ppm)
0		0.010	0	8.83614	2.61207
1	0.0071	0.010	0.71	8.83691	2.61224
3	0.0213	0.010	2.13	8.83693	2.61229
5	0.0355	0.010	3.55	8.83708	2.61211
7	0.0497	0.010	4.97	8.83779	2.61235
9	0.0639	0.010	6.39	8.83793	2.6124
11	0.0781	0.010	7.81	8.83804	2.61222
14	0.0994	0.010	9.94	8.83824	2.61223

Change in chemical shift ( $\Delta\delta$ )			
APTES $\mu$ L	[APTES]:[TNT]	Aromatic TNT	TNT Methyl
0	0	0	0
1	0.71	-0.00077	-0.00017
3	2.13	-0.00079	-0.00022
5	3.55	-0.00094	-4E-05
7	4.97	-0.00165	-0.00028
9	6.39	-0.00179	-0.00033
11	7.81	-0.0019	-0.00015
14	9.94	-0.0021	-0.00016



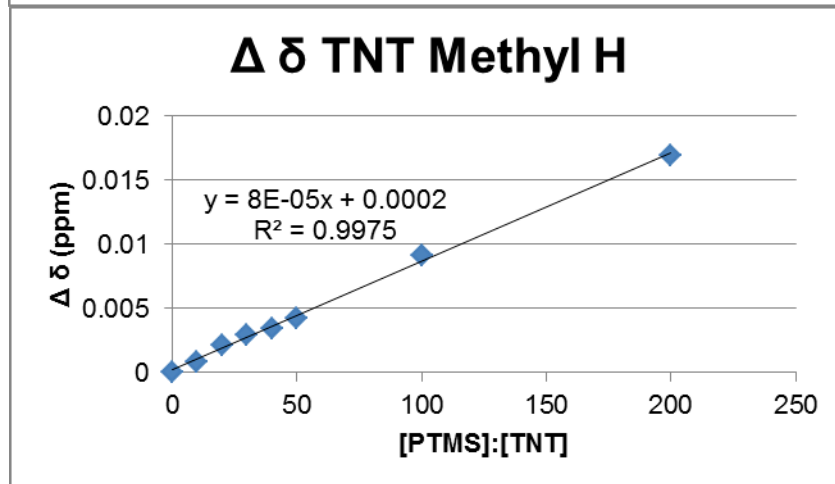
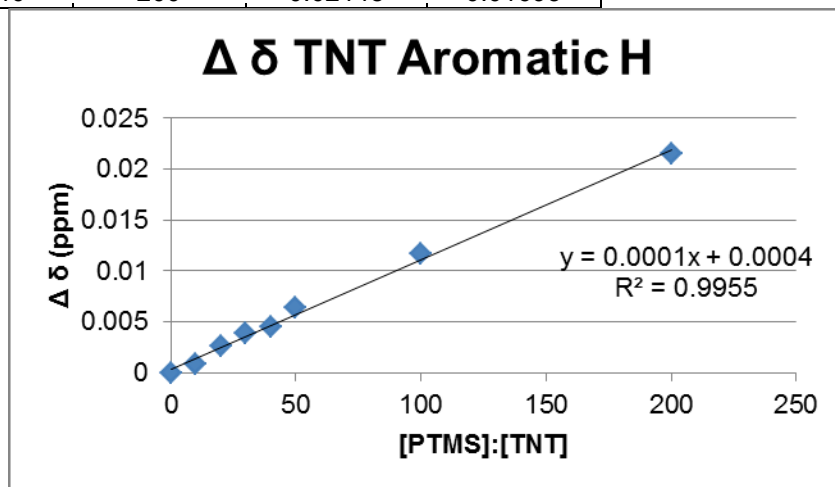
Titration of trinitrotoluene (TNT) with phenyltrimethoxy silane (PTMS)					
PTMS uL	[PTMS] M	[TNT] M	[PTMS]:[TNT]	Aromatic TNT (ppm)	TNT Methyl (ppm)
0	0	0.0177	0	8.84800	2.71767
2	0.0179	0.0177	1.01	8.84602	2.71601
4	0.0358	0.0177	2.02	8.84360	2.71383
6	0.0537	0.0177	3.03	8.84125	2.71222
8	0.0716	0.0177	4.05	8.83919	2.71042
10	0.0895	0.0177	5.06	8.83730	2.70891
12	0.1074	0.0177	6.07	8.83461	2.70671
14	0.1253	0.0177	7.08	8.83207	2.70471
16	0.1432	0.0177	8.09	8.82995	2.70285
18	0.1611	0.0177	9.10	8.82821	2.70150
20	0.179	0.0177	10.11	8.82589	2.69943
24	0.2148	0.0177	12.14	8.82106	2.69557
30	0.2685	0.0177	15.17	8.81542	2.69066
40	0.3580	0.0177	20.23	8.80500	2.68244

Change in chemical shift ( $\Delta\delta$ )			
PTMS uL	[PTMS]:[TNT]	Aromatic TNT	TNT Methyl
0	0	0	0
2	1.01	0.00198	0.00166
4	2.02	0.00440	0.00384
6	3.03	0.00675	0.00545
8	4.05	0.00881	0.00725
10	5.06	0.01070	0.00876
12	6.07	0.01339	0.01096
14	7.08	0.01593	0.01296
16	8.09	0.01805	0.01482
18	9.10	0.01979	0.01617
20	10.11	0.02211	0.01824
24	12.14	0.02694	0.02210
30	15.17	0.03258	0.02701
40	20.23	0.04300	0.03523



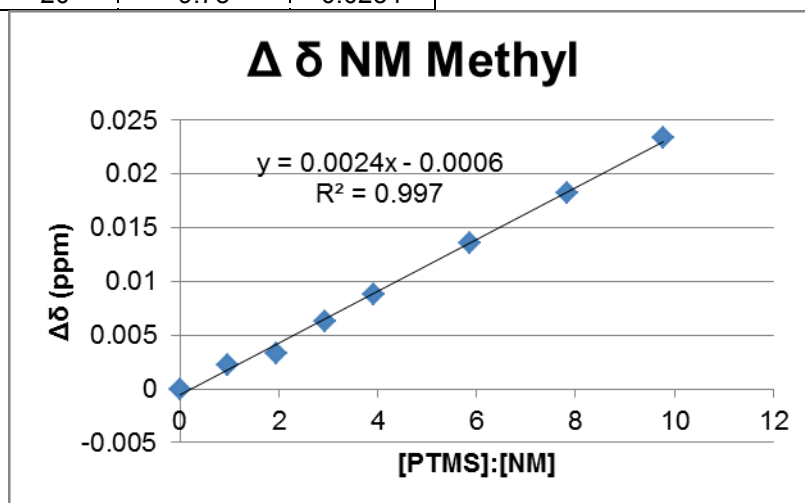
Titration of trinitrotoluene (TNT) with phenyltrimethoxy silane (PTMS)					
PTMS $\mu$ L	[PTMS] M	[TNT] M	[PTMS]:[TNT]	Aromatic TNT (ppm)	TNT Methyl (ppm)
0	0	0.0018	0	8.85048	2.71794
2	0.018	0.0018	10	8.84965	2.71707
4	0.036	0.0018	20	8.8479	2.71578
6	0.054	0.0018	30	8.84657	2.715
8	0.072	0.0018	40	8.84593	2.7145
10	0.09	0.0018	50	8.84401	2.71372
20	0.18	0.0018	100	8.83884	2.70877
40	0.36	0.0018	200	8.829	2.70101

Change in chemical shift ( $\Delta\delta$ )			
PTMS $\mu$ L	[PTMS]:[TNT]	Aromatic TNT	TNT Methyl
0	0	0	0
2	10	0.00083	0.00087
4	20	0.00258	0.00216
6	30	0.00391	0.00294
8	40	0.00455	0.00344
10	50	0.00647	0.00422
20	100	0.01164	0.00917
40	200	0.02148	0.01693



Titration of nitromethane (NM) with phenyltrimethoxy silane (PTMS)				
PTMS $\mu$ L	[PTMS] M	[NM] M	[PTMS]:[NM]	Methyl NM (ppm)
0	0	0.0183	0	4.3318
2	0.0179	0.0183	0.98	4.3296
4	0.0358	0.0183	1.96	4.3285
6	0.0537	0.0183	2.93	4.3255
8	0.0716	0.0183	3.91	4.323
12	0.1074	0.0183	5.87	4.3182
16	0.1432	0.0183	7.83	4.3136
20	0.1790	0.0183	9.78	4.3084

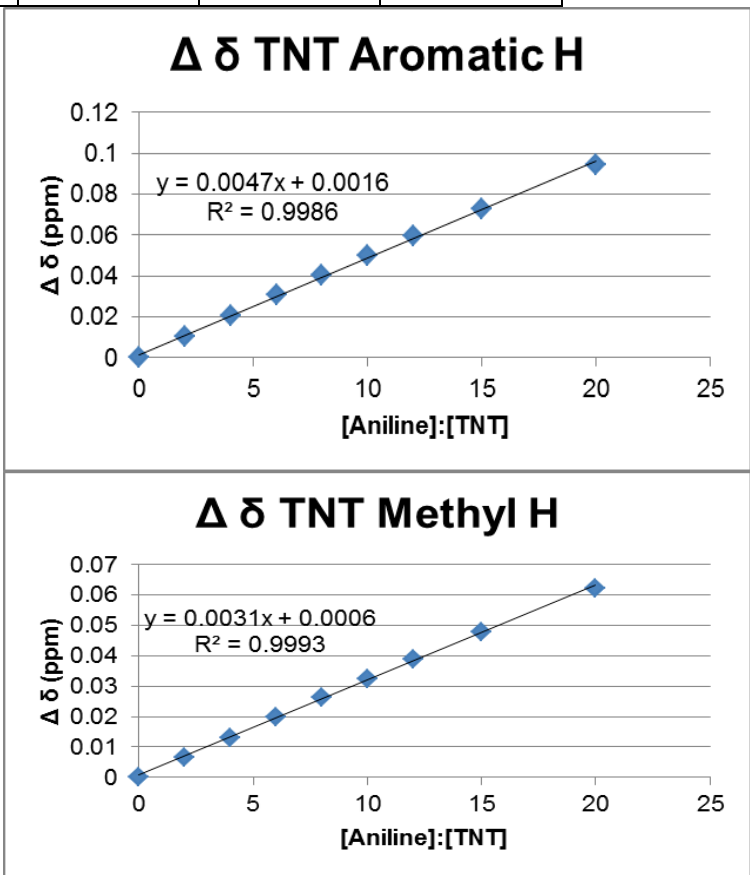
Change in chemical shift ( $\Delta\delta$ )		
PTMS $\mu$ L	[PTMS]:[NM]	Methyl NM
0	0	0
2	0.98	0.0022
4	1.96	0.0033
6	2.93	0.0063
8	3.91	0.0088
12	5.87	0.0136
16	7.83	0.0182
20	9.78	0.0234



Titration of trinitrotoluene (TNT) with aniline					
Aniline uL	[Aniline] M	[TNT] M	[Aniline]:[TNT]	Aromatic TNT (ppm)	TNT Methyl (ppm)
0	0	0.0177	0	8.85003	2.71818
4	0.0354	0.0177	2	8.83962	2.71159
8	0.0708	0.0177	4	8.82956	2.70509
12	0.1062	0.0177	6	8.81933	2.69847
16	0.1416	0.0177	8	8.80965	2.69205
20	0.177	0.0177	10	8.80001	2.68571
24	0.2124	0.0177	12	8.79061	2.67948
30	0.2655	0.0177	15	8.77719	2.67033
40	0.354	0.0177	20	8.75575	2.65591

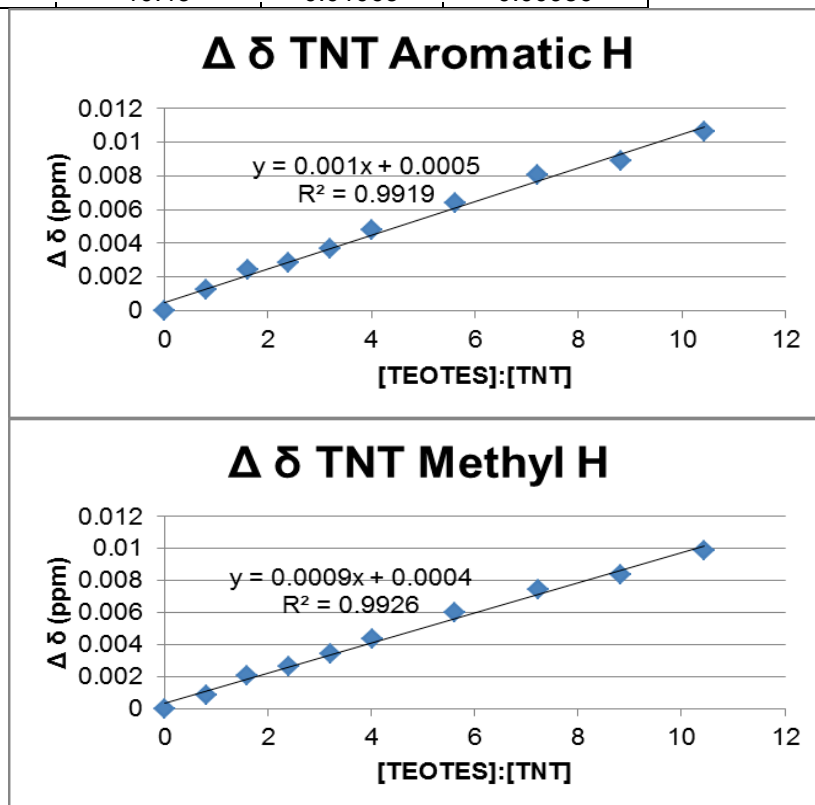
Change in chemical shift ( $\Delta\delta$ )			
Aniline uL	[Aniline]:[TNT]	Aromatic TNT	TNT Methyl
0	0	0	0
4	2	0.01041	0.00659
8	4	0.02047	0.01309
12	6	0.0307	0.01971
16	8	0.04038	0.02613
20	10	0.05002	0.03247
24	12	0.05942	0.0387
30	15	0.07284	0.04785
40	20	0.09428	0.06227



Titration of trinitrotoluene (TNT) with triethoxythienylsilane (TEOTES)					
TEOTES $\mu\text{L}$	[TEOTES] M	[TNT] M	[TEOTES]:[TNT]	Aromatic TNT ppm	TNT Methyl ppm
0	0	0.0177	0	8.85024	2.71855
2	0.0142	0.0177	0.80	8.84903	2.71768
4	0.0284	0.0177	1.60	8.84782	2.71647
6	0.0426	0.0177	2.41	8.84737	2.71589
8	0.0568	0.0177	3.21	8.84659	2.71515
10	0.071	0.0177	4.01	8.84545	2.71417
14	0.0994	0.0177	5.62	8.84384	2.71252
18	0.1278	0.0177	7.22	8.84216	2.71109
22	0.1562	0.0177	8.82	8.84132	2.71019
26	0.1846	0.0177	10.43	8.83961	2.70869

Change in chemical shift ( $\Delta\delta$ )			
TEOTES $\mu\text{L}$	[TEOTES]:[TNT]	Aromatic TNT	TNT Methyl
0	0	0	0
2	0.80	0.00121	0.00087
4	1.60	0.00242	0.00208
6	2.41	0.00287	0.00266
8	3.21	0.00365	0.0034
10	4.01	0.00479	0.00438
14	5.62	0.0064	0.00603
18	7.22	0.00808	0.00746
22	8.82	0.00892	0.00836
26	10.43	0.01063	0.00986



Titration of trinitrotoluene (TNT) with trimethoxytrifluoropropyl silane (TMOTFS)					
TMOTFS $\mu\text{L}$	[TMOTFS] M	[TNT] M	[TMOTFS]:[TNT]	Aromatic TNT ppm	TNT Methyl ppm
0	0	0.0177	0	8.85009	2.71812
2	0.0174	0.0177	0.98	8.85008	2.71846
4	0.0348	0.0177	1.97	8.85024	2.71825
10	0.087	0.0177	4.92	8.84967	2.71716
15	0.1305	0.0177	7.37	8.84965	2.71697
20	0.174	0.0177	9.83	8.84963	2.71636

Change in chemical shift ( $\Delta\delta$ )			
TMOTFS $\mu\text{L}$	[TMOTFS]:[TNT]	Aromatic TNT	TNT Methyl
0	0	0	0
2	0.98	1E-05	-0.00034
4	1.97	-0.00015	-0.00013
10	4.92	0.00042	0.00096
15	7.37	0.00044	0.00115
20	9.83	0.00046	0.00176

